Laboratory approaches for expanding the understanding of an emerging strain of *Erysipelothrix rhusiopathiae* in the Arctic

By

Yuk Ching Eugene Lau

BSc (Hons) in Veterinary Biosciences

Submitted in fulfilment of the requirements for the Degree of Master of Science by Research

University of Glasgow

School of Biodiversity, One Health and Veterinary Medicine

College of Medical, Veterinary and Life Sciences

October 2025

Abstract

Recent investigations into mass mortality events in the Canadian Arctic Archipelago have discovered that one singular 'Arctic clone' (Ac) of *Erysipelothrix rhusiopathiae* has been causing a large number of muskox die-offs. There is limited understanding of how this strain of the bacterium is maintained and transmitted, or why it is causing such high mortality in this wildlife population. Evidence suggests that this strain could be more virulent than other strains of *E. rhusiopathiae*. The aim of this project was to contribute to the further understanding of the Ac in the Canadian Arctic. Advances in animal welfare have redefined the ethics behind the use of mammalian models for scientific research. An emerging invertebrate disease model, using *Galleria mellonella* larvae as a host, has gained increasing recognition. The immune system of the larvae is similar to the mammalian innate immune system. Several successful examples using this model in studies of bacterial virulence suggest that this could be a useful tool to test the virulence of the Ac compared to non-Arctic clones (Nac) of *E. rhusiopathiae*. Since there were no prior investigations conducted on *E. rhusiopathiae* using this model, my first data chapter serves as an initial evaluation of its use. The experiments included the measurement of the growth kinetics and the inoculation of *G. mellonella* larvae in biological triplicate. Kaplan-Meier survival curves were generated to illustrate the larvae mortality over the course of the experiment. Up to 2.08×10^6 colony forming units of either Ac or Nac were injected into each larva but did not cause significant mortality during the 9-day observation period. The only experimental group that showed a significant difference was the undiluted Nac group (p-value of 0.049). The limited mortality observed across the majority of the test groups, and limited statistically significant differences in mortality in the treatment versus control groups (as shown using a Cox proportional hazards model) suggests that the *G. mellonella* is not a suitable model for studying the virulence of *E. rhusiopathiae* or the Ac. My results suggest that future studies to assess virulence of *E. rhusiopathiae* would best utilise other *in vivo* models.

The outbreak investigation of *E. rhusiopathiae* in muskoxen in the Canadian Arctic Archipelago has raised the need for a rapid and sensitive detection assay, particularly for identifying strains belonging to the Ac. I evaluated the design

and implementation of a triplex qPCR for simultaneous identification of three strains of interest. Signal leakage and limit of detection testing was conducted. An investigation was conducted to determine the cause of apparent false amplification of the Ac target in four outlier isolates. These 'imposter' isolates had cycle threshold (C_t) higher than other Ac isolates on the yellow channel; this observation was used to establish a trend between amplification of the *E. rhusiopathiae* and Ac targets to help spot future false positives or co-infections. Digital PCR established that true Ac isolates had around 500-600 copies/µL of the Ac target while the imposters had around 0.3 copies/µL and sequencing results from whole genome sequencing of the 'imposter' isolates were used to confirm the findings (i.e., that these isolates lacked the Ac-specific sequence) and concluded that the imposters were likely showing late amplification due to earlier contamination of the DNA extracts. The triplex qPCR I developed was further used for strain identification in DNA extracted directly from 367 samples collected from animal carcasses and carcass sites on Ellesmere Island and Axel Heiberg, where recent muskox die-offs occurred. Nearly 90% (n=329) of the samples tested were positive for Ac. Further optimisation is necessary for validation of the assay in different sample types and target concentrations, especially for samples with lower concentrations of the pathogen's DNA.

Overall, my Masters work has demonstrated that the *G. mellonella* larvae model is not suitable for *E. rhusiopathiae* infections at the studied conditions, helping redirect future virulence studies of the Ac towards other models. The development of the new triplex qPCR assay has provided a rapid, sensitive and cost-effective alternative to identify *Erysipelothrix* species and distinguish between Ac and non-Ac strains in infections in the Canadian Arctic.

Table of Contents

List of Tables

List of Figures

Acknowledgements

The sincerest, most heartfelt thank you is owed to my supervisors, Dr Taya Forde and Dr Katarina Oravcova. To Dr Forde, thank you for always being there for me, your constant guidance and support was always needed and welcomed. From scientific advice to friendly updates, you have always gone above and beyond what was expected. To Dr Oravcova, thank you for always providing me with detailed explanations whenever I required your microbiological expertise and other scientific advice. I have both of you to thank for the completion of this thesis, which is a culmination of two years' worth of hard work.

The constant stream of support that I have received in the last 2 years also extended to everyone who I have had the pleasure to work with and learn from. To Ryan Carter, without you, the OHRBID lab would not be as organised and well supplied, thank you for always being there, offering support and good company. A very big thank you to everyone at the OHRBID lab, for always offering advice during the fortnightly lab meetings and making me feel very welcomed in this work environment. Thank you to Manuel and Gwen at the bacteriology lab across the hall for providing me with the materials and advice I needed for my experiments. To all my collaborators turned friends in Calgary, thank you for always making sure that I am well supported, through work and other aspects of my stay. Thank you Dr Susan Kutz for allowing me this opportunity to discover the beautiful country that is Canada, and to work with the amazing team at the Calgary lab. Thank you, Caide, for your friendship and support, always offering me help whenever help was needed. To Angie, Fabien, Hailey, Will and Jessie, thank you for celebrating my birthday with me during my placement and showing me the north American way of life. You all made me feel warm even in the coldest months. I would like to acknowledge the CINUK programme grant for funding the ArcticEID project, which allowed me to work with the most wonderful people.

To all my friends who have kept me company and made sure that the two years during this Masters were filled with joy and support, who made sure I maintained a healthy balance of work and social life, I cannot thank you enough, for always making me laugh and making me feel supported. To Jen, my ever-supportive partner in crime, thank you for always being there no matter what. Last but

definitely not the least, a big thank you to my family, to say that I would be nowhere without you guys would be a massive understatement.

Author's Declaration

I, Yuk Ching Eugene Lau, declare that the research presented in this thesis is my own original work and has not been submitted elsewhere for the fulfilment of degree or diploma at any other university. The current word count does not exceed the 50,000-word limit (excluding table/figure legends, bibliography and appendices) set by the University of Glasgow. Original concept of this study was formulated by Dr. Taya Forde.

1 General Introduction

1.1 Setting the background

Bacteria and the diseases they cause are incredibly diverse (1). Bacteria constitute approximately 38% of human pathogens (2) and they have significant impact on public health due to the rising emergence of antimicrobial resistance (3). Pathogens such as *Mycobacterium tuberculosis*, *Klebsiella pneumoniae*, *Staphylococcus aureus* and extraintestinal pathogenic *Escherichia coli* were listed as priority endemic pathogens for vaccine research by WHO, with AMR being one of the main weighing criteria (4,5). Many of these pathogens are of One Health significance, meaning they can affect the health of people, animals and the ecosystem. Bacteria are also responsible for a range of important diseases of wildlife. Endemic diseases – those that maintain a relatively stable prevalence in a population and geographic region over time – can have major population-level impacts (6). Moreover, different factors can cause endemic diseases to increase in prevalence and re-emerge as more serious threats. The interaction between wildlife and domestic species is intricate due to frequent overlap of habitat, posing various risks of pathogen transmission (7).

The rate of emerging infectious disease is acknowledged to be increasing (8,9). Pathogens of wildlife populations that cause zoonoses and infect domestic animals account for a significant number of important diseases that are impacting human and veterinary health globally (2,10,11). An example of the crossover of bacterial disease between domestic animals and wildlife is *Mycobacterium bovis*, where the bacterium crossed into wildlife from infected cattle when the two populations shared a habitat and made contact with each other; the pathogen has since established itself in the free-ranging wild populations (12,13). An example of an emerging endemic pathogen is *Brucella suis* Biovar 4. It has long been an endemic disease in caribou in the Canadian Arctic, but recent investigations show that there is a shift in infection dynamics, with major increases in seroprevalence and diagnosed cases over the past decades (14). In addition to impacts on caribou populations, this could pose an increased risk for the local Inuit communities who rely on the wildlife as a key food (15,16). Bacterial infectious diseases have also been associated with major outbreaks in wildlife populations. An important example is the recent outbreak

of *Pasteurella multocida* which was implicated in a mass mortality event of saiga antelope in central Kazakhstan and highlights the severity of events and potential population-level impacts that can result from bacterial infection (17).

1.2 Setting the scene: a major infectious disease outbreak in muskoxen

The muskox is a keystone herbivore and an important species for subsistence and culture for the Inuit communities in the Canadian Arctic (18). In 2012, over 100 muskoxen were found dead on Banks Island, Northwest Territories (NWT), Canada, the cause of which was established to be the bacterium *Erysipelothrix rhusiopathiae* (19). Subsequent analyses determined that muskox mortalities on neighbouring Victoria Island, NWT and Nunavut, in 2010 and 2011 were also associated with this bacterium (19). This was the first time that *E. rhusiopathiae* was reported to cause large-scale mortalities in a wild ungulate population. Through later seroprevalence studies on the muskox populations in Alaska and the Canadian Arctic, the introduction of *E. rhusiopathiae* to the Canadian Arctic could be dated back to as early as 1991 (20). The population of muskoxen on Banks and Victoria islands suffered significant declines between 2001 and 2015 (21,22), a large part of which is likely attributable to these mortalities. Most recent reports conducted by the Government of the NWT indicates that these populations have not shown evidence of recovery (23,24). After a detailed genomic analysis of the isolates collected from the two islands, it was established that a single clonal strain of *E. rhusiopathiae* was responsible for the mass mortalities (25), discussed further in Section 1.3. Since the location of the mass mortality events is remote and not often visited by researchers, and with a sparce local human population across a vast area, understanding the epidemiology of *E. rhusiopathiae* in the Arctic is particularly challenging.

The Arctic Emerging Infectious Diseases (ArcticEID) project, funded through the Canada - Inuit Nunangat - UK Arctic research programme (CINUK) (26) aimed to address this knowledge gap. This project, to which my Masters research was connected, represented a collaboration between the people of Inuit Nunangat, the Kutz research group (27), who are based at the University of Calgary,

Canada, and our lab, One Health Research into Bacterial Infectious Diseases (OHRBID) (28), based at the University of Glasgow. The ArcticEID project combined scientific research with the knowledge of local communities and community-based wildlife surveillance. As part of the project, harvestors submitted a suite of samples for health and pathogen monitoring to collaborators at the University of Calgary. The results of these tests are related back to the communities who submitted the samples. Since this information may guide decisions about meat consumption, this underscores the need for a fast testing process, where the results can be relayed back to the communities in a timely manner.

Despite the progress that has been made in understanding *E. rhusiopathiae* epidemiology in the Arctic, several outstanding questions remain, including how the bacterium is maintained and spread within this landscape. It has been previously reported by Mavrot et al that *E. rhusiopathiae* has been detected in over thirty species of wild birds, fifty species of wild mammals and at least four species of fish globally (22). It is an opportunistic pathogen of domestic animals such as swine, turkey, sheep (29,30). In Arctic regions, it has been isolated from muskoxen, arctic foxes, caribou, moose, wolves, and bison (31). It was linked to a recent large scale mass mortality event of harbour porpoises in the Netherlands in 2021 (32) as well as increasingly-reported disease and mortalities in a range of marine mammals such as sea otters and beluga whales (33,34). Evidently the bacterium is a generalist and has a wide range of hosts (31,35), with many of them being asymptomatic carriers (36). It was proposed that climate change may be associated with the increasingly reported clinical cases across different marine wildlife hosts, with higher water temperatures contributing to an increased abundance of *E. rhusiopathiae*, or heat stress predisposing them to this opportunistic pathogen (34).

1.3 Erysipelothrix spp.

The genus *Erysipelothrix* contains a few main recognised species including *E. rhusiopathiae* (29,37,38), *E. tonsillarum* (39), *E. inopinata* (40), *E. larvae* (41) and *E. piscisicarius* (42). Emerging novel *Erysipelothrix* species are slowly being described as they are isolated from animal sources of individual cases or outbreaks (43,44). The genus was first isolated by Koch in 1878 when *E.*

rhusiopathiae was isolated from mice, at the time referred to as 'Bacillus of mouse septicaemia' (45). *E. rhusiopathiae* is a thin, pleomorphic, nonsporulating, Gram-positive rod. The bacteria can survive for long periods in the environment; it was previously reported for up to two weeks (46), however it may be as long as five years in animal carcasses under Arctic conditions (47).

E. rhusiopathiae can cause the disease known as erysipelas in swine and other animals. It can also be transferred zoonotically, and is known as erysipeloid in humans (48). In people, infections are most common among individuals who handle unprocessed meat and animal products, manifesting primarily as skin lesions (49). Erysipelas in swine is transmitted via oronasal secretions or through environmental contamination. The bacteria can be harboured in the tonsils and lymphoid tissues by apparently healthy individuals and shed through excretions and secretions of the host (50). There are three forms of swine erysipelas, namely acute septicaemia, sub-acute cutaneous infections, and chronic polyarthritis (51). The mortality rate can reach up to 40% in a naïve herd. Penicillin, cephalosporins and fluoroquinolones are used to treat infections with *E. rhusiopathiae* in both animals and people (52). Prevention in pig herds is accomplished via immunisation programs. Serotypes are strains that share antigenic properties (53,54). There are at least 28 different serotypes recognised for *E. rhusiopathiae*, with the majority of swine erysipelas caused by serotypes 1a, 1b or 2 (45). Vaccines based on serotypes 1 or 2 of *E. rhusiopathiae* are injected intramuscularly or supplemented into the drinking water for mass treatment (45,51).

Various studies have revealed several different virulence factors that are necessary for *E. rhusiopathiae* to cause disease. These include a combination of extracellular enzymes, surface protective antigens (*SpaA*) (38), *E. rhusiopathiae* surface proteins (55), adhesins (38), and phospholipidases (38). Extracellular enzymes produced by *E. rhusiopathiae* such as neuraminidase and hyaluronidase have been theorised to play essential roles in virulence. The former was described to be essential in the pathogenesis of arteritis and thrombocytopenia in rats (56,57), but there is conflicting evidence for hyaluronidase playing a crucial role in the pathogenesis of *E. rhusiopathiae* in murine models (58,59). While *E. rhusiopathiae* has mechanisms for cellular adhesion and can form a capsule proven to resist phagocytosis from certain leukocytes, it has also

mechanisms for cellular invasion and been shown to replicate within phagocytic cells (58,60). Its intracellular survival and replication within macrophages was also shown by Shimoji et al, where the *E. rhusiopathiae* Fujisawa-SmR reference strain (GenBank accession no. AP012027 (38)) was shown to be ingested by macrophages, survived and replicated within the phagocytic cells (58). The body of knowledge available on differential virulence among strains of *E. rhusiopathiae* is limited. It has been shown that the majority of virulence genes described in this species are core genes, i.e. they are harboured by most *E. rhusiopathiae* genomes (25). However, it has been proposed that non-synonymous mutations in virulence genes could lead to alternate protein structures and altered function of the membrane surface proteins (61).

Infection with *E. rhusiopathiae* can be diagnosed by culturing of biopsies or other tissue samples and/or using polymerase chain reaction (PCR). This bacterium can be grown using a generic bacterial medium such as blood agar or selective media for potentially contaminated samples (62). Colony morphology of the bacteria is usually small, circular, transparent and non-haemolytic on sheep blood agar (63). Colonies usually form after 24 h of incubation in 5% CO_2 (30,62). The bacteria are usually isolated from organs or tissues with gross lesions, although lesions may not be visible macroscopically, particularly in acute cases. Common postmortem samples include but are not specific to liver, spleen, bone marrow and kidneys. Bone marrow extraction is the most common method of isolation from wildlife mortalities due to its straightforward technique and its tendency to be preserved from autolysis and scavenging (31,62).

1.4 *E. rhusiopathiae* Arctic clone

Studies based on whole genome analysis of several *Erysipelothrix* isolates from various locations have classified *E. rhusiopathiae* into three distinct clades (1 to 3) and an intermediate clade between clades 2 and 3 (Figure 1-1) (64). Isolates from all three clades are found across multiple continents and host species (65). Through phylogenetic analysis of isolates collected from the Canadian Arctic, it was revealed that the outbreaks from 2010-2012, as well as more recent muskox mortalities in 2017 and 2021 were caused by a single strain of *E. rhusiopathiae* (61). A total of 139 muskox carcasses were sampled between 2021 to 2024;

through qPCR testing and culturing, 101 carcasses (72.6%) tested positive for Ac (66).This strain has been found exclusively in the Canadian Arctic and is therefore nicknamed the 'Arctic clone' (Ac). Using whole genome analysis, the Arctic clone falls within Clade 3 of the *E. rhusiopathiae* phylogenetic tree (25,61).

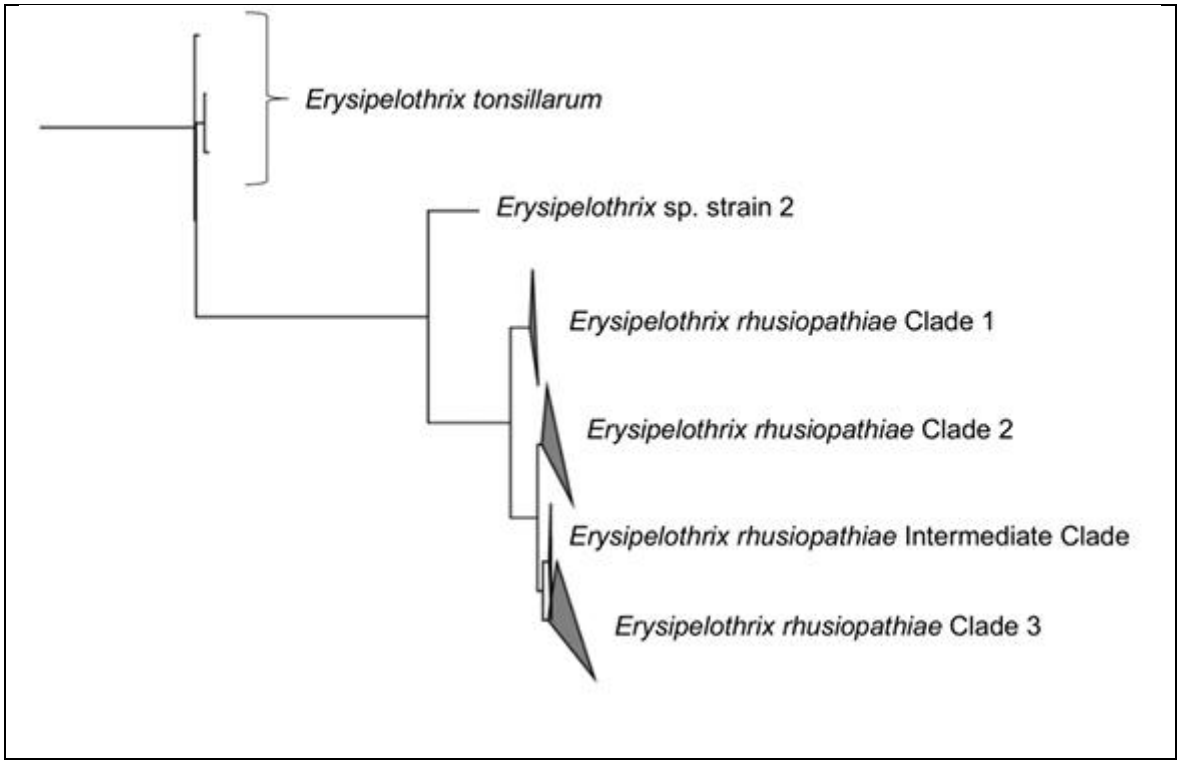

Figure 1-1 Phylogenetic tree which illustrates the three distinct clades of *Erysipelothrix rhusiopathiae* and the intermediate clade between clades 2 and 3. It also shows the relationship between *E. rhusiopathiae* and other closely-related *Erysipelothrix* species. This figure is adapted from Forde et al (2020) **(65)**.

The fact that this single clone has caused the first reported large-scale ungulate mortality event and has been found in widespread areas, reaching more than 1000 km apart across the Canadian Arctic Archipelago within just over 10 years, suggests that this strain of *E. rhusiopathiae* may possess additional genomic changes which make the clone more biologically 'fit' in comparison to the non-Arctic clone variants of *E. rhusiopathiae*, i.e. more virulent and/or host-adapted (47,61). No other single strain of *E. rhusiopathiae* has previously been connected with widespread mortalities in terrestrial wildlife.

The epidemiologic triad, described in the literature as early as 1974 (67), theorises that the ability of an infectious agent to cause disease is influenced by the combination of three factors: the agent, which in this case is *E.*

rhusiopathiae Ac; the host, which are the muskoxen; and the environment, which is the Canadian Arctic Archipelago (68). Using this framework, studies investigating these recent outbreaks should consider the three aspects of the disease to help understand the mechanisms behind the suspected high mortality and morbidity rates caused by the Ac, in hopes of designing appropriate management strategies.

One of the hypotheses behind the mass mortalities observed across the Canadian Arctic Archipelago is that muskoxen have an increased susceptibility to infectious diseases. A few factors could be associated with this, including their well-documented low genetic diversity (69,70) which could predispose them to environmental stressors (18). The environment itself could in turn have an impact on the susceptibility of the muskox population. The effects of climate change, such as the increase in global temperature and the frequency of heat waves (71) and the rise in humidity (72), could be associated with the dispersal and the persistence of bacteria in the environment.

Finally, factors associated with the bacterium itself could explain the high mortality and rapid dispersal within these muskox populations. For instance, *E. rhusiopathiae* Ac may contain virulence factors that affect the pathogenicity of the bacterium, therein making the strain more deadly. Bacterial pathogenicity can be defined as the capacity of a bacterial strain for causing disease in a host in a process which requires the bacteria to be virulent and bypass the immune defences of the host (73,74). Different virulence factors are coded by virulence genes, which can have a direct effect on the pathogenicity of the bacterium. These virulence genes can potentially be characterised using whole genome sequencing and comparing against other strains of *E. rhusiopathiae* (61). Alternatively, differential virulence can be tested through a range of different *in vivo* models.

Phylogenetic analyses of some of the key *E. rhusiopathiae* virulence genes, comparing amino acid sequences derived from Arctic clone (Ac) genomes to those from non-Arctic strains, found four virulence genes with distinct sequences (61). These four unique virulence gene variants found in Ac were adhesin (locus tag: ERH_1356)(38), rhusiopathiae surface protein A (*rspA*) (55), choline binding protein-B (*cpbB*) (75) and CDP-glycerol glycerophosphotransferse (*tagF*) (76)

(Figure 1-2). The genomic positions according to the Fujisawa reference strain (AP012027) (38) were at nucleotide positions 471,205 – 472,350 for *tagF*, 1,418,103 – 1,419,023 for adhesin, 813,020 – 814,840 for *cbpB* and 701,546 – 707,524 for *rspA*. These Ac-specific gene variants have been hypothesized as a mechanism that could explain why the Ac appears to be more virulent (61); however, no *in vitro* or *in vivo* testing has been undertaken to assess for differential virulence, or to assess this specific mechanism.

Two of the virulence factors with amino acid sequences unique to the Ac – adhesin and *cbpB* – have a role in adhesion. Adhesins allow bacteria to attach to host cells or tissues, with possible subsequent interactions such as biofilm formation and maintenance (77). They are highly diverse, and use specific mechanisms for different bacterial species (78,79). These adhesins help the invading bacteria to bind to the host cells by attaching to host receptor sites such as proteins, lipids, carbohydrates and their potential combinations (80). The process of adhesion provides various functional advantages: this includes acute colonisation, where the short binding allows for rapid utilisation of resources and reproduction at the binding site and prevents the shedding of the bacteria before the reproduction processes are finished (81). In the case of *E. rhusiopathiae*, protein *CbpB* has been shown to act both as adhesin and host plasminogen- and fibronectin-binding protein (75).

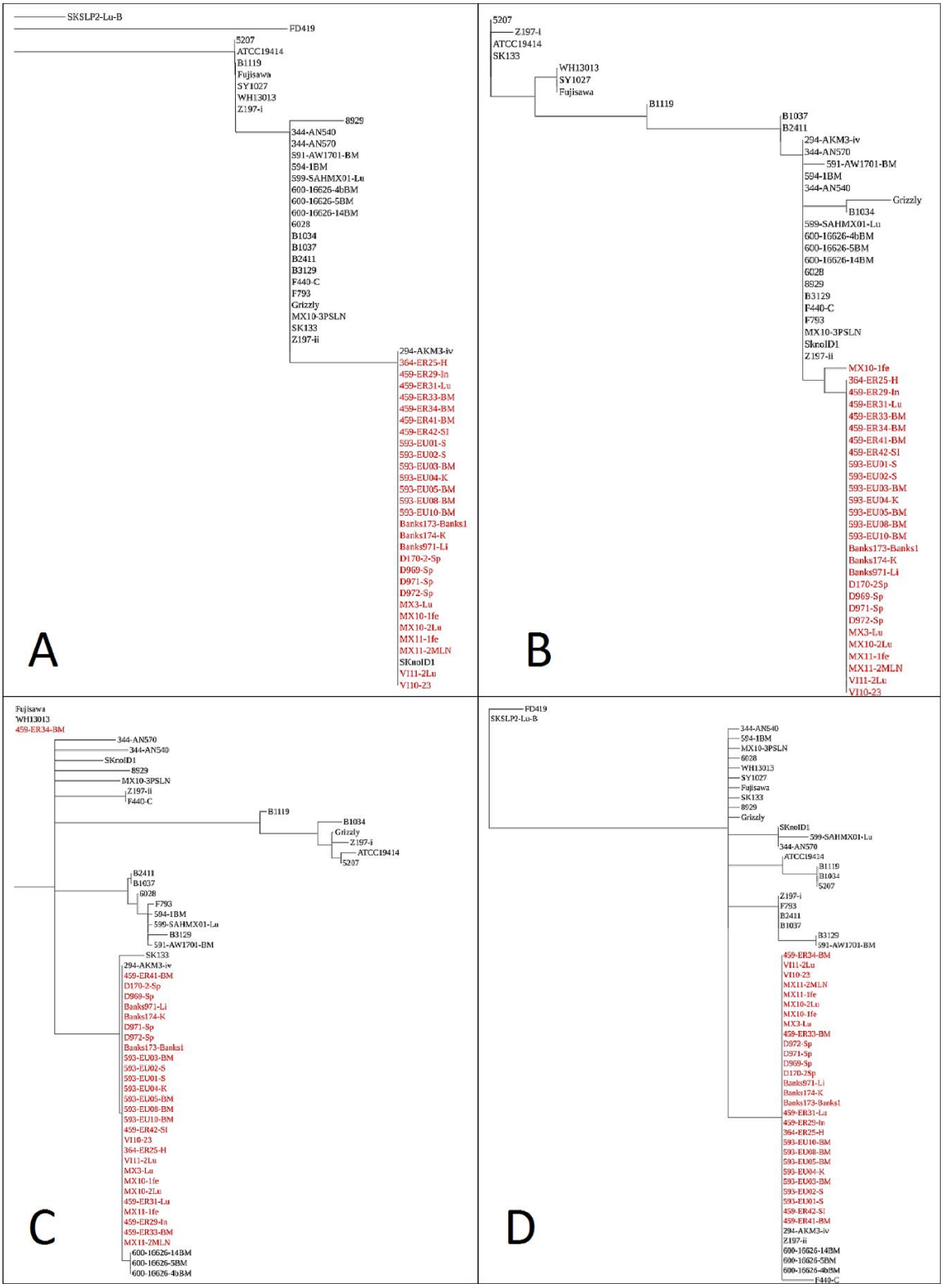

Figure 1-2 *Erysipelothrix rhusiopathiae* virulence genes with distinct amino acid sequences in Arctic clone (Ac) genomes compared to other genomes. Taken from Seru et al (2024) (61). Sequences belonging to the Ac are shown in red text. For these four genes, sequences deriving from Ac genomes largely clustered together and separately from those from other *E. rhusiopathiae* isolates. Panel A shows adhesin, panel B shows choline binding protein-B, panel C shows rhusiopathiae surface protein-A and panel D shows CDP-glycerol glycerophosphotransferase.

E. rhusiopathiae surface protein A, another key virulence factor with variants specific to the Ac, is involved in biofilm formation (61). Biofilm formation in *E. rhusiopathiae* is also supported by other virulence factors such as rhusiopathiae surface protein B (*rspB*) (82). While extensive studies into the role of biofilms in *E. rhusiopathiae* infections are absent, Shimoji et al suggests that the surface proteins can bind to biotic and abiotic surfaces to initiate in vivo colonisation (82). Biofilms are defined as "fixed microbial communities encased in extracellular polymeric substances"(83). They shield the organisms within them from pH changes, blood pressure, and osmotic current, concentrate nutrients, and help prevent detection of foreign microbes by the host's immune system. Bacteria in close proximity within biofilms communicate in the form of quorum sensing and horizontal gene transfer (84,85). A well-known example of a bacterium whose virulence is mediated by biofilm formation is *Pseudomonas aeruginosa*, which can develop a biofilm that cause serious infection in the lungs. This biofilm is surrounded by thick mucus which makes it hard for the bacteria to be eradicated (86).

CDP-glycerol glycerophosphotransferase (*tagF*) has been theorised to support the structural integrity and pathogenic potential of the bacterium by encoding a component in the cell wall (76,87). The precise mechanism includes the polymerisation of the main chain of teichoic acid which was the result of sequential transfer of the glycerol-phosphate units into linkage unit lipid in the CDP-glycerol (88,89).

The process of metal acquisition, specifically iron, is another important virulence mechanism, as metals are vital in fundamental life processes such as redox reactions, hydrolysis, DNA synthesis and cell signalling (90). There are three main classes of metal acquisition systems: elemental metal import, extracellular metal capture via siderophore and host protein metal extraction (91). Although *E. rhusiopathiae* doesn't produce siderophores, it encodes for metal ion transporters and surface receptors, but their role in *Erysipelothrix* virulence is not fully understood yet (92).

Exotoxin production is another common virulence factor. Toxins can be secreted to create pores and result in the leakage of host ions and ATP (93). An example is cholera toxin, which can lead to loss of body weight (94). Toxins can also

affect cell signalling, such as oedema toxin bypassing the G protein complex in the host immune system in *Bacillus anthracis* infections (95,96). While no toxins have been described for *E. rhusiopathiae* (58), Seru et al found that a putative toxin gene, annotated as the 'toxin B' gene, was over-represented among Ac genomes in a genome-wide association study of *E. rhusiopathiae* genomes (61). This toxin can be found in cases caused by *Clostridium difficile* and causes cytotoxicity within the host cell (97,98). Further work has not been done to determine whether this putative toxin gene truly encodes an exotoxin that might be associated with *E. rhusiopathiae* virulence.

1.5 Knowledge gaps and thesis outline

To aid in the investigation into the outbreak of Ac in the Canadian Arctic Archipelago, i.e. to tease apart the different components of the epidemiological triad, the virulence of the Ac must be studied further. The use of *in vivo* models could shed light into differences of pathogenicity between the Ac and the non-Arctic clone (Nac) strains of *E. rhusiopathiae*. One promising *in vivo* model is that of *Galleria mellonella* (Greater Wax moth) larvae. While this model has been used for the study of other species of bacteria (99–102), it has – to our knowledge – never been tested with *E. rhusiopathiae*. Investigating the effects of *E. rhusiopathiae* on *G. mellonella* larvae and demonstrating it to be an effective model for virulence in this bacterial species could allow evidence to be generated to explore differences in pathogenicity between Ac and Nac. In Chapter 2 of this thesis, I conduct experiments to assess *G. mellonella* as a model system to study *E. rhusiopathiae* virulence.

While molecular methods are commonly used for confirmation of the *E. rhusiopathiae* species (103), there are not yet molecular assays published for the detection of key strains, such as the Ac; its identification currently relies on WGS and genomic comparisons. A Masters student at the University of Glasgow recently developed a single-plex qPCR assay which specifically targets the Ac (104), although with minimal validation conducted. This single-plex assay could be combined with other assays for distinguishing *Erysipelothrix* spp. (103) to develop a multiplex assay which could simultaneously identify species and strain-type of *Erysipelothrix* spp. in outbreak investigations or wider research studies, particularly in the Arctic, thereby reducing the cost and amount of

laboratory and bioinformatics labour required. In Chapter 3 of this thesis, I develop and evaluate a multiplex qPCR assay to contribute towards rapid and cost-effective *Erysipelothrix* diagnostics.

2 *Galleria mellonella* infection model

2.1 Introduction

To understand the role of bacterial virulence factors and microbial pathogenicity, various *in vivo* models have been studied. Mice and pigs have been commonly used in *E. rhusiopathiae* vaccine efficacy studies, where success is measured by protection against lethal challenge with the bacteria, administered subcutaneously or intramuscularly (105,106). While murine models have been hugely informative for the study of microbial infections, including virulence studies, they have been at the centre of social and ethical concerns (107–109). Additionally, the cost for the maintenance of sufficient animals to obtain statistically relevant data is high. In recent years, alternative host models have been used instead of the traditional murine models as part of the '3Rs alternatives' which are replacement, reduction and refinement (110). This principle aims to minimise the potential for animal pain and distress in biomedical research (111). As an alternative to rodent models, simple invertebrate hosts such as *Caenorhabditis elegans* and *Drosophila melanogaster* are used for the genetic analysis of the host and the bacteria to identify the virulence factors and host immune mechanisms (112). Another commonly used invertebrate model for early-stage virulence studies is the *Galleria mellonella* larvae model (100).

Galleria mellonella, or the Greater Wax moth, is a holometabolous insect that has a varying lifecycle of weeks to months. It has four distinct life stages: egg, larva, pupa and adult. It is one of the most important pests of honeybee products as it feeds on pollen, honey and wax (113). *G. mellonella* lacks an adaptive immune system but its innate system shares many similarities with mammals, specifically with its cellular response where haemocytes -which are similar to mammal neutrophils - are the key actors responsible for cellular events (101). These haemocytes are found in the haemolymph of the larvae (where the bacterial inoculum is injected during infection trials) or attached to the internal organs such as the digestive tract or the heart surface (101). The limitation to an innate immune response allows for the study of host-pathogen interactions without the interference of the adaptive immune system (114). The

larvae can also be kept in 37 °C which is the equivalent of the body temperature of mammals, where it has an effect on microbial virulence factors (115).

Various studies have utilised the survival of *G. mellonella* larvae to study the virulence, host immune responses and effects of different chemical compounds, providing a simple, cost-effective and ethically more acceptable option compared with rodent models. The melanisation of larvae caused by infection is linked to the prophenoloxidase-activating system of humoral immunity (116). This increase in melanin results in the darkening of the larva and has been used to observe presence of infection (102).

The *G. mellonella* model has been used to study a wide range of microorganisms and has proven to provide a good representation of virulence, including for Gram-positive bacteria (e.g. *Streptococcus pyogenes* (117), *Streptococcus pneumoniae* (118), *Enterococcus faecalis* (119); Gram negative bacteria (e.g. *Escherichia coli* (100)); and fungi (e.g. *Cryptococcus neoformans* (120)). Many studies have successfully shown dose dependent killing or differences in survivability when exposed to different strains of the same bacteria (121,122). *E. rhusiopathiae* has not yet been tested with the *Galleria* model or any other invertebrate. If shown to work as a model for this species, it could provide insights into the virulence of the Ac compared to other strains of *E. rhusiopathiae* and other microorganisms to establish if the virulence of the Ac is the key contributor to the mass mortality events observed in Arctic muskoxen. The fact that the same clone of *E. rhusiopathiae* has spread across such a wide area within such a short time span, combined with the high mortality rate observed in muskoxen, suggests that the Ac may be particularly virulent. To test this hypothesis, *in vivo* assays to assess the virulence of this clone, such as with the invertebrate infection model *Galleria mellonella* larvae, would be of high interest.

The aim of this chapter was to evaluate the *Galleria mellonella* larvae model as a potential tool for assessing the virulence of *E. rhusiopathiae* strains.

2.2 Materials and methods

2.2.1 *G. mellonella* larvae source, maintenance and preparation

Ethical approval for this work was received from the University of Glasgow School of Biodiversity, One Health & Veterinary Medicine Research Ethics Committee (ref EA04/24). *G. mellonella* larvae were sourced from a producer of live insects for pet food (Livefoods UK Ltd, Somerset, UK) using 'research grade' larvae (123). Each batch of larvae was prepared and transported on a Tuesday then delivered to the lab via Royal mail on a Wednesday afternoon or Thursday morning. Physiological state of the larvae, dependent on the larval age, transport conditions and the length in transit, was inspected upon arrival. For each batch of experiments, roughly 250 larvae (~75 g) were delivered in varying states of wellness. The transport box was unsealed to allow for adequate airflow, and the box of larvae was kept in the coldest and darkest part of the lab, to prolong the larval stage before pupation.

The larvae were stored for one day upon arrival, which allowed them to acclimatise to room temperature (typically 17°C - 21°C). An hour before injection of the inoculum, freshly disinfected containers (cleaned with standard laboratory procedures: wipe with 1% bleach, followed by water and then 70% ethanol rinse) were prepared and the larvae were taken out of their storage container and organised using sterile forceps. Larvae that were most reactive to external stimuli (light and touch, i.e. those deemed to be the healthiest) were selected for the experiment and were placed in a separate container. Dead and unhealthy larvae, i.e. with signs of melanisation and less reactive to external stimuli, were discarded. The selected larvae were disinfected by spraying with 50% ethanol, placed in a clean box and left to be air-dried before injection.

2.2.2 Bacterial cultures and growth quantification

Two strains of *E. rhusiopathiae* – a strain of Arctic clone (Ac) (Isolate number: 358-DMX014.2-He, isolated from a muskox carcass on Victoria Island in July, 2015) (124) and a strain of non-Arctic clone (Nac) (Isolate number: 620-A1627895, isolated from a humpback whale from Alaska in 2015) (34) – were used in this study. Both isolates were kept for long term storage in 20% glycerol at -80°C. They were resuscitated by culture on 5% Columbia sheep blood agar

(E&O Laboratories Ltd, Bonnybridge, Scotland) incubated aerobically at 37°C for 24 hours (h). Isolated colonies were used for further subcultures and growth rate measurement. In a BSL-level 2 compliant biosafety cabinet (BSC), a sterile cotton swab was dipped into the glycerol stock and transferred onto a 5% Columbia sheep blood agar (SBA) plate. The quadrant streaking technique (125) was used to dilute the bacteria to isolate a single colony. Inoculated plates were incubated at 37°C for 24 h, after which a single colony from the fourth quadrant of the plate was picked up using a sterile inoculating loop and spread evenly across a new SBA plate to ensure that the culture was pure. The sub-cultured plates were placed in the incubator for 24 h. Bacterial growth was established by culturing the strains in brain heart infusion broth (BHI, Sigma-Aldrich, Dorset, UK) supplemented with 5% foetal bovine serum (GIBCO, Paisley, UK). Foetal bovine serum (FBS) was syringe filtered using a 50 mL sterile plastic Luer-Lok syringe (BD, New Jersey, USA) and a PES sterile 0.22 µm filter (Starlab, Hamburg, Germany). A volume of 9.5 mL of the sterilised BHI solution was aliquoted into 15 mL Falcon tubes (Thermo Fisher Scientific, Waltham, MA, USA) in the BSC and supplemented with 0.5 mL of FBS freshly before the experiment. Due to serum stability, the supplemented broth was used within a week. The growth medium was made the day before the experiment and stored in the fridge overnight. Overnight cultures were prepared by inoculating a loopful of each strain from SBA into 10 mL of freshly prepared 5% FBS-BHI medium. A separate tube with broth only was used as negative control. Cultures were incubated aerobically at 37°C for 16-20 h. After the overnight incubation period, 100 µL of the overnight culture was sub-cultured into a sealed culture tube of 4.9 mL 5% FBS-BHI and incubated until early- mid exponential growth (for 6 h). Swabs from each broth negative control were taken and plated on SBA to check for possible issues of contamination (i.e. presence of bacterial growth). After the 6 h incubation, the centrifuge tube was vortexed to ensure the culture was homogenous. An aliquot of 100 µL of each culture was transferred to fresh tubes of 9.9 mL 5% FBS-BHI broth (BHIB). To quantify bacterial growth, the culture tubes were vortexed and 500 µL aliquots were withdrawn for colony forming unit (CFU) counts and optical density (OD) measurements in 1 h intervals. Of the 500 µL, two aliquots of 200 µL were used for OD measurement at 600 nm (OD_{600}); the remaining 100 µL was used for the counting of the CFU. OD_{600} was measured in 96-well flat bottom plates (Corning Incorporated, Corning, USA) using a

Multiskan FC plate reader (Thermo Fisher Scientific, Waltham, MA, USA). Viable bacterial concentrations were established as CFU/mL using the Miles and Misra technique (126). A ten-fold dilution series of the culture was conducted to dilute the bacterial culture to enable the growth and observation of individual colonies. An aliquot of 100 µL of the bacterial culture was added to 900 µL of pre-aliquoted sterile phosphate buffered saline (PBS) in 1.5 mL Eppendorf tubes and vortexed to produce a one in ten dilution and the process was repeated according to Table 2-1.

Table 2-1 *Erysipelothrix rhusiopathiae* decimal dilutions used to estimate bacterial concentration over 9 h of culture. Each row details the maximum dilution level from the original stock plates on the 5% Colombia sheep blood agar. Each number in the dilution column represents the dilution factor, where -2 means that it has a dilution factor of 1:100, or 1 x 10^{-2}.

Time point post inoculation	Dilutions to plate on SBA
0h	-2, -3, -4
1h	-2, -3, -4
2h	-2, -3, -4
3h	-3, -4, -5
4h	-4, -5, -6
5h	-5, -6, -7
6h	-5, -6, -7, -8
7h	-5, -6, -7, -8
8h	-5, -6, -7, -8

Three to four sections were divided on each SBA and labelled according to the dilution factor. The diluted suspensions were vortexed. Three 20 µL droplets from the pre-determined dilutions were pipetted onto each agar section and left to soak into the agar in the BSC until the solution suspension could no longer be seen. The plates were then incubated for 18-24 h at 37°C. Following incubation, colonies per droplet were counted and recorded. An average was taken between the three droplets of the same dilution factor. If the number of colonies was too high (i.e., where it was no longer feasible to count individual colonies), a picture of the plate was taken and uploaded to the computer and opened with the photo application. The paint function was used to track which colonies were counted until all the colonies were covered by the paint. An example of this can be seen in Figure 2-1.

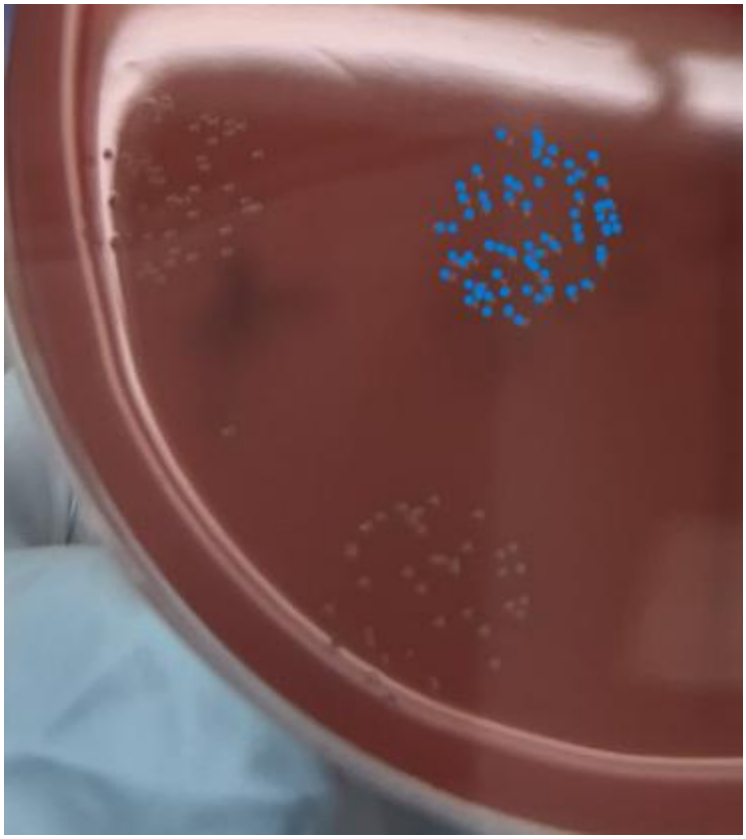

Figure 2-1 An example of colony forming units on agar inoculated with decimally diluted suspensions of *Erysipelothrix rhusiopathiae* culture. Three drops of a serial dilution plated on 5% Columbia sheep blood agar. Each drop consists of 20 µL of a 6 h culture. Blue dots were used to keep track of the colonies that were counted during the colony count using a photo application.

The following equation was used to estimate the concentration (c) of the culture at a given timepoint in CFU/ml:

c(CFU/ml) = average number of colonies per dilution × 50 × dilution factor

A repeat of the same procedure was conducted to produce the growth curve of two replicates of the Nac.

2.2.3 *G. mellonella* larvae injections

Both Ac and Nac strains were grown as described above. Nine different groups of larvae were included in each experiment. Three controls were used: i) a 'No touch' (NT) control where the larvae were only sterilised and manipulated with forceps, nothing was injected; ii) a 'PBS' control to ensure that the injection technique used, and the PBS solution used in the serial dilution, did not affect the larvae vitality, and iii) a 'BHIB' control, to ensure that the culture medium also did not have an effect on the larvae. Both Ac and Nac strains in exponential growth phase were injected into the larvae. The strain with the higher OD_{600} was

diluted with BHIB to match the OD_{600} of the slower strain to ensure that a similar concentration of bacteria was injected for both strains. The larvae were inoculated with 10 µL of three different concentrations of either strain (undiluted or 'neat'; 1:10; 1:100). These made up the remaining six experimental groups.

Sterile Petri dishes were used as containers for the inoculated larvae. A sheet of Whatman 90 mm diameter filter paper (1001-090, Grade 1, CYTIVA, Marlborough, US), was used to line the bottom of each plate. The NT controls were placed in these first, since they did not require any injection, followed by the other two controls following injection.

Injections were performed on the larvae, prepared as described above (larvae preparation). Syringes (1750 RN 500 µL, Hamilton, Timis, Romania) and needles (26S gauge, 50.8 mm length, point style 4 (30°), Hamilton) were sterilised with a 4-step cleaning process: 1% bleach, sterile water wash 1, 70% ethanol, sterile water wash 2. The syringe was filled and soaked in the bleach solution for three minutes, then it was flushed with sterile water, soaked in the ethanol for another three minutes before being flushed again with sterile water. The syringe was sterilised with the 4-step cleaning process between each inoculum.

Before injection, bacterial cultures were brought to homogenous suspension by vortexing. A total of 200 µL of the inoculum was taken up the syringe. Each larva was double checked for signs of melanisation before injection. The larvae were flipped upside down and immobilised with sterile forceps. The needle was carefully injected to the front right proleg of the larvae, making sure the proleg was well-positioned while the needle went in. An aliquot of 10 µl of a suspension was injected into each larva. After the inoculum was injected into the larva, the needle was removed carefully, and the larva was placed in its corresponding Petri dish. This step was repeated until all 15 larvae were injected with each treatment. This was done in following order: the two inoculation controls, then the bacterial inoculum of the lowest concentration (2.08×10^4 CFU/larva), i.e., highest dilution of Ac (100-fold) was injected, followed by the 10-fold and the undiluted. The syringe was thoroughly cleaned again for the injection of Nac.

2.2.4 Evaluation of injection results

Larvae were incubated at 37°C, aerobically and in the dark and observed for physiological changes and survival vs. mortality once a day until larvae showed signs of pupation (up to a maximum of 10 days). Larvae were considered dead when there was a combination of melanisation and/or lack of reaction to external stimuli. At each observation, the number of dead larvae were scored, and the state of the surviving larvae was recorded according to Table 2-2. For 'Dead' and 'Alive' and 'Movement', the number of larvae corresponding to each condition was recorded. For melanisation, the number of larvae corresponding to each condition state as described in Figure 2-2 was recorded.

Table 2-2 Scoresheet used for measuring the physiological state and survival of *Galleria mellonella* larvae post-injection. Each batch was injected with either *Erysipelothrix rhusiopathiae* Arctic clone (Ac) or non-Arctic clone (Nac) strains at different concentrations, as well as control conditions of 'No touch', phosphate buffered saline (PBS) and 5% brain heart infusion broth (BHIB) supplemented with foetal bovine serum. The number of larvae corresponding to each of the different conditions (columns) were noted daily for up to 10 days. For movement, + and – signs were used to indicate how many surviving larvae were responding to touch (e.g., 11+,2-). Melanisation was scored according to the scale in Figure 2-2.

Date/Time	Day 1			
Parameters	Dead	Alive	Movement	Melanisation
No touch				
PBS				
BHIB				
Ac (Undiluted)				
Ac (10-fold dilution)				
Ac (100-fold dilution)				
Nac (Undiluted)				
Nac (10-fold dilution)				
Nac (100-fold dilution)				

M0/- (No melanisation) | M1/+ (On the end) | M2/++ (Midline) | M3/+++ (Half melanised) | M4/++++ (Entire body)

Figure 2-2 *Galleria mellonella* scoring scale for melanisation. The states of the larvae range from least severe on the left (M0) to the most severe (M4) on the right.

The observation period ended when the number of surviving larvae in the control batches fell below 10 or when all the larvae incubated started pupating (Figure 2-3). To euthanise the surviving larvae, all plates containing larvae were placed at -20°C for at least an hour before being disposed of in the biological waste bin and sterilised in an autoclave.

Figure 2-3 *Galleria mellonella* larvae in different developmental states of pupation. The larva on top is pupating, and the bottom one is not pupating.

2.2.5 Statistical analyses

Using the 'Survival' package installed in R studios, using R version 4.4.2 (127), a Cox proportional hazards model was run to compare the survival probability among the different test conditions in the experimental batches. The reference category was set as the NT control and the exp(coef) was used to determine if particular test groups were statistically more likely to die or to survive. Analysis of variance (ANOVA) tests combined with a post-hoc Dunnett's test were performed to determine if there were differences between the mean larvae in the controls and in the different test groups. The NT control group was set as a reference, and the other test groups were analysed to identify any trends in i) pupation and ii) melanisation. Dunnett's correction for multiple tests was used to adjust the p-value to account for the 8 test groups when comparing against the reference. A p-value of <0.05 means that that the null hypothesis was rejected. The null hypothesis was that the survival distributions were identical across all test groups.

2.3 Results

2.3.1 Growth curve

The growth of bacteria was measured using optical density (OD_{600}) of the culture and measured at hourly intervals (Table 2-3). Growth curves were plotted as OD_{600} values of two biological replicates against their respective incubation times (Figure 2-4). The lag phase of the two isolates continued past the three-hour mark, with the inflection point being approximately halfway between the 3 and 4-h marks. The exponential phase started four h post inoculation and continued until hour 7, where the plateau phase occurred. Although small differences were observed around the 5-hour mark, both replicates had largely similar growth kinetics. The replicates reached final concentrations of $1.62 \times 10^{11} \pm 0.23 \times 10^{11}$ CFU/mL and $1.73 \times 10^{11} \pm 0.29 \times 10^{11}$ CFU/ml, respectively.

Table 2-3 Optical density (OD_{600}) for two replicates of *Erysipelothrix rhusiopathiae* non-Arctic clone. Measurements were taken in duplicates. The absolute OD values (as plotted in Figure 2-4) were calculated by subtracting the mean of the repeated OD_{600} readings of the blanks (OD blank1 and OD blank2) from the culture (OD culture 1 and OD culture 2).

Nac 1				
Culture (h)	OD blank1	OD blank2	OD culture1	OD culture2
0	0.348	0.355	0.343	0.357
1	0.343	0.364	0.353	0.358
2	0.346	0.348	0.353	0.356
3	0.340	0.352	0.378	0.376
4	0.348	0.357	0.407	0.407
5	0.344	0.356	0.489	0.492
6	0.342	0.351	0.570	0.571
7	0.341	0.359	0.615	0.621
8	0.340	0.357	0.603	0.629
9	0.335	0.353	0.598	0.639
Nac 2				
Culture (h)	OD blank1	OD blank2	OD culture1	OD culture2
0	0.329	0.351	0.347	0.356
1	0.337	0.358	0.335	0.356
2	0.343	0.345	0.353	0.365
3	0.340	0.370	0.369	0.388
4	0.348	0.362	0.399	0.413
5	0.339	0.353	0.422	0.454
6	0.335	0.361	0.543	0.553
7	0.346	0.352	0.592	0.617

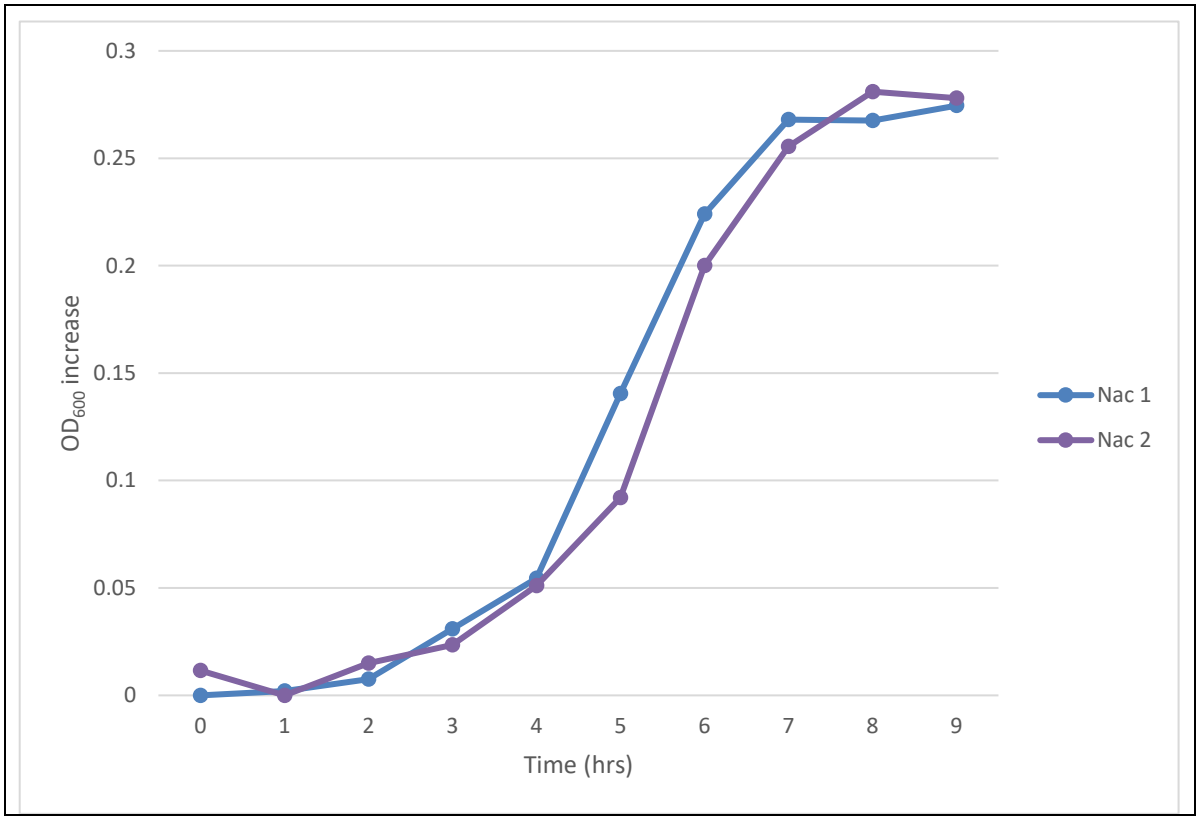

Figure 2-4 Growth curve of two replicates of *Erysipelothrix rhusiopathiae* non-Arctic clone (Nac). Optical density (OD_{600}) values are shown hourly over 9 h for the two technical replicates of the same Nac strain 620-A1627895 (Nac 1 and Nac 2). OD_{600} of the blank was subtracted from the OD_{600} measurement of the bacterial culture to provide the final OD_{600} values of the replicates.

2.3.2 *Erysipelothrix rhusiopathiae* injection of *Galleria mellonella* larvae

2.3.2.1 Establishing bacterial concentrations

The mean CFU/mL of *E. rhusiopathiae* in the injected dose was estimated to be $2.08 \times 10^8 \pm 0.81 \times 10^8$ CFU/ml. This was obtained from the mean CFU/mL from all six bacterial isolates used in batches 1 to 3 described below (triplicates of Ac and Nac). Values for each isolate/batch are provided in Table 2-4. Each larva was injected with 10 µL of the culture, which means that the undiluted experimental group of larvae was injected with roughly 2.08×10^6 CFU of bacteria, with the 10-fold dilutions injected containing roughly 2.08×10^5 CFU and 100-fold dilutions injected containing roughly 2.08×10^4 CFU.

Table 2-4 Final concentration of each *Erysipelothrix rhusiopathiae* isolate used for *Galleria mellonella* injection.

E. rhusiopathiae Isolate	concentration (CFU/ml) ($\times 10^8$)
Ac 1	1.33
Nac 1	2.45
Ac 2	1.23
Nac 2	1.64
Ac 3	2.24
Nac 3	3.60
Mean CFU/mL	2.08

2.3.2.2 Larval survival and pupation

The larvae arrived in a very good state; the majority were deemed to be healthy for the inoculations. The weight distribution of the larvae ranged from 3.57 g to 3.96 g per larval group, which works out to be 0.25 g per larva. Pupation started on day 3 for both controls and the inoculated groups. The observations of the inoculated larvae lasted 9 days before the pupating larvae could finish their pupating stage and become wax moths. The frequency of pupating larvae increased as the observation period went on. There were more pupating larvae in the control groups (Table 2-5; Supplementary Table 1). All pupating larvae were kept in the same Petri dishes as their experimental group and were counted as alive by the end of the 9 days. All pupating larvae were still alive by the end of the experiment and all larvae that were recorded as dead died as larvae.

Table 2-5 Survivability of *Galleria mellonella* larvae when injected with different concentrations of *Erysipelothrix rhusiopathiae* Arctic clone (Ac) and non-Arctic clone (Nac). Three control groups were included: No touch (NT), phosphate buffered saline (PBS) and brain heart infusion broth (BHI). Each experimental group contained 15 larvae. A simplified table only containing results of batch numbers 1-3 on days 1 and 9 is shown here. Full results are provided in Supplementary Table 1. The number of larvae showing different levels of melanisation (from most to least severe: M2, M1, and M-) at each time point are shown. The % total calculated at the bottom of the table was calculated by dividing the total of the column by the total number of starting larvae (135). Al = number of larvae alive; Pu = number of larvae that have pupated.

Day	1					9					
State	M2	M1	M-	Al	Pu	M2	M1	M-	Al	Pu	Dead
Groups											
NT1	0	2	13	15	0	0	1	2	14	11	1
PBS1	0	0	15	15	0	0	1	0	15	14	0
BHI1	0	1	14	15	0	0	0	3	13	10	2
Ac1(Undil)	3	2	10	15	0	3	3	7	13	0	2
Ac1(10-fold)	0	3	12	15	0	1	4	0	10	5	5
Ac1(100-fold)	0	0	15	15	0	0	0	1	15	14	0
Nac1(Undil)	1	4	9	14	0	0	2	0	12	10	3
Nac1(10-fold)	0	1	14	15	0	0	2	1	13	10	2
Nac1(100-fold)	0	2	13	15	0	0	1	1	15	13	0
NT2	0	0	15	15	0	0	2	0	14	12	1
PBS2	0	0	15	15	0	0	1	2	15	12	0
BHI2	0	0	15	15	0	1	2	0	6	3	9
Ac2(Undil)	1	1	11	13	0	0	3	0	8	5	7
Ac2(10-fold)	0	2	13	15	0	0	2	1	13	10	2
Ac2(100-fold)	0	0	15	15	0	1	2	2	13	8	2
Nac2(Undil)	0	2	13	15	0	0	2	0	12	10	3
Nac2(10-fold)	0	0	15	15	0	0	1	0	14	13	1
Nac2(100-fold)	0	0	15	15	0	0	0	3	12	9	3
NT3	0	0	15	15	0	0	1	0	14	13	1
PBS3	0	0	15	15	0	1	6	0	13	12	2
BHI3	0	0	15	15	0	0	1	0	15	14	0
Ac3(Undil)	9	2	3	14	0	6	1	0	11	4	4
Ac3(10-fold)	0	1	14	15	0	1	3	0	15	11	0
Ac3(100-fold)	0	0	15	15	0	0	1	0	14	13	1
Nac3(Undil)	0	5	9	14	0	3	1	0	10	6	5
Nac3(10-fold)	0	0	15	15	0	1	1	0	11	9	4
Nac3(100-fold)	0	0	15	15	0	0	0	0	15	15	0
total	14	28	358	400	0	18	44	23	345	266	60
% total	3.5	6.9	88.4	98.8	0.0	4.4	10.9	5.7	85.2	65.7	14.8

By day 9 of batches 1-3, 119 of the 135 (88%) control larvae were still alive, with 101 (85% of those alive) at varying stages of pupation. This was similar to the larvae injected with bacteria: by day 9, 226 of the 270 (84%) inoculated larvae were still alive, with 165 of those (73%) pupating by the end of the experiment. In batches 1 and 3 (shown below to be the two valid experimental batches), 74 out of the 84 (88%) larvae alive in the control group were pupating on day 9, while 110 of the 154 (71%) alive in the test groups were pupating. Table 2-5 also shows that pupation was more frequently observed in populations that were exposed to lower concentrations of bacteria. For the undiluted inoculations, 66 of the 90 (73%) larvae injected were alive by the end of the experiment, with 31 (47%) pupating. In contrast 160 of 180 (89%) in the combined 1:10 and 1:100 dilutions for both Ac and Nac were still alive at the end of the experiment, with 130 of the 160 larvae (81%) in the pupating stage.

The ANOVA test combined with a post-hoc Dunnett's test was used to test for differences in the number of pupating larvae on day 9 in each test group in batches 1 and 3 compared to the NT control (Table 2-6). There were only two groups (Ac and Nac 100-fold dilution) which had more pupating larvae, with the mean difference being 1.5 larva and 2 larvae. All the other groups were less likely to pupate, with mean difference ranging from 1 (PBS) to -10 (Ac undiluted). Only one group was statistically significant compared to the control: Ac undiluted.

Table 2-6 Analysis of variance (ANOVA) results of the pupation numbers in batches 1 to 3 of *Galleria mellonella* injections with *Erysipelothrix rhusiopathiae*. Diff shows the mean difference compared to the 'no touch' control and a p-value of less than 0.05 (Pr(>|z|)) shows that the reference (no touch) was statistically different compared to the test group (shown by asterisk *). 'PBS' = phosphate buffered saline controls; 'BHI' = brain heart infusion broth controls; 'Ac' = Arctic clone of *E. rhusiopathiae*; 'Nac' = non-Arctic clone.

Test group	Diff	P value
PBS	1.0	0.999
BHI	0.0	1.000
Ac Undiluted	-10.0	0.011*
Ac 10-fold	-4.0	0.452
Ac 100-fold	1.5	0.984
Nac Undiluted	-4.0	0.452
Nac 10-fold	-2.5	0.835
Nac 100-fold	2.0	0.932

A series of Kaplan-Meier curves were generated in R studio to compare the survival probability among the different test conditions in batches 1-3. Figure 2-5 compares the combined results of the three batches of undiluted Ac vs. Nac inoculations, along with the three control groups. Both the NT and the PBS control groups had the least number of mortalities overall, with survival probability to the end of the experiment above 88%. Ac undiluted had the lowest survival probability (~70%), followed by Nac undiluted and the BHI control group (~75%). All curves show a gradual decrease over the course of the experiment. The p-value generated using the Log-rank test was 0.0035, which was lower than 0.05 meaning that that the null hypothesis was rejected. In this instance, the null hypothesis was that the survival distributions were identical across groups.

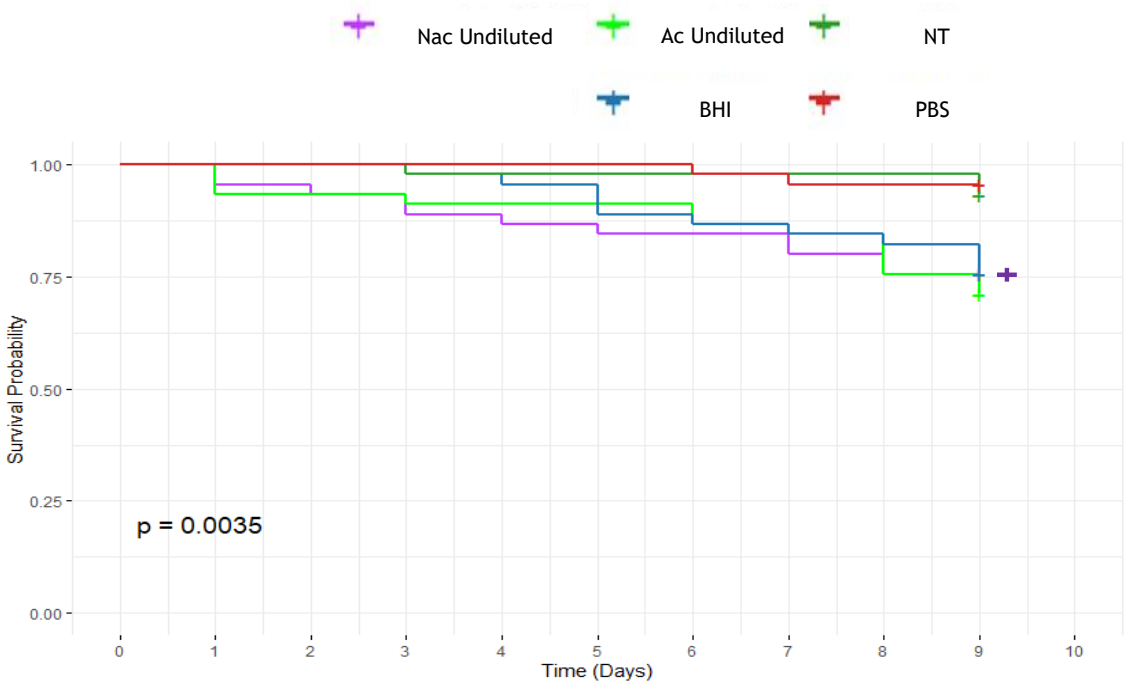

Figure 2-5 Kaplan-Meier survival curves of the three batches of *Galleria mellonella* inoculations of undiluted strains of *Erysipelothrix rhusiopathiae* Arctic clone (Ac) and non-Arctic clone (Nac). Results from the three batches of the experiment are combined. 'NT' represents the no touch controls, 'BHI' represents the brain heart infusion broth controls, and the 'PBS' represents the phosphate buffered saline controls. The p-value refers to the Log-rank test conducted along with the 'Survival' package in R studios. A value of less than 0.05 means that the 5 test groups have distribution curves that are statistically different from each-other.

Further, a Cox proportional hazards model was performed to estimate the risk of one or more variables (such as the strain type) on the hazard rate (death or survival). Results from the Cox proportional hazards model are shown in Table 2-7 (Column 1, Cox 1), with NT controls taken as the reference category. Values >1 suggest members of the group were more likely to die, vs. <1 were more

likely to survive. A coefficient of 1 shows that the experimental group has the same chances of death as the reference, 2 means it has double the chances of death, etc. 'Ac Undiluted' had the highest chances of dying, being 4.99 times more likely to die compared to the NT group, followed by 'Nac Undiluted' at 4.30 and 'BHI control' at 4.07. Both 'Ac 10-fold' and 'Nac 10-fold' were at similar levels, around 2.42 and 2.46, followed by the 100-fold dilutions of Ac and Nac, at 0.99 and 1.02. The only group that was less likely to die compared to the NT group was the 'PBS control' group. The values in the column Pr(>|z|) show the p value compared to the reference group 'NT'. Any value in that column <0.05 means that the experimental group was statistically different from the reference. There were only three groups that were statistically different from the reference: 'Ac Undiluted', 'Nac undiluted', and 'BHI control'.

Table 2-7 Cox proportional hazards models of the survivability of *Galleria mellonella* at the end of the observation period. The mean of each experiment group was taken to calculate the exp(coef), which shows the rate of hazard compared to the reference 'no touch' control. In Cox 3, data from the two Ac dilutions (10- and 100-fold) were combined. A p-value of less than 0.05 shows that the reference was statistically different compared to the test group (shown by asterisk *). 'PBS' = phosphate buffered saline controls; 'BHI' = brain heart infusion broth controls; 'Ac' = Arctic clone of *Erysipelothrix rhusiopathiae*; 'Nac' = non-Arctic clone.

	Cox 1 (Batch 1-3)		**Cox 2 (Batch 1 and 3)**	
Test group	Exp(coef)	p-value	Exp(coef)	p-value
PBS	0.667	0.658	1.012	0.990
BHI	4.066	0.031*	0.990	0.992
Ac undiluted	4.987	0.012*	3.194	0.155
Ac 10-fold	2.420	0.200	2.570	0.260
Ac 100-fold	0.997	0.997	0.494	0.565
Nac undiluted	4.301	0.025*	4.716	0.049*
Nac 10-fold	2.462	0.192	3.267	0.147
Nac 100-fold	1.024	0.977	0.000	0.997

To explore why the BHI control group showed similar mortality levels in the combined results to those of the experimental groups, Kaplan Meier curves for each batch were generated to further investigate this trend (Figure 2-6). Panels A (Batch 1) and C (Batch 3) show expected trends, with the three control groups maintaining a similar if not higher survival probability compared to the inoculated groups. Panel B (Batch 2) clearly shows that the BHI control group

had a lower survival probability compared to all the other control and test groups. Batch 1 had 13 and batch 3 had 15 of 15 BHI-inoculated larvae remaining alive, compared to 6 alive at the end of day 9 of Batch 2. This corresponded to a survival probability of around 40% for the BHI control group of Batch 2, while the undiluted Nac larvae, which have the lowest survival probability in the other 2 batches, had a probability of around 56%. We take this to suggest that there was likely an issue of contamination in this batch. From the log-rank test, only panel B was shown to have groups which were statistically significantly different from each other; panels A and C both had values above 0.05, which meant that the null hypothesis should not be rejected.

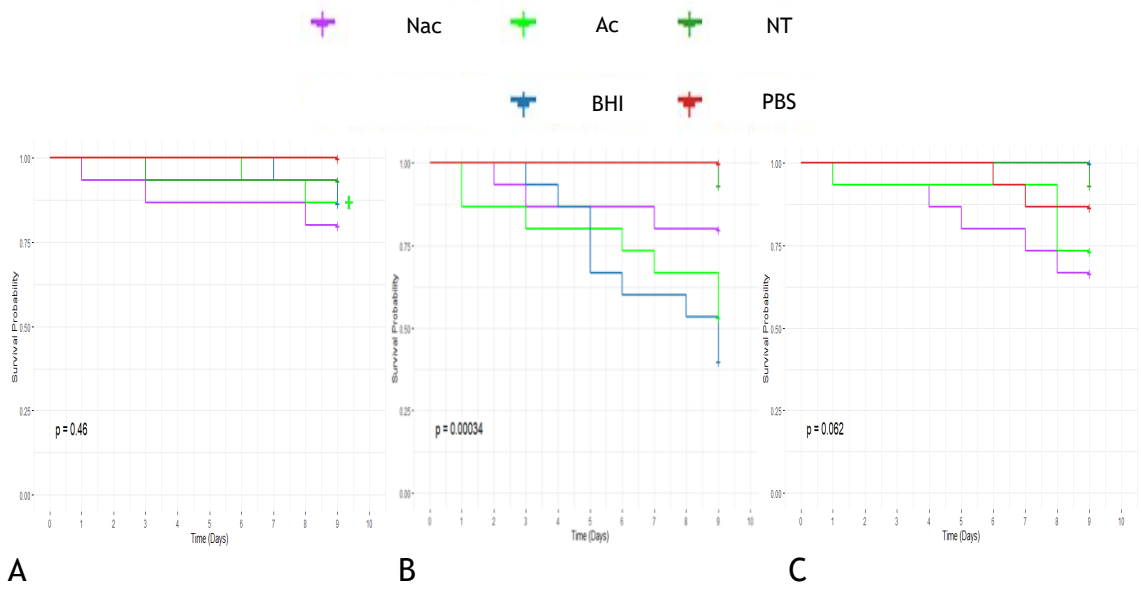

Figure 2-6 Kaplan Meier survival curves comparing the survivability of *Galleria mellonella* larvae of the three batches when injected with *Erysipelothrix rhusiopathiae* Arctic clone and non-Arctic clone. Panel A represents batch 1, panel B for batch 2 and panel C for batch 3. 'NT' represents the no touch controls, BHI represents the brain heart infusion broth controls, and the 'PBS' represents the phosphate buffered saline controls. The p-value on the graph was generated from a Log-rank test. A value of less than 0.05 means that the five test groups have distribution curves that are statistically different from each-other.

A second Cox proportional hazards model was run (Cox 2, Table 2-7) using the same parameters, with Batch 2 removed from the dataset, since we suspected issues of contamination due to the disproportionate number of dead larvae in the BHI control group compared to other experimental groups (Figure 2-6, panel B).The new Cox test shows that the BHI control group now is almost as likely to experience the hazard as the NT control, going from 4 times as likely, with the inconsistent data from Batch 2, to being 0.99 times as likely to be killed in the newer model. It also shows that only the Nac undiluted is statistically significant

when compared to the controls. This test provided the necessary justification to remove Batch 2 from all statistical testing from this point onwards.

For the different dilutions of Ac-injected larvae, no clear dose-dependent survival was observed. The neat inoculum was expected to have a lower survival probability compared to the lower concentrations. Each dilution group was plotted against the controls in Figure 2-7 to identify trends more easily. In panel A, the 10-fold dilution had the lowest survival probability (~65%), followed by the undiluted (~88%). Panel B became redundant due to the BHI anomaly which makes the results unreliable. Panel C had a p-value above 0.05 which meant that the test groups are not statistically different. It can be concluded that none of the panels showed evidence of dose-dependent mortality for the Ac-strain of *E. rhusiopathiae*.

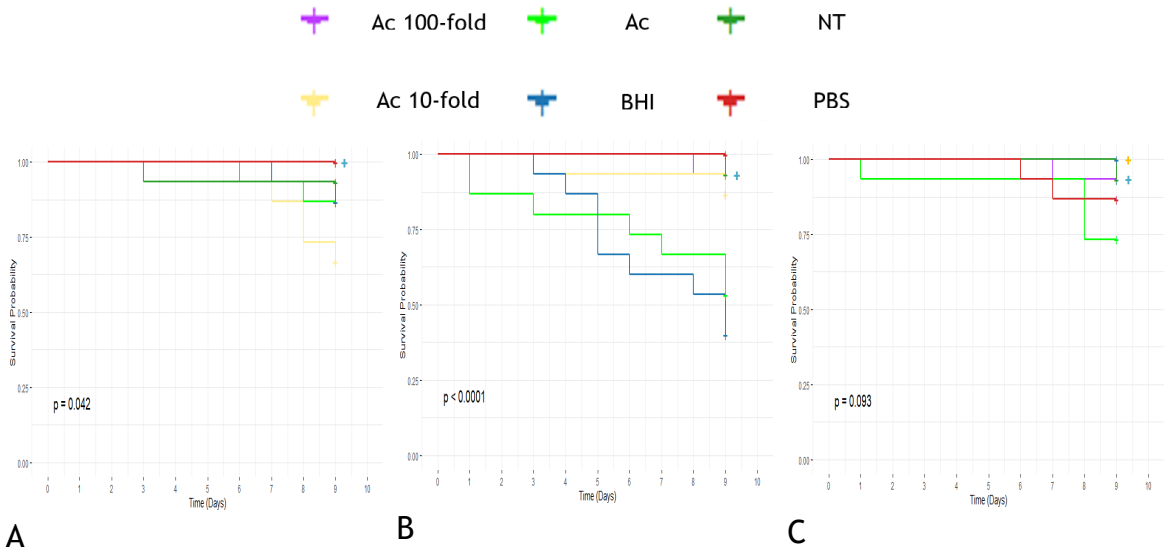

Figure 2-7 Kaplan-Meier survival curve comparing the survivability of *Galleria mellonella* larvae inoculated with the Arctic clone (Ac) strain of *Erysipelothrix rhusiopathiae* to visualise dose-dependent survival probability. For batch 1 (panel A), 2 (panel B) and 3 (panel C) of the experiment, undiluted, 10-fold diluted, and 100-fold diluted stock of the Ac culture was injected into 15 larvae per condition. 'NT' represents the no touch controls, BHI represents the brain heart infusion broth controls, and the 'PBS' represents the phosphate buffered saline controls. The p-value on the graph was generated from a Log-rank test. Values of less than 0.05 mean that the five test groups are significantly different from each-other.

Similarly for the non-Arctic clone, the 10-fold and 100-fold dilutions were plotted against the undiluted inoculations and the controls (Figure 2-8). Batch 1 Nac (Panel A) had a p-value above 0.05, which meant that the test groups are statistically not significantly different from each-other. Panel B had the BHI anomaly, which contributes to the p-value being significantly lower than the

0.05 threshold. Panel C is the only experimental batch showing evidence of *E. rhusiopathiae* dose-dependent larval mortality. The survival probability of larvae injected with undiluted culture was the lowest (~65%), followed by the 10-fold dilution (~74%). The 100-fold had the same survival probability as the BHI control (~100%). The p-value was <0.05 which meant that the null hypothesis is rejected and that the test groups are significantly different.

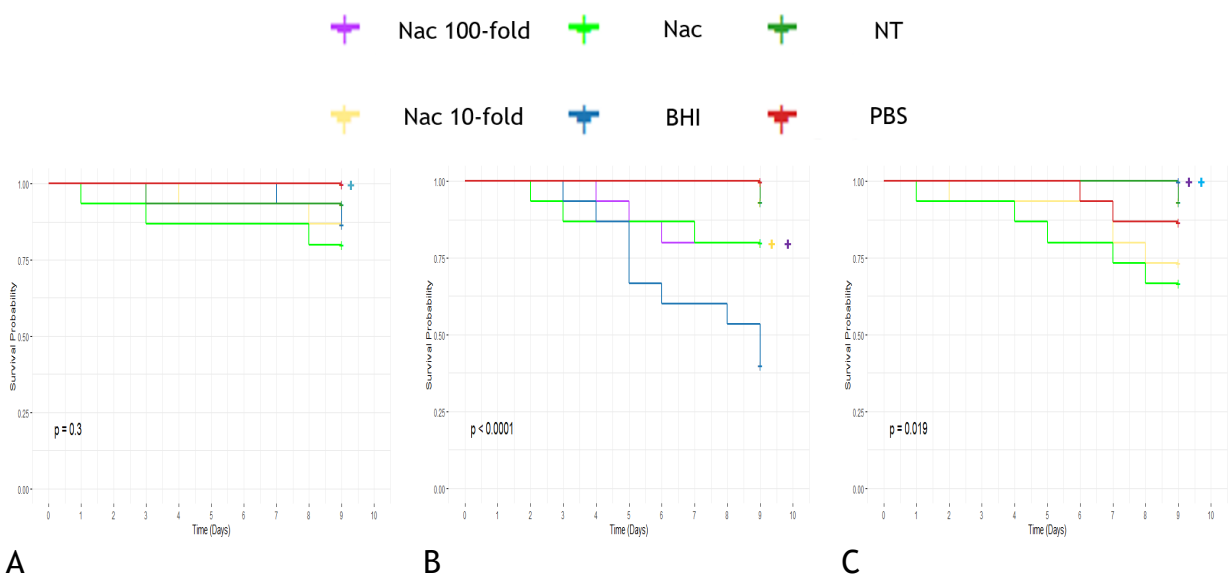

Figure 2-8 Kaplan Meier survival curve comparing the survivability of *Galleria mellonella* larvae inoculated with non-Arctic clone (Nac) strain of *Erysipelothrix rhusiopathiae* to visualise dose-dependent survival probability. For batch 1 (panel A), 2 (panel B) and 3 (panel C) of the experiment, undiluted, 10-fold diluted, and 100-fold diluted stock of the Ac culture was injected into the larvae. 'NT' represents the no touch controls, BHI represents the brain heart infusion broth controls, and the 'PBS' represents the phosphate buffered saline controls. The p-values were generated from a Log-rank test. For $p<0.05$, the five test groups were significantly different from each-other.

2.3.2.3 Melanisation

The numbers of larvae at four stages of melanisation (M-, M1, M2, M3) were recorded daily, with observations from days 1 and 9 shown in Table 2-5; no larvae at stages M3 were observed. The number of larvae alive (Alive, Al) and the number of larvae pupating (Pu) were also recorded at each time point to calculate the percentage of larvae at each melanisation level. The number of pupating larvae was subtracted from the number of alive non-pupating larvae to obtain the number of larvae relevant for melanisation observations. The number of larvae with no melanisation went from 358/400 (90%) down to 23/79 (29%) over the course of the experiment. From day 1 to day 9, larvae at M1 went up from 28/400 (7%) to 44/79 (56%) and the larvae at M2 increased from 14/400 (4%) to 18/79 (23%).

The number of larvae at each melanisation stage in batches 1 and 3 (Table 2-5) was also subjected to ANOVA and Dunnett's tests to test for differences among inoculation groups. The mean differences varied slightly for the larvae with no melanisation (M-) (Table 2-8), from -0.5 for Ac 100-fold and Nac 10- and 100-fold, to 2.5 in Ac undiluted. None of the test groups were found to be statistically significant compared to the NT reference. It can be concluded that there was no significant difference between the number of larvae with no melanisation in the test groups.

For larvae classified as M1, the same tests were run and again, most groups were within 0.5 mean difference compared to the reference. The PBS control and the Ac 10-fold dilution had the highest difference, both having a mean difference of 2.5 more larvae at M1 stage of melanisation. All test groups were statistically similar to the reference.

Larvae classified at M2 had the highest amount of variance in the dataset of batches 1 and 3. Ac undiluted had the highest mean difference across all melanisation stages (4.5). All the other test groups were within the mean difference of 0.5 to 1. P-values classified only the Ac undiluted group as statistically significant compared to the NT reference, making it the only test group to be statistically significantly different in all three observed melanisation stages.

Table 2-8 Results of the analysis of variance (ANOVA) tests comparing the number of *Galleria mellonella* at the different melanisation stages in all test groups in batches 1 and 3. The Diff shows the mean difference compared to the 'no touch' control and a p-value of less than 0.05 (Pr(>|z|)) shows that the reference (no touch) was statistically different compared to the test group (shown by asterisk *). 'PBS' = phosphate buffered saline controls; 'BHI' = brain heart infusion broth controls; 'Ac' = Arctic clone of *Erysipelothrix rhusiopathiae*; 'Nac' = Non-Arctic clone.

	ANOVA 1 (M-)		ANOVA 2 (M1)		ANOVA 3 (M2)	
Test group	Diff	P value	Diff	P value	Diff	P value
PBS	-1.0	0.995	2.5	0.411	0.5	0.997
BHI	0.5	1.000	-0.5	1.000	0.0	1.000
Ac Undiluted	2.5	0.691	1.0	0.971	4.5	0.011*
Ac 10-fold	-1.0	0.995	2.5	0.410	1.0	0.895
Ac 100-fold	-0.5	1.000	-0.5	1.000	0.0	1.000
Nac Undiluted	-1.0	0.995	0.5	1.000	1.5	0.624
Nac 10-fold	-0.5	1.000	0.5	1.000	0.5	0.997
Nac 100-fold	-0.5	1.000	-0.5	1.000	0.0	1.000

2.4 Discussion

Recent mass mortality events of muskoxen in the Canadian Arctic have shown that these populations are susceptible to the Ac strain of *E. rhusiopathiae*. Many questions remain as to how the pathogen is maintained and spread across the different islands in the Arctic and why the muskoxen are so vulnerable to this bacterium. There was an interest in determining to what extent the high rate of *E. rhusiopathiae*-related mortalities could be associated with pathogen-related factors, such as Ac-specific virulence (61). The *G. mellonella* larvae model has been proven successful as an alternative to murine models to study virulence and host response effects for a range of Gram positive and negative bacteria (116,120,128). In this study, we aimed to determine whether this could also be a suitable model to test the different virulence traits or determinants of *E. rhusiopathiae* isolates. To our knowledge, the *Galleria* model has not been evaluated for this species before. Here, within two independent experimental replicates conducted, we found minimal *E. rhusiopathiae* related mortality, which suggests that *G. mellonella* may not be a suitable model to assess the virulence of this bacterial species, regardless of possible strain-level differences.

2.4.1 Experimental changes

The lack of standard practise of the use of the *G. mellonella* model has resulted in several inconsistencies between this methodology used for this experiment when compared to others. Some of the changes were made to make the experiment more time-efficient while others were made to account for discoveries made during the practise round and the experimental round.

For the sterilisation of the larvae pre-inoculation, 50% ethanol was used to spray clean the larvae. The rationale behind this was to clean the injection sites of pathogens that could also infect the larvae via the injection site. During the practice rounds of larvae injections, 70% ethanol was used instead but it was discovered that the larvae would become inactive within 10 min of the sterilisation stage and this would cause death, even with the ‘No touch’ controls. The decrease in alcohol content to 50% prevented this from happening and remained standard practice ever since.

A common practice conducted by various *G. mellonella* studies is the use of a PBS wash of the culture to remove any secreted virulence factors and toxins so that any changes to the viability of the larvae can solely be contributed to the bacteria post-inoculation (129,130). This was not conducted in this round of experiments. In the literature to date, there is no evidence that *E. rhusiopathiae* secretes toxins (58), the main method of pathogenicity is the use of virulence factors such as neuraminidases for attachment and invasion, capsular polysaccharides for phagocytic resistance and the need for intracellular survival for replication, which is why the inoculum consists of whole bacterial cells. The overall inoculum injected into the larvae did not show evidence of *E. rhusiopathiae*-associated mortality during our studies, which strongly suggests that the exclusion of extracellularly secreted virulence factors would not likely have made a difference in the experimental results.

The final deviation from what was previously described in prior *G. mellonella* studies was the injection site of the larvae. While the site of injection in most studies uses the posterior proleg of the larvae (131,132), some studies used other injection sites such as the anterior proleg (133) or simply just described it as 'injection into the abdominal spiracle area' (122). The main cause for the deviation of the methodology I used was mainly due to significant difficulties encountered during the practice injections, where the increased manipulation of the larvae for the injection of the inoculum into the hind proleg caused deaths within the controls. Through a review of the literature, it was discovered that most justification for the use of the left proleg was to minimise the damage done to the midgut and to provide more space for the needle (134,135). The understanding was that the choice of injection site was mainly to reduce the variability of the larvae from trauma caused by the injection, therefore, as long as the injection sites remain consistent for all injection, and that there were no significant deaths caused by the trauma from the needle, the results remain valid.

2.4.2 Multiple strains of *E. rhusiopathiae* have limited impact on *G. mellonella* survival

In this study, *E. rhusiopathiae* caused only limited mortality in injected *G. mellonella* compared with what has been observed in 'successful' bacterial virulence studies using this model system. For illustrative purposes, two Kaplan-Meier curves taken from two different studies using the *G. mellonella* model – on *Micrococcus luteus* and *Leptospira* spp. (121,122) – are compared with that generated from the two successful experimental replicates of this study (Figure 2-9). Both studies injected the *G. mellonella* larvae with around 1×10^6 CFU per larva and observed survival over the course of at least 7 days in a 37°C environment. Despite having a similar CFU injected into the larvae, the survival probability greatly differs between the three curves. Within one day of injection, larvae inoculated with 1×10^6 of *M. luteus* fell from 100% to just below 10%. A similarly dramatic decrease was also observed in the same experiment for inoculations of the bacteria as low as 1×10^4 CFU (122). The two strains of *Leptospira* inoculated had different survival probabilities due to differences in pathogenicity (121). For the pathogenic strain at 1×10^6 CFU, there was a sharp decrease in survival probability one day post infection, decreasing to ~25%. The non-pathogenic strain had a sharp decrease on day 6 and ended up with around 40% survival on day 11. This is in contrast to the *E. rhusiopathiae* Kaplan-Meier curve, with survival rates of ~ 75% to 80% for both strains at the end of the experiment (Figure 2-9). The lack of a steep decrease in survival probability as seen on day 1 in the survival curves generated by Banfi et al (109) and by Prakoso et al (121) would indicate that the *G. mellonella* larvae are not as susceptible to *E. rhusiopathiae* as *M. luteus* and *Leptospira* spp. and *Saprolegnia parasitica* (136).These examples showcase the fact that not all bacterial species affect *G. mellonella* the same way. The 50% lethal dose (LD_{50}) is a recognised unit of measurement for the toxicity of a substance, it accounts for the dose of the substance required to kill 50% of the population (137). The LD_{50} of *E. rhusiopathiae* varies depending on the strain, infected organism, the route of inoculation and disease presentation, wherein acute forms of the bacteria can disseminate through the bloodstream. The Fujisawa strain was described to have a subcutaneous LD_{50} of $10^{1.2}$ CFU while intraperitoneal injection has a LD_{50} of $10^{3.5}$ CFU (138). Another study found that a strain isolated from dead pig tissue in an outbreak in China had the minimum lethal dose of <10

CFU in piglets and mice (139). The findings of these studies suggest that the injected doses of *E. rhusiopathiae* in the larvae (~2.08 $\times 10^6$ CFU) were significantly higher than those typically used in mammalian models. That being said, future studies using higher infectious doses of *E. rhusiopathiae*, i.e. by concentrating the bacteria through centrifugation of the liquid culture prior to inoculation, would be worth attempting.

The lack of significant mortalities in the test groups precluded our ability to identify any strain level differences between the two strains. While it could be argued that using one of the injected groups would have represented a better comparison group than the NT controls to show pathogen-specific differences in mortality (since these take injection-induced trauma into account) (140), given that the Cox proportional hazards of the two injection controls were similar to the NT, this choice is unlikely to have influenced our conclusions. Overall, the *G. mellonella* model does not appear to be well-suited for the *in vivo* study of *E. rhusiopathiae* or its Arctic clone strain.

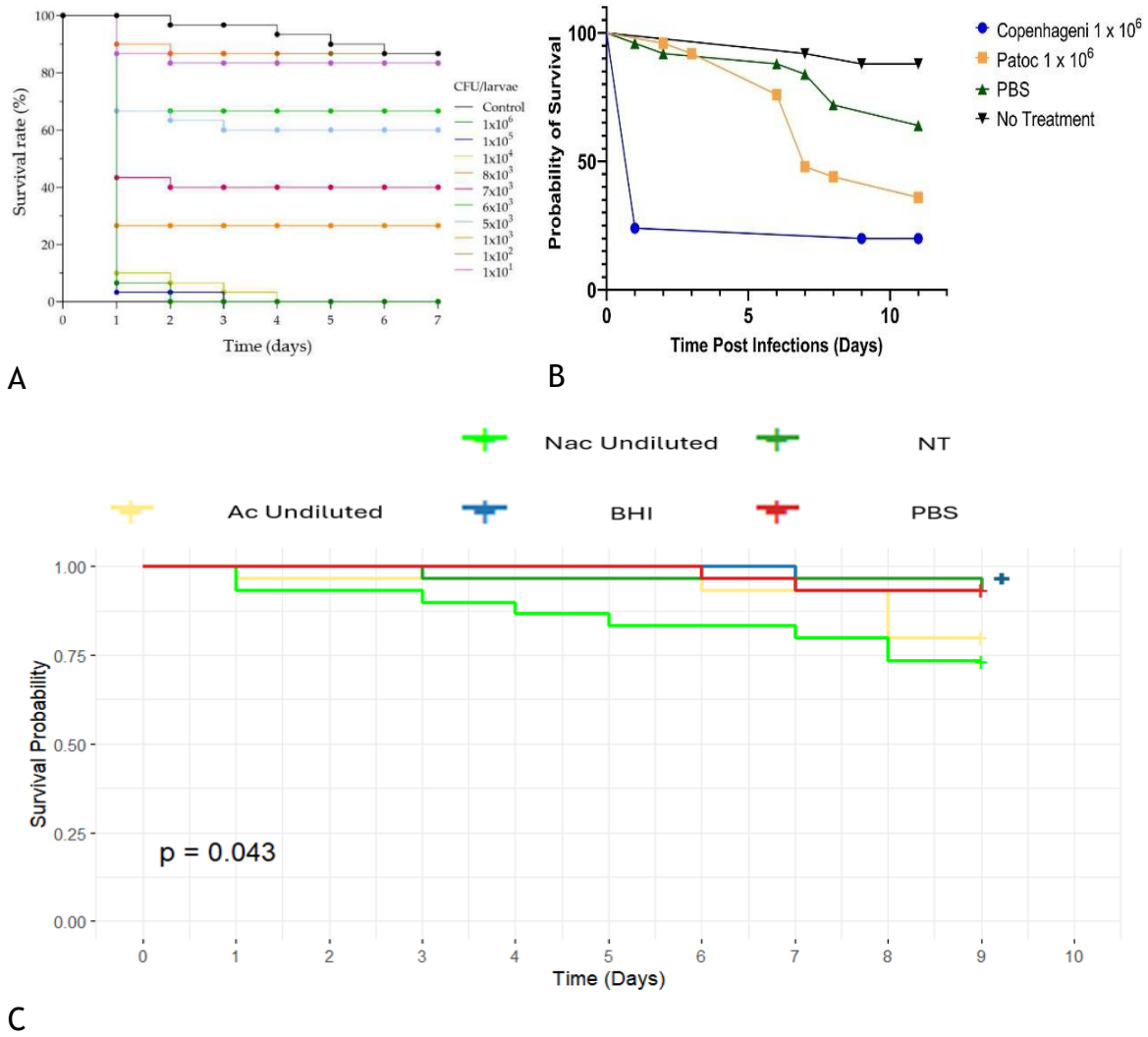

Figure 2-9 Comparisons between Kaplan-Meier survival curves generated for two different studies of bacterial virulence using the *Galleria mellonella* model alongside the curve generated from this study (panel C). The survival curve generated by Banfi et al **(122)** (panel A) investigated the survivability of *Galleria* larvae when exposed to various concentrations of *Micrococcus luteus* in a 7-day period, and Prakoso et al **(121)** (Panel B) investigated the difference of survival probability between pathogenic (blue) and non-pathogenic strains (orange) of *Leptospira* over 11 days.

There are a few reasons as to why the *G. mellonella* model may not be suitable for the study of *E. rhusiopathiae* infection. The different infection route could result in a different immune response. The difference between infection of muskoxen via the oral-nasal route and the injection of bacteria directly into the haemolymph of the larvae could yield different results. The use of this model is also strictly limited to the innate immune system, since the larvae do not possess an adaptive immune response (do not produce T or B cells, no antibodies). They can, however, exhibit “immune priming”, such as through enhanced haemocyte activity and co-presentation of antimicrobial peptides (141,142) that is comparable to mammals, including ungulates. Pathogens whose

role in pathogenicity critically depends on interactions with the adaptive immune system cannot be fully assessed using *G. mellonella*.

Although recent studies have discovered several unique virulence gene variants related to the Ac, there was no solid confirmation on the specific mechanism of action. Most bacteria in mammals are commensals, and some commensals can form biofilms. Biofilms are often multi-species communities and are important in many infections. The occurrence of pathogen co-infection in mammals has been described in many studies. Examples include infectious diarrhoea in dogs caused by a combination of canine parvovirus type 2 and *Cryptosporidium spp.* and *Giardia spp.*(143) or the co-infection of cattle with *Mycobacterium bovis* and liver flukes (144). The formation of biofilms can , which increases the resistance to antimicrobial agents as reported by Nishi et al (145), cause the major infection or co-infection. The possibility of co-infection predisposing muskoxen to disease with *E. rhusiopathiae* has previously been proposed (146). Studies have found that *Streptococcus suis* and *E. rhusiopathiae* were the cause of porcine endocarditis (147). However, in recent outbreak investigations on Ellesmere Island, tests for anthrax, yersiniosis, salmonellosis and orf virus on a limited number of carcasses all yielded negative results (66). Alternatively, its environmental persistence could be an important factor, since the Ac is hardy and ubiquitous in nature, being able to be cultured from carcass sites five years post-mortem (which is the longest reported *ex-vivo* survival time for *E. rhusiopathiae* to date) and from the faeces of several other wildlife species (27, 117). High temperatures – leading to heat stress in muskoxen – have been proposed to predispose these cold-adapted animals to disease caused by opportunistic bacterial like *E. rhusiopathiae* (25). While local weather data, as well as communications with the local weather station and documentarians, suggests that there was an absence of extreme weather events associated with the recent mortalities on Ellesmere and Axel Heiberg Islands (66), more in-depth analyses of climatic data are required before any firm conclusions are drawn related to this factor. More broadly, there is evidence of climate-driven range expansion of bacterial infections and an increase of emerging disease globally, including in the Arctic (71,148).

Further studies could benefit from investigating any co-factors that could affect the survival probability of the larvae, such as tissue cultures. Alternatively,

while less ideal from ethical and financial perspectives, a different model could be used to study the virulence of the Ac. Other animal models have been used for vaccine trials targeting *Erysipelothrix* spp. These include porcine, avian and murine models (45). Clear *E. rhusiopathiae*-induced mortality can be observed in these species in the absence of immune protection (105,106). Moreover, clear differences in strain-level virulence have been observed using such models (149).

2.4.3 Dose dependent mortality

One of the hypotheses associated with infection models is that higher bacterial loads will be associated with a lower survival probability. Indeed, in 'successful' *Galleria* infection models, the trend of dose-dependent infection can be clearly observed in the Kaplan Meier curves (122,150). This was observed to a degree in our current study, in that most mortalities occurred in the undiluted injections of 2×10^6 CFU. While there was a general trend of lower mortality in the lower dilutions, the difference between the serial dilutions was not statistically significant. Cox 2 of Table 2-7 shows that only the Nac undiluted test group was statistically different from other treatment groups using the Cox proportional hazards model; all the other test groups, including the Ac undiluted test group, were not statistically significant and had p-values of >0.05. This shows that there is an absence of dose-dependent infection from the results of this experiment.

2.4.4 Melanisation vs infection

The inoculation of bacteria into the *Galleria* larvae invokes an innate immune response similar to the response exhibited by mammals. The haemocytes have been shown to possess the ability to phagocytose and eliminate pathogens (100,151). Melanisation is caused by the phenoloxidase activation reaction which is secreted following pathogen recognition using pattern recognition receptors (116,152). The presence of dark spots on the body of the larvae is an important sign of the immune system's recognition of an infection. Several studies have observed that the larvae exhibited dose-dependent melanisation. In a study of *Brucella*-host interaction, Elizalde-Bielsa et al (102) noticed that the *Brucella suis* biovar 2 strains they used were not causing melanisation, whereas their positive control *Klebsiella pneumoniae* strain showed intense melanisation 6 h

post inoculation. It was concluded that this was because the *Brucella* inoculated did not activate innate immunity because it was not recognised by the immune system (102). In our study, immediate melanisation was not observed 24 h post inoculation; instead, from day 1 to 9 post-inoculation, the number of larvae in melanisation stage 1 (M1) increased from 28/400 (7%) to 44/79 (56%) and the larvae at stage 2 (M2) increased from 14/400 (4%) to 18/79 (23%). Due to the large number of larvae per experimental batch (n = 135), it was nearly impossible to label each larva and monitor them individually. From recorded results (Supplementary Table 1), the number of larvae with severe melanisation on the first day usually corresponded to the number of dead larvae found on the following day, and this is supported by other studies (153). Statistical tests of the three observed melanisation stages showed that most test groups had the same melanisation rate as the NT control group (Table 2-8). All of the larvae with no melanisation and stage 1 melanisation showed no statistically significant differences to the NT control (p-value >0.05) (ANOVA 1, Table 2-8); the only test group that was statistically significant compared to the control was the Ac undiluted in melanisation stage 2 (ANOVA 3, Table 2-8). These results seem to indicate that both *Erysipelothrix* strains were not efficiently recognised by the host immune system and further supports the conclusion that the *G. mellonella* model may not be suitable for the virulence testing of *Erysipelothrix rhusiopathiae*.

2.4.5 Pupation

The life cycle of the *G. mellonella* larvae switched from larva to pupa over the course of the test period. In batches 1 and 3, 74 out of the 84 (88%) larvae alive in the control group were pupating on day 9, while 110 of the 154 (71%) alive in the test groups were pupating. Pupation began as early as day 3 in the experiment; all pupating larvae were counted as alive until the end of day 9. ANOVA testing of the number of pupating larvae in batches 1 and 3 concluded that only the Ac undiluted test group was statistically significant ($p < 0.05$) (Table 2-6); all the other test groups, including the Nac undiluted test group, had mean values that were statistically similar to the reference NT control group. In its natural breeding ground in a beehive, wax moth larvae pupate when they can find a safe environment (154). It was reported that temperature affects the speed of pupation. Śmietanko et al reported that a temperature of 18°C has

a strong inhibitory effect on *G. mellonella* larvae pupation, while D. Beck reported that chilling larvae delayed the rate of pupation by making the part of the brain in control of endocrinology less competent (155,156). This was in line with what was observed as part of the current experiment. Not all the larvae received in each shipment were inoculated. The larvae that were not chosen for the injections were kept in their original delivery container, at room temperature, in the dark. By day 9, when most of the control larvae used in the experiment were pupating, most of the larvae that were kept out of the incubator did not pupate. Pupation could also be interpreted as a stress response. A study was conducted by Copplestone et al to investigate the effect of radiation on *G. mellonella* larvae and found that in larvae exposed to a higher dose of radiation, there was an increased rate of pupation, leading them to theorise that the stress caused by the hazard led to developmental dysfunction (157). They also cited other studies which showed a similar trend, where the introduction of a stressor decreased the expression of a protein (SOD2) which contributes to pupation in some species of insects (158,159). The incubation of larvae at 37°C, combined with the introduction of a stress event in the form of an injection, could explain the high abundance of pupating larvae in the test groups while the warm temperature alone would explain the high pupation rate of the NT control group. Further testing could be done to identify the effect of stress on specific gene expression that affects the rate of pupation, but this was beyond the scope of the current project.

2.4.6 Experimental constraints

Re-examination of the methodology used in the current experimental development presented many potential limitations, which were the result of this being an initial screening of this model in the lab and on this bacterium. The potential limitations encountered for the duration of this experiment are listed below (Table 2-9).

Injection techniques had to be refined prior to the experimental phase to establish a suitable technique (160). Various studies have noted that due to a lack of standardised procedures, it is difficult to obtain consistent results, resulting in conflicting reports (101,128). The importance of standardising the protocols for the handling and maintenance of larvae pre-inoculation is high. The

numerous different inconsistencies highlight the need for a standard stock centre for *G. mellonella* research to provide reliable and reproducible results. Since all the larvae used in batches 1-3 of the experiment reported in this thesis were from the same batch of larvae from the same supplier, this minimises any potential inconsistency of the larvae survivability.

Leading up to the experimental work reported here, six earlier batches of *G. mellonella* injections were conducted, some of which were run under different conditions; these were considered invalid for different reasons. Table 2-9 shows why the results from the initial batches were discarded. The final three batches on which I report were the most comparable between the two strains of *E. rhusiopathiae*, since the OD_{600} values of the 6-hour cultures were within 0.05.

Table 2-9 Factors that were potentially encountered during the *G. mellonella* inoculation experiments.

Limitation	Description	Reference
Larvae source	Different rearing systems, quality standards between suppliers. Suppliers have been reported to use antibiotics, which affects the susceptibility to pathogens.	(153,161,162)
Temperature	Temperature fluctuates between transport and storage. Increased temperature stimulates immune response.	(128,163,164)
Larval size at the start of the experiment	Increased weight leads to increased volume of haemolymph.	(165)
Lab handling	Sterilisation techniques differ, leading to the difference in coverage of clean vs unclean larvae.	(128,166)
Equipment failure	The CO_2 incubator had inconsistent CO_2 levels, which led to earlier batches being discarded. We later decided to use only aerobic incubation.	(167,168)
Culture contamination	The growth media (BHI supplemented with HS) was not selective for *E. rhusiopathiae*, leading to frequent contamination issues and led to an earlier batch of inoculations being discarded.	(169,170)
Inconsistent growth	The starting OD_{600} value is too different between Arctic clone (Ac) and non-Arctic clone (Nac) *E. rhusiopathiae* strains, making it impossible to make direct comparisons between groups. Later tests made sure that the OD_{600} was used to standardise bacteria concentration.	N/A

Poor lab technique	The pipette tips used for the serial dilution were not changed for each dilution, resulting in inaccurate dilutions in earlier batches.	(171)

The inoculation concentration of the *G. mellonella* larvae is currently limited due to the methodology established prior to the experiment. A wider range of inoculations could be tested and has the potential to show significant results regarding larvae mortalities. This overnight culture of *E. rhusiopathiae* could be concentrated to achieve a higher infectious dose. This could be achieved by spinning the culture down using a centrifuge and resuspending in a lower volume of PBS. This step could be conducted in future research to re-assess the potential of using the model for *E. rhusiopathiae*.

E. rhusiopathiae was able to replicate within macrophages post phagocytosis (58) and enters the host via the tonsillar crypt epithelium in pig infections (172). This evidence suggests that infections in mammals relies on mammalian cell types and could provide a reason as to the lack of mortalities within the *G. mellonella* model. The model lacks the features of the typical route of infection in murine and porcine models and therefore is not fully representative of a typical infection. Another limitation of the *in vivo* model is the inability to represent the environmental stressors experienced by the muskoxen in the wild. Chronic stress was noted as a potential factor which may predispose the host to infection, as evident by the cortisol levels found within the qiviut (wool undercoat) of the muskox (173); this could be related to the increased global temperature, which changes the distribution of the already scarce plant life in the Canadian Arctic, causing a cascade in compromised nutrition which leads to reduced immunity (174). The environment where the muskox resides is harsh and unforgiving, and the conditions are impossible to replicate in a laboratory environment. The inability to simulate these stressors that could predispose the host to opportunistic infections may therefore affect the results.

2.4.7 Conclusions

Numerous studies have shown that the *G. mellonella* larvae model can provide great value in the study of virulence for different bacterial species and strains. From the results of this study of *E. rhusiopathiae* and its Arctic clone, there is a lack of evidence that *E. rhusiopathiae* causes physiological changes and mortality in the *G. mellonella* larvae model, including high dose-associated mortality when compared with other pathogens studied with this model. Future investigations of *E. rhusiopathiae* virulence factors, co-infections and the role of stress, including climate-induced, should be conducted. Virulence studies of this bacterium may require the use of more traditional *in vivo* infection models. If pursuing *G. mellonella* infection studies, further testing could involve increasing the injected dose of the bacteria, as well as different stressors to mimic the environmental stress that the muskox population experiences in the Canadian Arctic – predisposing them to opportunistic infection.

3 Development of a diagnostic qPCR to distinguish among *Erysipelothrix* spp.

3.1 Introduction

Polymerase chain reaction (PCR) is a very useful tool in molecular diagnostics. The first instance of any mention of the techniques used in the process of a PCR came from a paper published by Kleppe et al in 1971 (175), and the first PCR protocol was developed by Mullis et al (176). The mechanisms of this reaction were later refined: this included a newly increased thermal-threshold, larger fragments were amplified, the incidence of non-specific binding was reduced, and the DNA fragments could be detected in agarose gels stained by ethidium bromide (177–179). In 1993, Huguchi et al described 'a simple, quantitative assay for any amplifiable DNA sequence that uses a video camera to monitor multiple polymerase chain reactions' (180). Using the fluorescence from the binding of ethidium bromide to the new DNA sequence, the video camera was able to accumulate the data and relate that to the starting number of DNA copies. This was the first step in the development of real-time PCR, or quantitative polymerase chain reaction (qPCR).

Quantitative PCR is the modern standard for microbial diagnostics (181). There were two main ways to allow for real-time visualisation of amplified DNA: fluorescent dyes (SYBR green) that intercalate between double-stranded DNA (182), and sequence-specific fluorescent labelled probes (TaqMan®) (180,183,184). Recently, digital PCR (DPCR) was developed as an offshoot qPCR. DPCR has the ability to dilute and divide the initial DNA sample into many reaction chambers. This process allows for the detection of a single copy of the template, which results in an increased sensitivity (185). Using the aforementioned techniques, PCR assays have been developed to detect different bacterial species and strains. These assays can de designed to detect small amounts of DNA from a wide range of different samples from various sources such as DNA extracted from bacterial isolates, or directly from different samples (e.g. blood, tissue, faeces etc.) (186,187). With the incorporation of a forward and reverse primer which flanks the sequence of interest, deoxynucleoside triphosphates (dNTPs), Taq polymerase, in the presence of magnesium ions (Mg^{2+}), the PCR can theoretically amplify any sequence of DNA, provided that it

was present in the sample (186). Due to its simplicity, speed and accuracy, it is used widely in molecular diagnostics (188).

Numerous studies have designed strain-specific qPCR assays based on sequence data generated by next-generation sequencing (189,190). The sequencing data can be used to distinguish between different strains to detect the differences in specific gene sequences or the presence/absence of genetic markers. The qPCR assay is used to target the specific alleles/genotypes based on the strain-specific amplicon sequences, which allows the qPCR to detect strain differences within a sample (191,192). Since DNA can persist in the environment regardless of host (i.e. bacterial survival), the qPCR can detect the presence of the pathogen DNA even if the bacterial cell is not culturable or no-longer viable. The speed and simplicity of qPCR, the possibility of multiplexing, and the wide possible sample range it can be applied to makes qPCR ideal for identification of the Arctic clone of *E. rhusiopathiae* involved in the recent outbreak in the Canadian Arctic.

Infection with *E. rhusiopathiae* is commonly diagnosed by culture of viable bacteria or by identification of its specific DNA sequences, as described in the General Introduction. A qPCR assay was previously developed by Pal et al (103) that was able to distinguish among multiple species of *Erysipelothrix* spp. in one qPCR reaction. The primers and probes used in their study were manually designed based on BLAST analysis of the DNA sequences of the genomic region coding for the rRNA gene cluster (Figure 3-1). The primers and probes were designed to attach to a tRNA sequence (ERH_RS05350), which was upstream of the rRNA cluster on the Fujisawa reference genome (38). A single set of primers was used, with three different probes used to distinguish among the species *E. rhusiopathiae*, *E. tonsillarum and Erysipelothrix* sp. strain 2 (now *E. piscisicarius*) (193,194). These sequences were chosen for their weak homology with each other, thus enabling discrimination among the species.

E. tonsillarum, a morphologically and biochemically similar species to *E. rhusiopathiae*, was previously found in the Canadian Arctic. In the paper published by Forde et al (2016), it was shown that certain isolates that had the expected morphology for *E. rhusiopathiae* tested negative on the species-specific qPCR. Subsequent testing using the *E. tonsillarum* probe showed positive amplification results (25). Since these species may both be found in the Arctic

and sometimes co-occurring in the same sample, both these species probes were retained in the currently developed multiplex qPCR.

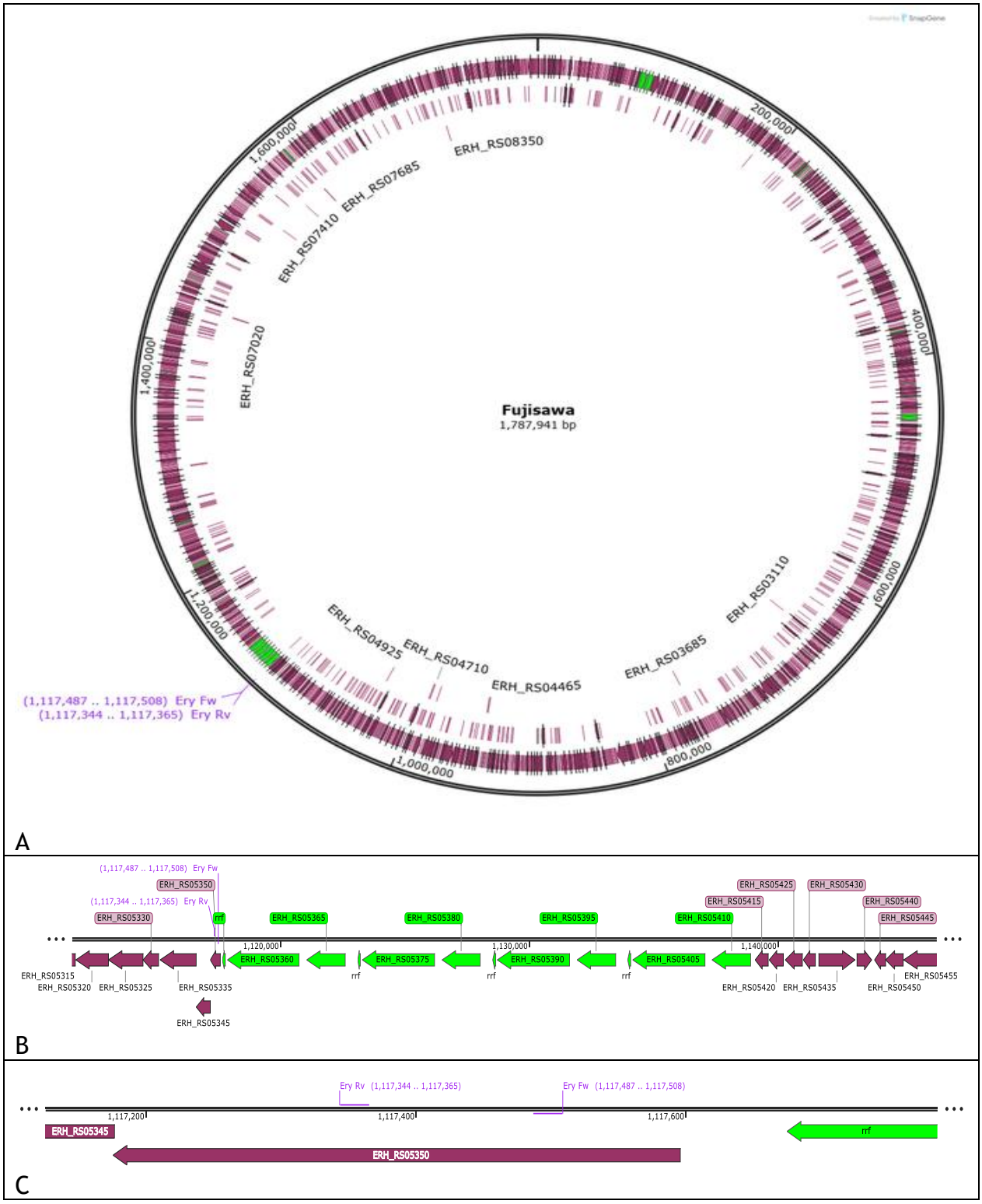

Figure 3-1 The location of the amplicon sequence for *Erysipelothrix* spp. designed by Pal et al (103). Location is mapped to the *E. rhusiopathiae* Fujisawa reference genome (Accession AP012027) using SnapGene viewer **(195)**. The forward and reverse primers are labelled in purple font as Ery Fw and Ery Rv. The primers target a specific tRNA located just upstream of an rRNA cluster (green arrows). Panel A – circularised genome. Panel B – zoom in to rRNA gene cluster. Panel C – further zoom in to primer binding locations on the tRNA (ERH_RS05350).

For the detection of the Ac of *E. rhusiopathiae* specifically, the primers and probe were designed by a past MSc student in the University of Glasgow, Tianjiao Fang, as part of her final MSc project. The primers and probe were designed to bind to the unique gene, *hhaIM*_1, which encodes a putative DNA methyltransferase enzyme of the restriction modification system, and is only found in isolates belonging to the Ac and not in non-Arctic clone (Nac) or other bacterial species (61).

The aim of this chapter was to contribute to the development and evaluation of diagnostic tools for *E. rhusiopathiae* – and the Ac in particular – by combining previously developed single-plex and duplex assays to design and optimise a multiplex qPCR assay capable of detecting the species *E. rhusiopathiae* and *E. tonsillarum*, and for the former, determining whether it is the Arctic clone.

3.2 Methods

3.2.1 DNA samples

DNA samples used in the testing of the qPCR assays were isolated and extracted from bacterial isolates obtained from a variety of different hosts (Table 3-1). *E. rhusiopathiae* Ac and Nac isolates were first selectively cultured by collaborators in the University of Calgary, using the methods detailed in . The QIAGEN DNA Blood & Tissue kit (QIAGEN, Hilden, Germany) was used for the DNA extraction and the DNA was stored at -80°C (34,61); *E. tonsillarum* isolates were provided by T. Opriessnig (Roslin Institute, University of Edinburgh), and extracted by T. Fang during her Masters thesis work. Aliquots of each DNA extract from Calgary were diluted 100-fold in nuclease-free water (QIAGEN, Hilden, Germany) to preserve the original samples and ensure that there was enough DNA available for all testing planned. These diluted DNA extracts were kept in a -20°C freezer for quicker thawing and easier access. Sample numbers 1,2,7,8,13 and 14 were chosen as 'representatives' of the three target strains for certain validation steps (described below). The original concentration of all undiluted DNA extracts was determined using the Invitrogen Qubit high sensitivity assay (ThermoFisher Scientific, MA, USA) following manufacturer's instructions.

Table 3-1 General information of the samples used for the qPCR optimisation. The list includes sample identification (ID) name and number, strain identity, collection year, and the host species source of the isolates, and the identity of the three *Erysipelothrix rhusiopathiae* clades (as described in Forde et al., 2016 **(64)** to which the isolates belong. (N/A = not applicable).

Sample ID	Sample number	Species/clone	Collection year	Host species	Clade
358-DMX014.2-He	*1*	*E. rhusiopathiae rhusiopathiae*-Arctic clone (Ac)	2015	Muskox	3
358-DMX07.1-Lu	*2*	*E. rhusiopathiae*-Ac	2015	Muskox	3
459-Mould1-BM	*3*	*E. rhusiopathiae*-Ac	2017	Muskox	3
459-Mould2-Lu	*4*	*E. rhusiopathiae*-Ac	2017	Muskox	3
593-EU01-Sp	*5*	*E. rhusiopathiae*-Ac	2021	Muskox	3
593-EU04-Kid	*6*	*E. rhusiopathiae*-Ac	2021	Muskox	3
620-A1627895	*7*	*E. rhusiopathiae*-non Arctic clone (Nac)	2015	Humpback whale	3
622-2019384	*8*	*E. rhusiopathiae*-Nac	2019	Beluga whale	3
622-2019387	*9*	*E. rhusiopathiae*-Nac	2019	Beluga whale	3
622-2019396	*10*	*E. rhusiopathiae*-Nac	2019	Beluga whale	2
622-2020230	*11*	*E. rhusiopathiae*-Nac	2020	Beluga whale	2
622-2021136	*12*	*E. rhusiopathiae*-Nac	2021	Beluga whale	3
ERY0041	*13*	*E. tonsillarum*	Pre-1986	Fish	N/A
ERY0037	*14*	*E. tonsillarum*	1975	Pig	N/A

3.2.2 Primer design and targets

The qPCR assays (primers and probes) used to identify *E. rhusiopathiae* and *E. tonsillarum* were designed by Pal et al (103), based on sequences found in a non-coding region of a tRNA (near the rRNA gene cluster) as described above. The Arctic clone (Ac) single-plex reaction was designed by a past Master's student (T. Fang) (104) using a combination of Primer-BLAST (196) and Primer 3 (197); the primer sizes were 19 and 20 base pairs (bp) and the amplicon length was 111 bp. This third diagnostic target in the triplex qPCR developed in this chapter was included to distinguish among Arctic clone (Ac) and non-Arctic clone (Nac) strains of *E. rhusiopathiae*. The sequences of the primers and probes are all listed in Table 3-2.

All primers and probes were ordered from IDT (Integrated DNA Technologies Europe, Leuven, Belgium) and reconstituted using nuclease-free water to achieve a concentration of 100 µM. The emission wavelength of the probes was as follows: FAM at 520 nm, HEX at 555 nm, and Cy5 at 668 nm. Dilutions were made using nuclease-free water to make up the working concentration solution of 20 µM for the primers and 10 µM for the probes. In order to identify the amplification of three different targets in a single qPCR reaction, the strain/clone-specific probes were labelled with three different fluorophores as indicated in Table 3-2.

Table 3-2 Primer and probe sequences used for the triplex qPCR. The three target strains are: *Erysipelothrix rhusiopathiae* Arctic clone (Ac), *E. rhusiopathiae* non-Arctic clone (Nac), and *E. tonsillarum*. 'Ery' primers amplify an *Erysipelothrix* genus-specific sequence, whereas the 'Rhus' and 'Tons' probes detect *E. rhusiopathiae* and *E. tonsillarum,* respectively. HEX, FAM, and Cy5 probes' fluorescence are detected on in the yellow, green and red channels, respectively.

Primer/probe name	Sequence
Ac Forward (Old)	5'-AAAATCGCTCGGCCATTT-3'
Ac Forward (New)	5'-CGTAAAGCCGGAAACTGATTTG-3'
Ac Reverse	5'-TAGTGATTCTCGTGGCGTCA-3'
Ery Forward	5'-ATTTCTCTAGCAGGTGATTTGG-3'
Ery Reverse	5'-ACCCTCTAATCGATATGCATCA-3'
Ac probe	5'-HEX-TCACTGTTGATGGAAAACTTCGGAGA-3IABkFQ-3'
Rhus probe	5'-FAM-AACGAAACGATTAGTAGTCCAACA-3IABkFQ-3'
Tons probe	5'-Cy5-AAATATTCATGAGACAATCAGCAGT-3IAbRQSp-3'

3.2.3 Multiplex qPCR Assay Development

3.2.3.1 Single-plex testing

Three single-plex qPCR reactions were initially tested with the cycling conditions as used for *E. tonsillarum* and *E. rhusiopathiae* in the study conducted by Forde et al (64), modified from Pal et al (2010): denaturation at 95°C, followed by 40 cycles of 95°C for 10 s and then 57°C for 30 s, and fluorescence measurement after each cycle for all three fluorophores (HEX, FAM and Cy5) on a RotorGene Q PCR instrument (Qiagen). The purpose of these test runs was to confirm the assay was functioning correctly within our laboratory set-up, and to determine whether these cycling conditions would be adequate for incorporating the Arctic clone single-plex PCR into the previously described duplex assay which detects *E. rhusiopathiae* and *E. tonsillarum*. The original assay developed by T. Fang used slightly different cycling conditions, which were: 1 cycle of pre-denaturation at 95°C for 3 min, 40 cycles of denaturation at 95°C for 10 s, annealing at 60°C for 10 s and extension at 72°C for 30 s and fluorescence measurement (104). Three different probes and corresponding channels were assigned to each of the three variants of *Erysipelothrix* spp., as described above. All 14 DNA extracts of all three *Erysipelothrix variants* (Table 3-1) were tested against each single plex reaction in three separate runs, one run for each primer and probe combination. This was done to observe for any false positive or false negative amplification off-target. The final 20 µL reaction consisted of 10 µL of Brilliant III Ultra-Fast QRT-PCR Master Mix (Agilent, Santa Clara, USA), 2 µL of

DNA template, 1 µL of each primer (20 µM), 0.1 µL of the corresponding probe (10 µM) and 5.8 µL of nuclease-free water (Table 3-3).

3.2.3.2 Duplex testing

Once the single-plex reactions had been validated to successfully detect their respective targets extracts, duplex testing was conducted on a representative subset of the samples described in Table 3-1 to observe for any interactions between the different primer and probe combinations and for any significant variation in reaction efficiency, potentially represented by deviations of their threshold cycle (C_t) values (i.e., lower efficiency of duplex when compared with single-plex). Three tests were done, each combining two different sets of primer and probe combinations. The cycling conditions were kept the same as the single-plex reactions. The primer and probe combinations used and the volumes of each are described in Table 3-3. The final master mix 20 µL reaction consisted of 10 µL of Brilliant III master mix, 2 µL of DNA template, 1 µL of each primer, 0.1 µL of the corresponding probe and 3.6/5.6 µL of nuclease-free water depending on whether two or one set of primers were used (Table 3-3).

3.2.3.3 Multiplex qPCR development

After testing the duplex reactions and finding no significant deviation of C_t values between the single and duplex qPCRs assays, the testing moved on to the triplex stage where all three reactions were combined into one. All three primer and probe combinations were combined into a single qPCR reaction (Table 3-2). The cycling conditions remained the same as prior tests, with the final master mix containing all 3 primer and probe sets (Table 3-3).

3.2.3.4 PCR protocol

The multiplex protocol was developed and optimised using a QIAGEN Rotorgene-Q machine and accompanying software (198) (QIAGEN, Hilden, Germany) in the OHRBID lab at University of Glasgow. There were two versions of the PCR cycling conditions used during the development of the multiplex qPCR. The initial cycling parameters were taken from Forde et al (2016) (64), as described above (single-plex testing). with 95°C for 3 min for the denaturation step, followed by 40 cycles of 95°C for 10 s and 57°C for 30 s with fluorescence measurement at

the end of this step. The multiplex qPCR mixture had a total volume of 20 µL. The mixture consisted of 10 µL of Brilliant III Ultra-Fast QRT-PCR Master Mix (Agilent, Santa Clara, USA), 3.4 µL of nuclease-free water, 2 µL of the DNA template, 1 µL (20 µM) of each of the forward and reverse primers for Ac and Ery, and 0.2 µL (10 µM) of each of the three multiplex probes (Table 3-2). A negative PCR control was included in each run. The results were analysed using the Rotor-Gene Q Series Software (198) (QIAGEN). The C_t thresholds were set automatically by the software and adjusted manually to reflect the inflection points on the individual amplification curves set based on the log scale visualisation of the fluorescence amplification curves, the threshold value was set at the halfway point of the Log curve of the initial triplex qPCR channel (199). Outlier removal was used to remove background interference, the level was set at 10%. The fluorescence activity of all three channels was recorded for every test regardless of the presence of the primers and probe for that particular channel.

Table 3-3 Volume of the components of the master-mix used in the qPCR. Volumes of the master-mix may change depending on the target of the assay; these are provided as examples. 'Ac' represents *Erysipelothrix rhusiopathiae* Arctic clone, 'Ery' stands for *Erysipelothrix* spp., 'Rhus' stands for *E. rhusiopathiae* and 'Tons' stands for *E. tonsillarum*. Ac primers and probe are limited for reactions that detect the Arctic clone, the Ery primers are universal for all *Erysipelothrix* variants.

	Single-plex (Ac)	**Duplex (Rhus + Tons)**	**Triplex (Ac + Rhus + Tons)**
Reagent	Volume (µL)		
Master mix	10	10	10
Ac Forward (20 µM)	1	0	1
Ac Reverse (20 µM)	1	0	1
Ery Forward (20 µM)	0	1	1
Ery Reverse (20 µM)	0	1	1
Ac Probe (10 µM)	0.2	0	0.2
Rhus Probe (10 µM)	0	0.2	0.2
Tons Probe (10 µM)	0	0.2	0.2
DNA template	2	2	2
Nuclease-free water	5.8	5.6	3.4

3.2.3.5 Triplex PCR Specificity Testing

A series of opportunistically selected DNA extracts from different bacterial species were used to test the *in vitro* specificity of the qPCR triplex assay. These isolates were extracted by a PhD student at the OHRBID lab. The 16 samples included six Gram-positive species, six Gram-negative species and four fungal

species (Table 3-4). An extract of each of the three strains of *Erysipelothrix* from Table 3-1 was included in the qPCR to function as a positive control for the reaction.

Table 3-4 Information of the 16 isolates used for *in vitro* specificity testing. The isolate ID, species and Gram staining results are shown. The default cycling conditions, and triplex master-mix combination were used.

Isolate ID	Species	Gram staining
ATCC 35218	*Escherichia coli*	-ve
ATCC 700603	*Klebsiella quasipneumoniae*	-ve
ATCC 27853	*Pseudomonas aeruginosa*	-ve
ATCC 12453	*Proteus mirabilis*	-ve
ATCC 13076	*Salmonella enteritidis*	-ve
ATCC 8090	*Citrobacter freundii*	-ve
NCTC 12493	*Staphylococcus aureus*-MRSA	+ve
ATCC 9491	*Staphylococcus epidermidis*	+ve
ATCC 19615	*Streptococcus pyogenes*	+ve
ATCC 6303	*Streptococcus pneumoniae*	+ve
ATCC 29212	*Enterococcus faecalis*	+ve
N/A	*Streptococcus agalactiae*	+ve
ATCC 5314	*Candida albicans*	N/A
N/A	*Cryptococcus neoformans*	N/A
N/A	*Rhodotorula mucilaginosa*	N/A
N/A	*Meyerozyma guilliermondii*	N/A

3.2.3.6 Further Assay Optimization

The 100-fold diluted stock of DNA extracts from isolates ID 358-DMX014.2-He (Ac), 620-A1627895 (Nac) and ERY0041 (*E. tonsillarum*) (Table 3-1) were chosen as representatives of the three target strains for the triplex qPCR. Unless otherwise stated, these three isolate DNA extracts were used for the tests described below, including limit of detection, serial dilutions, signal leak and false-positive testing. These tests were aimed to investigate the limit of detection of the triplex qPCR, and the specificity and the sensitivity of each channel to their targets. Depending on the test parameters, these samples were used as the positive controls of the tests or as a representative of a potential 'contaminant' spiked into the DNA extracts to test the specific fluorescence of each channel used.

3.2.3.6.1 Efficiency comparison

To test for any interference or potential loss of efficiency between single-plex, duplex and triplex PCRs in identification of the respective targets, runs of all combinations of the qPCRs were conducted to observe the difference of efficiency at each stage of the qPCR development. The tests comprised single-plex qPCRs of all three channels, three duplex qPCRs of the three available combinations of channels, and a triplex qPCR. The C_t values were used to compare the efficiency between each stage of the qPCR. The six representative isolates described in 3.2.1 were used, and the tests were conducted in the same qPCR run. Seven different master-mixes were made, each with different volumes of components and tailored to the reaction.

3.2.3.6.2 Limit of detection

The limit of detection was determined on a series of decimally diluted DNA. No duplicates of the samples were run; each sample was run individually. Standard curves were constructed automatically using the Rotor-Gene Q software by plotting the C_t values against the calculated DNA concentration of the samples from the original Qubit measurements. The limit of detection was determined as the lowest DNA concentration producing positive amplification on the triplex qPCR. The C_t values of the qPCR were compared to the Qubit results of the DNA extract to identify the detection limit of the qPCR.

3.2.3.6.3 Channel fluorescence interactions

We also wanted to see whether any leakage of fluorescence signal occurred across channels. In particular, we were concerned about the potential for the FAM probe, which normally emits strong fluorescence at 520 nm (detected on the green channel), to ‘leak’ fluorescence signal, i.e. that is incorrectly detected by neighbouring channels, particularly the yellow channel that should detect HEX (556 nm) (200,201). Fluorescent signal leakage was tested by comparing two runs of an Nac isolate. Two sets of the serially diluted Ery Nac were aliquoted into the respective PCR tubes, and two different master mixes were made: one containing all primers and probes for the triplex qPCR and one containing everything in the reaction apart from the 0.2 µL of FAM probe, which was replaced with the same volume of nuclease-free water.

3.2.3.6.4 Detection of mixed strains

Previous work has suggested that samples collected from wildlife may contain both *E. rhusiopathiae* and *E. tonsillarum* (25) or multiple strains of *E. rhusiopathiae* (e.g. Ac and Nac) simultaneously (Wooten et al., unpublished data). To test the ability of the triplex qPCR to detect and distinguish among two different targets simultaneously (e.g. in total DNA extracted directly from animal and environmental samples), a series of two 'co-infection' tests were conducted. We aimed to test whether low levels of Ac or *E. tonsillarum* DNA could still be detected in the presence of larger amounts of Nac DNA.

Two qPCR runs were conducted; each consisted of a serial dilution of either *E. rhusiopathiae* Ac or *E. tonsillarum*. To each PCR tube of both dilutions, 2 µL of 100-fold diluted Nac added. The same cycling parameters were used as for the triplex described above in '3.3.3.4 PCR protocol'. The volumes of the master-mix for the qPCR were adjusted to allow for 4 µL of DNA templates when two DNA samples were added to the reaction mix, reducing the volume of nuclease-free water from 3.4 µL to 1.4 µL.

Any amplification that did not follow the conditions detailed in Table 3-5 would be considered an outlier (i.e. potential mixed infection). Any amplification in the yellow or red channels was classified as having the presence of Ac or Tons.

Table 3-5 Summary of the primer and probe combinations for each target strain. Each row details which primer and probe combination would be expected to bind and amplify the DNA of that strain. Ery primers bind to all *Erysipelothrix* spp. 'Y' means yes, 'N' means no.

			Yellow channel	**Green channel**	**Red channel**
Target	Ac primers	Ery primers	Ac probe (HEX)	Rhus probe (FAM)	Tons probe (Cy5)
***E. rhusiopathiae* Arctic clone (Ac)**	Y	Y	Y	Y	N
E. rhusiopathiae	N	Y	N	Y	N
E. tonsillarum	N	Y	N	N	Y

3.2.3.7 Testing of false positives

A collection of isolate DNA was received from collaborators at the Kutz group from the University of Calgary to the OHRBID lab as part of a related project. All the extracts were whole genome sequenced on an Illumina platform, and a single-plex qPCR for the Arctic clone was run in the meantime. Certain isolates (Table 3-6) were shown to deviate from the sequencing data, wherein amplification of the Ac target was observed for extracts whose sequencing results showed them to be other strains/species; we refer to these four isolates from hereon as 'imposters'. The triplex qPCR was used to determine if the new reaction assay could illuminate the problem with the initial discrepancies between qPCR and sequencing results of the imposter isolates. These four samples were put through the triplex qPCR along with four other suspected Ac extracts.

To assess the relationship between DNA concentration and C_t value, a standard curve was constructed by plotting the C_t values of the *E. rhusiopathiae* qPCR (yellow channel) vs. the respective DNA concentrations as measured by the HS dsDNA Qubit for each isolate. We theorised that if the 'imposters' fall outside of the C_t trend while having similar DNA concentrations as DNA from pure isolates, this would indicate differences in copy numbers of the *hhalM-1* gene (i.e. that not all bacteria extracted were Ac and represented contamination). The following experiments were conducted to better understand the reasons for these unexpected 'false positive' amplifications.

Table 3-6 Isolate information of the *Erysipelothrix* spp. extracts which generated inconclusive results on the qPCR ('imposters'). The isolate ID, sample collection year and the host sources of the isolates were provided by collaborators from the University of Calgary.

Isolate ID	Collection year	Isolate host source	Whole genome sequencing results
659-MX-WilRiv-BM	2022	Muskox	*E. rhusiopathiae* non-Arctic clone
637-BIS-22-779-Spleen	2022	Bison	*E. rhusiopathiae* non-Arctic clone
616-Bathurst-BM – Rib	2022	Muskox	*E. rhusiopathiae* non-Arctic clone
683-PB-Skin	2023	Polar bear	*E. tonsillarum*

3.2.3.7.1 Troubleshooting of Arctic clone 'imposters'

3.2.3.7.1.1 Cycling parameters

Upon re-examination of the reference guide for the Brilliant III Ultra-Fast QRT-PCR Master Mix (202), it was discovered that the recommended temperature profile for the mixture differs from the initial qPCR cycling conditions, specifically the annealing step. It was recommended that the annealing stage should remain as close to 60°C as possible and should only be between 10-20 s (202). From this point on, the following conditions were used (i.e. final cycling parameters): 95°C for 3 min, followed by 40 cycles of 95°C for 10 s followed by 60°C for 20 s.

3.2.3.7.1.2 Primer redesign

Due to the amount of qPCR tests being run, over time, a series of qPCR tests showed signs of contamination, most likely due to the opening of the nested qPCR tubes (associated with other experiments not shown). All samples, including the negative qPCR controls, had late amplification in the yellow channel, with the Arctic clones at around C_t 12 to 14, imposters at around C_t 23 to 27 and the negative controls at ~C_t 34. Since the yellow channel was Ac specific, it was theorised that there were Ac amplicons in the lab environment. To counter the issue, it was decided that a new forward primer should be designed to increase the specificity of the qPCR protocol and avoid amplification of any pre-existing amplicons. Using the sequence of the Ac amplicon from the *hhalM*-1 gene, the initial binding location of the forward and reverse primers and the probe were identified using SnapGene and Geneious Prime (203,204). A new forward primer was developed designed to target the sequence just upstream of the original amplicon, and the compatibility of the melting temperature and the self-complementarity were tested using the primer design tool provided on the National Library of Medicine website (196). The new forward primer increased the amplicon length by 22 bases, which brought the amplicon length to 133 bases.

3.2.3.7.1.3 Outlier identification

A scatterplot of Ac amplification was generated by plotting the C_t values obtained on the yellow channel against a) C_t values obtained on the green channel and b) the respective DNA concentrations. Using the Qubit High Sensitivity DNA quantification kit, the DNA concentration of 20 Ac isolate

extracts, including the selection mentioned in Table 3-1 were measured, along with the isolates described in Table 3-6. Using the C_t values of the same isolates obtained from the yellow channel of the triplex qPCR, two scatterplots were generated ion Microsoft Excel and a trendline was used to help identify outliers.

Using R studios (R version 4.3.1), an Analysis of Variance (ANOVA) test was conducted to determine whether the differences between the C_t values of the 20 Ac isolates and the four 'imposters' were statistically significant. The ANOVA test compared the mean of two independent groups (205). The R codes shown below (Table 3-7) were used to generate a p-value, where a value less than 0.05 means that the difference between the two groups was significant and not due to chance.

Table 3-7 Codes used in R studio to perform an Analysis of Variance (ANOVA) test. These codes were used for within R studio 2025.05.1 Build 513, using R version 4.3.1.

data$Ct <- as.numeric(ANOVA_AC$Ct)
data$group <- factor(ANOVA_AC$Group, levels = c("Ac", "Imp"))
aov_mod <- aov(Ct ~ Group, data = ANOVA_AC)
summary(aov_mod)

3.2.3.7.1.4 Sequencing data

To further investigate the reasons behind the amplification of the Ac amplicon in genomes that did not classify as the Ac in the WGS data, the existing genomic data were analysed to identify any sequences with close matches with the primer and probes used for the qPCR assay. The raw read files (fastq) and assembly DNA sequences (fasta and GenBank formats) of the four isolates were obtained from the biotech company MicrobesNG, (Birmingham, UK). BLAST searches were conducted using Geneious Prime, wherein the primers, then later the full amplicon sequence, were searched for within the genome assembly.

After the analysis of the sequencing data, it was decided that there was a high probability that the DNA extracts of the imposter isolates were contaminated prior to the qPCR assays. The original bacterial isolates, which were stored in the -80°C freezer in the lab, were located and thawed. The cryotubes were vortexed, then a 10 µL sterile plastic inoculation loop (VWR International, Radnor, USA) was submerged in the tube and swabbed on a 5% Columbia sheep blood agar plate (SBA) (EO LABS, Stirlingshire, Scotland) using the quadrant streaking technique. The SBA plates were incubated overnight at 37°C and a

single colony was sub-cultured onto another SBA plate but this time the colony was streaked across the entire SBA plate and left to incubate for another 24 h at 37°C. The final sub-cultured bacterial isolate was then collected using an autoclaved cotton swab and suspended in 200 µL of sterile phosphate-buffered saline (PBS) to be extracted using a QIAGEN DNeasy Blood and Tissue kit (QIAGEN, Hilden, Germany). The 'Purification of Total DNA from Animal Blood or Cells (Spin-column Protocol)' provided with the kit was used to extract the DNA from the *Erysipelothrix* spp. colonies. The eluted DNA was stored in autoclaved sterile 1.5 mL Eppendorf tubes in the -20°C freezer for later use.

3.2.3.7.1.5 Digital PCR

An opportunity to utilise digital PCR (DPCR) to confirm the suspicion of post-extraction contamination was brought up within the School of Biodiversity, One Health and Veterinary Medicine (SBOHVM) at the University of Glasgow. A QIAGEN QIAcuity dDPCR machine (185) was lent to a neighbouring lab at SBOHVM as a demo machine. The following samples were tested: two of the imposter DNA extracts (Table 3-6), along with two Ac and two Nac extracts (Samples 1,2,7,8, Table 3-1). The original contaminated extracts of the imposters were used, as the purpose of the DPCR testing was to identify the copy number of the Ac amplicon in each of the extracts. The qPCR protocol and reaction mix were adapted to suit the requirements of the DPCR system. Each reaction mix was limited to 12 µL per well. QIAcuityDx Universal MasterMix, provided by QIAGEN, was used. The volume of reagents used is detailed in Table 3-8. The new cycling conditions established in the cycling parameters section 3.3.3.7.1.1 above were used. The QIAcuity Software Suite was used to analyse the results of the DPCR. A triplex qPCR of the same samples was conducted to obtain a correlation between C_t of the current triplex qPCR and the copy number obtained from the results of the DPCR. The Qubit results of the extracts, the C_t values of the qPCR and the copy number from the DPCR were used in conjunction with each other to confirm whether the 'false positives' were due to contaminated extracts and to establish a standard curve to root out future false positives/mixed infections.

Table 3-8 Digital polymerase chain reaction (DPCR) reagent mix used in the identification of copy numbers of *Erysipelothrix rhusiopathiae* and Arctic clone (Ac) amplicons.

Reagents	Volume per well (µL)
DPCR master-mix	3
E. rhusiopathiae Ac forward primer (20µM)	0.6
E. rhusiopathiae Ac reverse primer (20µM)	0.6
Erysipelothrix spp. (Ery) forward primer (20µM)	0.6
Erysipelothrix spp. (Ery) reverse primer (20µM)	0.6
E. rhusiopathiae Ac probe (HEX) (10µM)	0.12
E. rhusiopathiae probe (FAM) (10µM)	0.12
DNA template	2
Nuclease-free water	4.36

3.2.4 Diagnostic application of the developed triplex qPCR

The opportunity to test the triplex qPCR assay for diagnostic samples was presented during my 3-month exchange to the University of Calgary. A collection of samples (n = 606) collected in 2024 from the Canadian Arctic region were selectively cultured by me and Caide Wooten, the PhD student in charge of the outbreak investigation, for *E. rhusiopathiae*. The method includes the homogenisation of 1 g of tissue in 10 mL of brain-heart infusion broth (BHIB) supplemented with 5% horse serum (HS) using a gentleMACS™ Octo Dissociator with Heaters (Miltenyi Biotec, Inc., San Diego, CA, USA), followed by incubation at 5% CO_2 at 37°C for 24 h in 10 mL of BHIB with 5% HS. A selective broth containing the following was prepared: 5% HS + BHIB, kanamycin (40 µg/mL), neomycin (50 µg/mL) and vancomycin (25 µg/mL). From the 24-h culture with the 10 mL of 5% HS + BHIB, 0.3 mL was aliquoted into 2.7 mL of the selective broth and incubated with at the same conditions as before for 72 h. A selective agar was prepared containing 5% HS + BHI agar, the same concentrations of the three antibiotics, 1 ml/l of 1 % crystal violet solution and 1 g/l of sodium azide. After the plates were set, 100 µL of the 72-h selective culture was plated on the agar and incubated in the same conditions for another 72 h. Any colonies observed after the incubation period were sub-cultured onto a SBA plate and incubated overnight in at the same incubator conditions (62,206,207). The resulting colonies were then collected and stored in a 20% glycerol solution to be stored in -80°C for DNA to be extracted later. A KingFisher Apex System (ThermoFisher Scientific, Waltham, MA, USA) was used to extract the DNA from

both culture positive and culture negative all samples along with *E. rhusiopathiae* isolates collected from the Canadian Arctic in 2024.

Using the MagMAX™ CORE Nucleic Acid Purification Kit (Applied Biosystems, Foster CIty, CA, USA), all collected samples were extracted for qPCR. The triplex qPCR protocol was adapted to suit the availability of equipment and resources in this lab. Due to the use of a different qPCR machine, QuantStudio™ 5 system (ThermoFisher Scientific, MA, USA), a new fluorophore was used for the Arctic clone channel, moving from HEX to TAMRA. Instead of the Rotorgene-Q machine developed by QIAGEN, the qPCR machine in the Calgary lab used was the QuantStudio™ 5 system (ThermoFisher Scientific, MA, USA). The qPCR cycling conditions and master-mix volumes remained the same as the final Glasgow protocol. The mastermix used was the TaqMan® Fast Advanced Master Mix (Applied Biosystems). All results were analysed using QuantStudio™ Design and Anaylsis Software (version 1.5.3).

A collection of 367 DNA extracts from a mixture of isolates and samples that had previously tested positive with *E. rhusiopathiae* qPCR were also tested on the triplex qPCR to determine whether the isolates were Ac.

3.3 Results

3.3.1 Single-plex qRCR

Three single-plex qPCRs were run, using cycling conditions described in the 'Single-plex testing' section 3.2.3.1 in the Methods section. All three fluorophores were tested on in their corresponding fluorescence channel to test the cycling conditions and the probes' reaction efficiency. The colour scheme used to represent the test results corresponds to the expected channel of amplification: the Ac amplicon amplification curves were colour coded to be orange (for better visualisation than yellow), *E. rhusiopathiae* (any strain) was coloured green, and *E. tonsillarum* was coloured red. In this way, if there were a mismatch of the colours of the amplification curve compared to the channel colour, it would be clear that there was a false positive amplification. All single-plex reactions (Figure 3-2) showed amplification of the correct targets: on the red channel, only *E. tonsillarum* samples amplified, on the green channel, both *E. rhusiopathiae* Ac and Nac amplified, on the yellow channel, all Ac samples amplified. Since the correct targets were amplified in their corresponding channel, it was concluded that the cycling conditions work for all three primer and probe sets and could be used for the triplex and that the duplex series of tests could move forward.

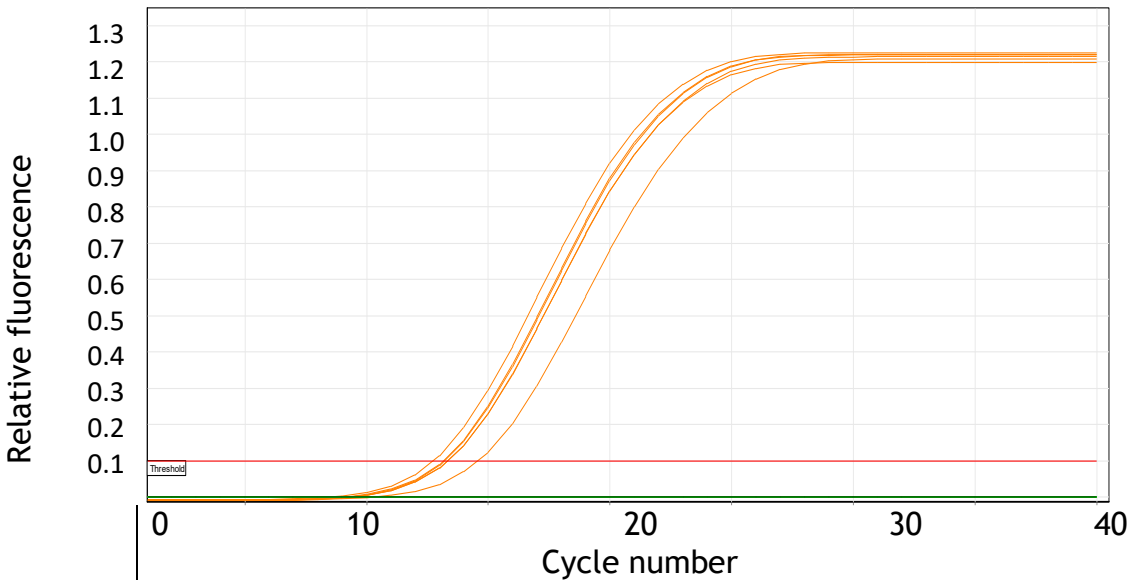

A) Yellow channel (Arctic clone specific)

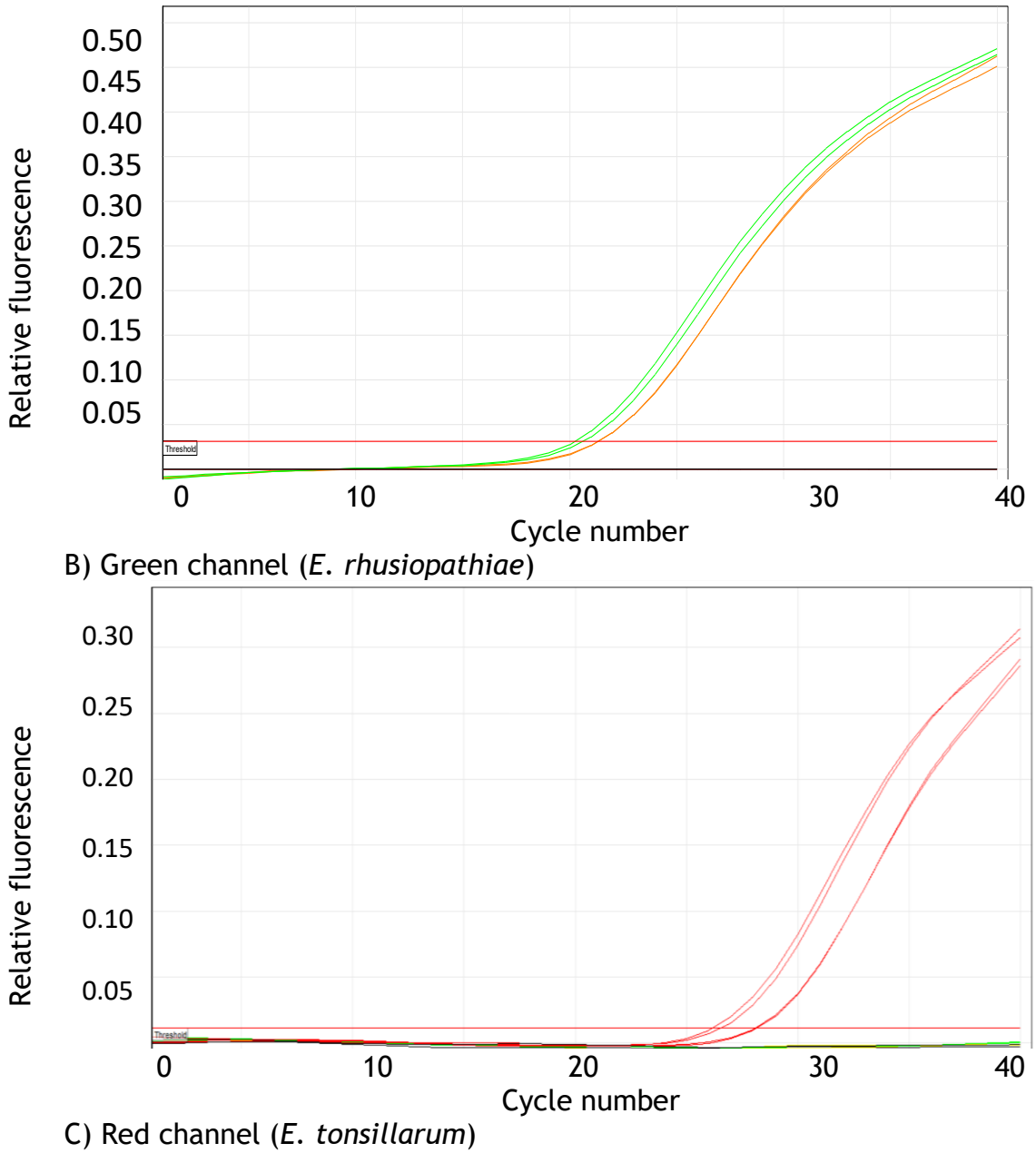

Figure 3-2 Amplification curves of three single-plex qPCR assays on their target channels. The different colours used represent the predicted channel of amplification. A) Arctic clone (Ac) samples in the yellow channel; B) *Erysipelothrix rhusiopathiae* samples in the green channel; C) *E. tonsillarum* in the red channel. Each reaction showed amplification of the target strain, and no non-specific amplification. All qPCR reports were subjected to 10% outlier removal using the Rotorgene Q series software.

3.3.2 Duplex qPCR

Duplex qPCRs were conducted to observe any potential interactions between two different channels and to observe fluorescence signal leaks. All qPCRs share the same cycling conditions but different primers and probes depending on the targeted reaction. The C_t of the duplex reactions were summarised in Table 3-9 and shown in Figure 3-3. The first two duplex assays showed amplification of all the expected samples. The final test, between Ac and *E. tonsillarum* showed unexpected amplification of Nac and *E. tonsillarum* samples in the yellow channel (panel E, Figure 3-3). The unexpected amplification observed was likely due to the template spilling over between the qPCR tubes (i.e. cross-contamination). As a precaution, new aliquots of the reagents were made before proceeding with the triplex series of testing to correct any potential issues of contamination.

Table 3-9 Summary of the threshold cycle (C_t) of the three duplex qPCR tests using isolate DNA extracts from *Erysipelothrix rhusiopathiae* Arctic clone (Ac), non-Arctic clone (Nac) and *E. tonsillarum* (Tons). Panels with N/A shows expected lack of amplification and panels with * shows unexpected amplification.

Target	Yellow channel	Green channel	Red channel
Duplex of Ac and Nac			
E. rhusiopathiae (Ac) (1&2)	17.84/17.61	23.90/23.62	N/A
E. rhusiopathiae (Nac) (7&8)	N/A	22.87/22.59	N/A
E. tonsillarum (13&14)	N/A	N/A	N/A
Duplex of Nac and Tons			
E. rhusiopathiae (Ac) (1&2)	N/A	19.55/19.22	N/A
E. rhusiopathiae (Nac) (7&8)	N/A	18.40/17.99	N/A
E. tonsillarum (13&14)	N/A	N/A	27.87/27.33
Duplex of Ac and Tons			
E. rhusiopathiae (Ac) (1&2)	7.19/9.87	N/A	N/A
E. rhusiopathiae (Nac) (7&8)	31.01/27.15*	N/A	N/A
E. tonsillarum (13&14)	24.63/24.45*	N/A	21.16/21.96

Duplex of Ac and Nac

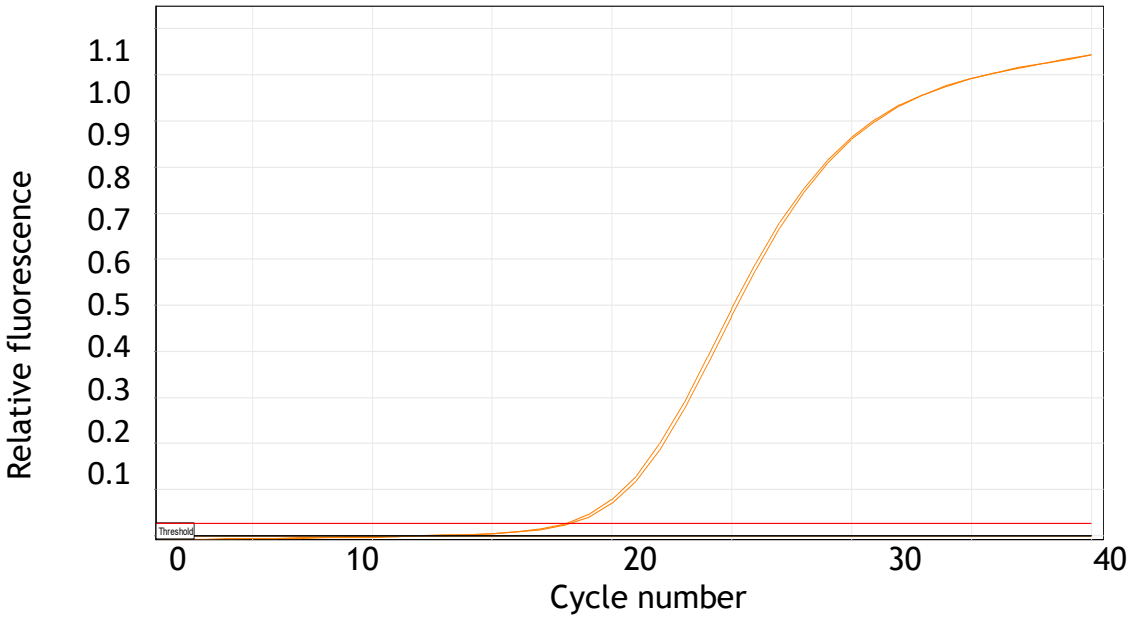

A) Yellow channel (Arctic clone specific)

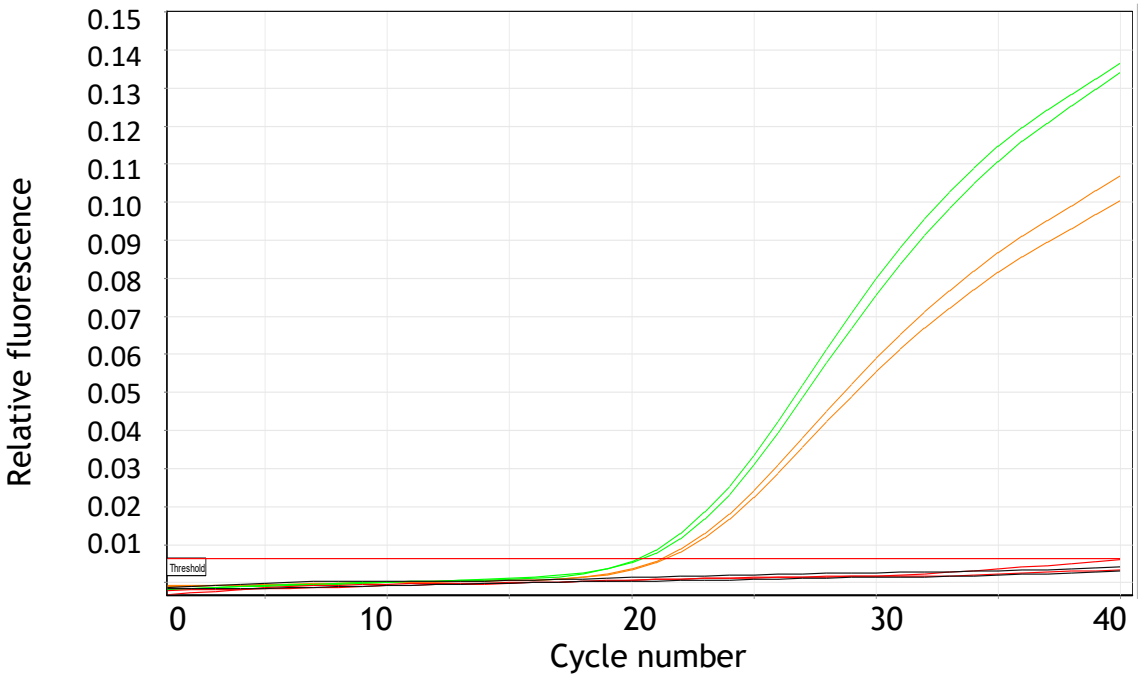

B) Green channel (*E. rhusiopathiae*)

Duplex of Nac and Tons

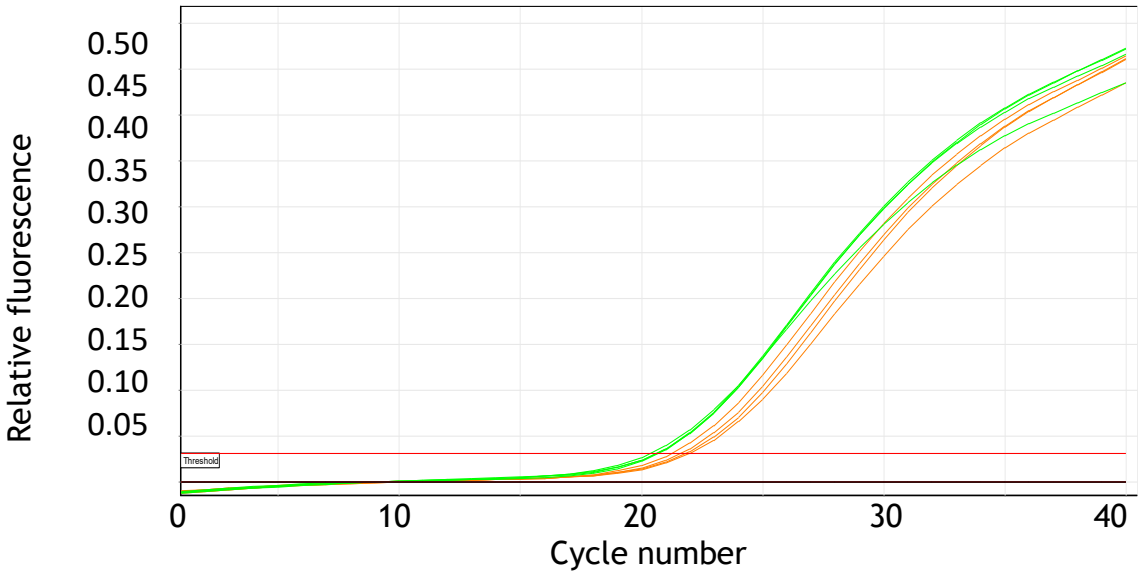

C) Green channel (*E. rhusiopathiae*)

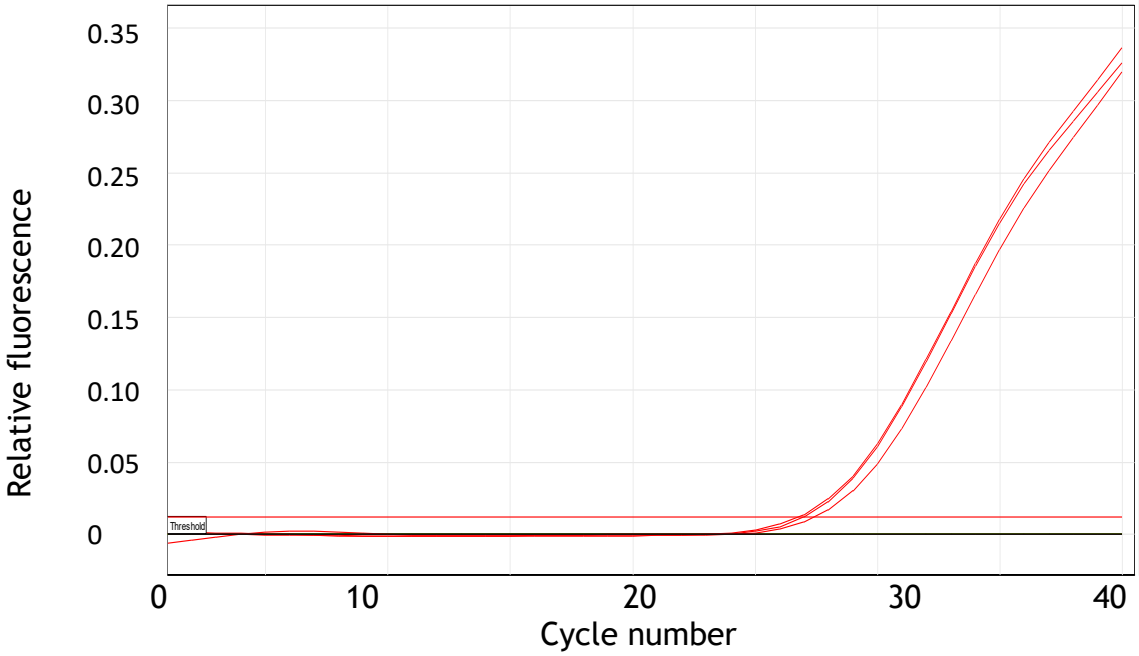

D) Red channel (*E. tonsillarum*)

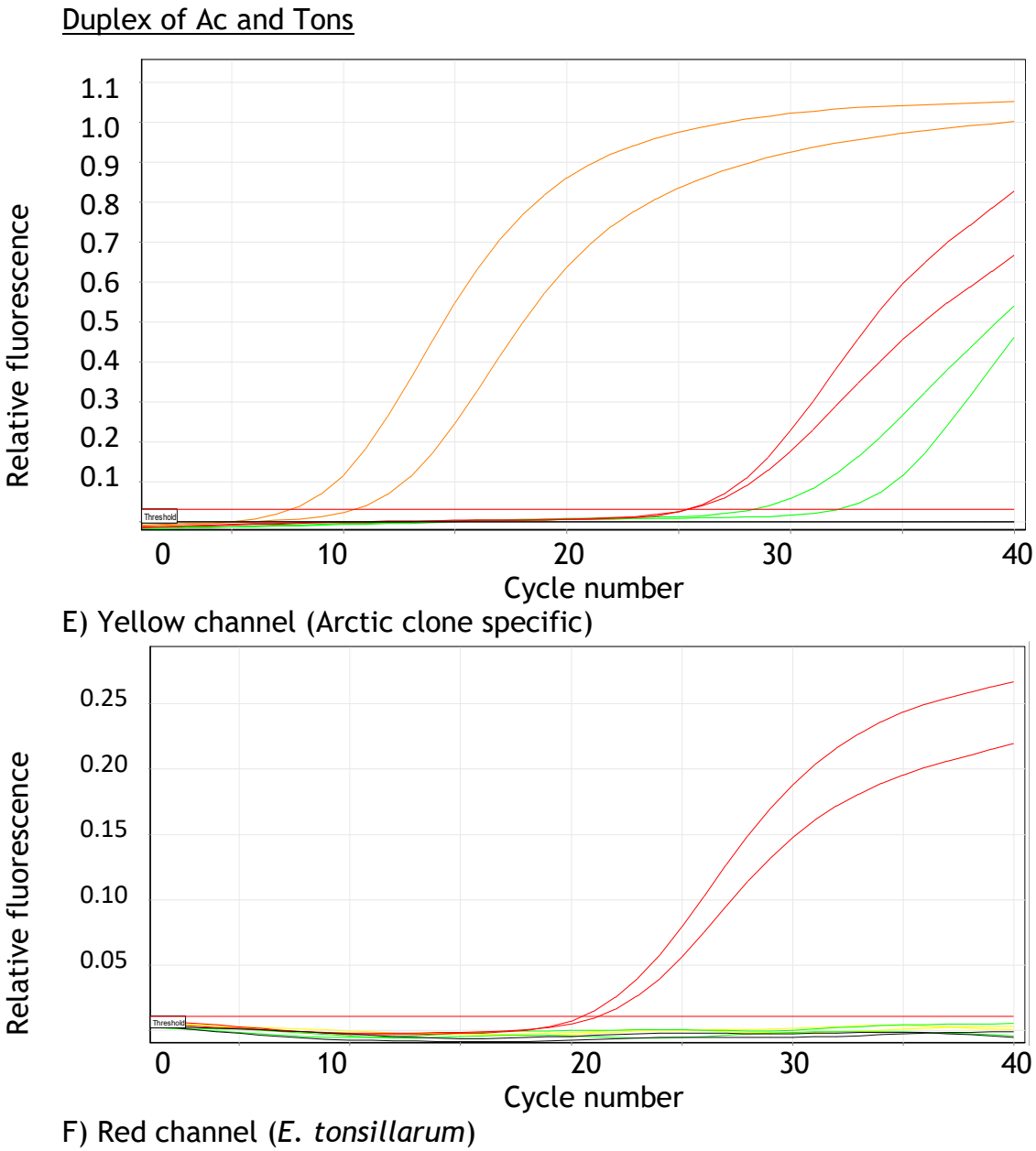

Figure 3-3 Duplex qPCR reactions of the three different combinations of primers/probes. All three combinations of the three targets were tested in the same run to observe interactions between the channels. DNA extracts representing all three *Erysipelothrix* variants were included in each duplex reaction. Top row represents the combination of *Erysipelothrix rhusiopathiae* Arctic clone (Ac) and non-Arctic clone (Nac). Middle row represents the combination of Nac and *E. tonsillarum* (Tons). Bottom row represents Ac and Tons. Orange amplification curves are Ac, green are Nac and red are Tons.

3.3.3 Triplex qPCR

All three sets of the primers and probes were combined into the same master-mix for the first test of the qPCR triplex. The threshold used to determine the C_t was different for each channel based on numerous factors, including but not limited to the signal strength of the fluorophores, the qPCR machine and the property of the DNA template. The yellow channel (Ac) threshold was set at 0.02, the green channel (Ery) was set at 0.012 and the red channel (Tons) channel threshold was set at 0.016 and Figure 3-4 shows the C_t and the three amplification curves generated by the same run of a single qPCR, using the representative subset of two samples from each strain type in Table 3-1 described in 3.3.1. The triplex results showed that the contamination observed in the duplex runs was eliminated by making new aliquots of reagents and taking care during addition of DNA template. The results observed show that the triplex qPCR can differentiate between the three different strains using the current cycling conditions.

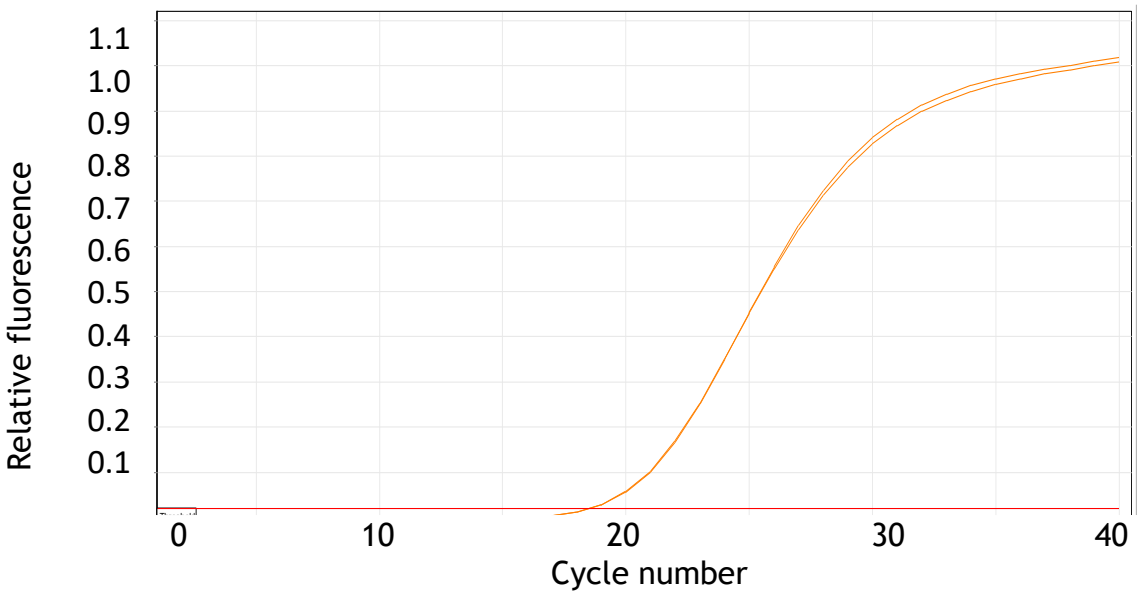

A) Yellow channel (Arctic clone specific)

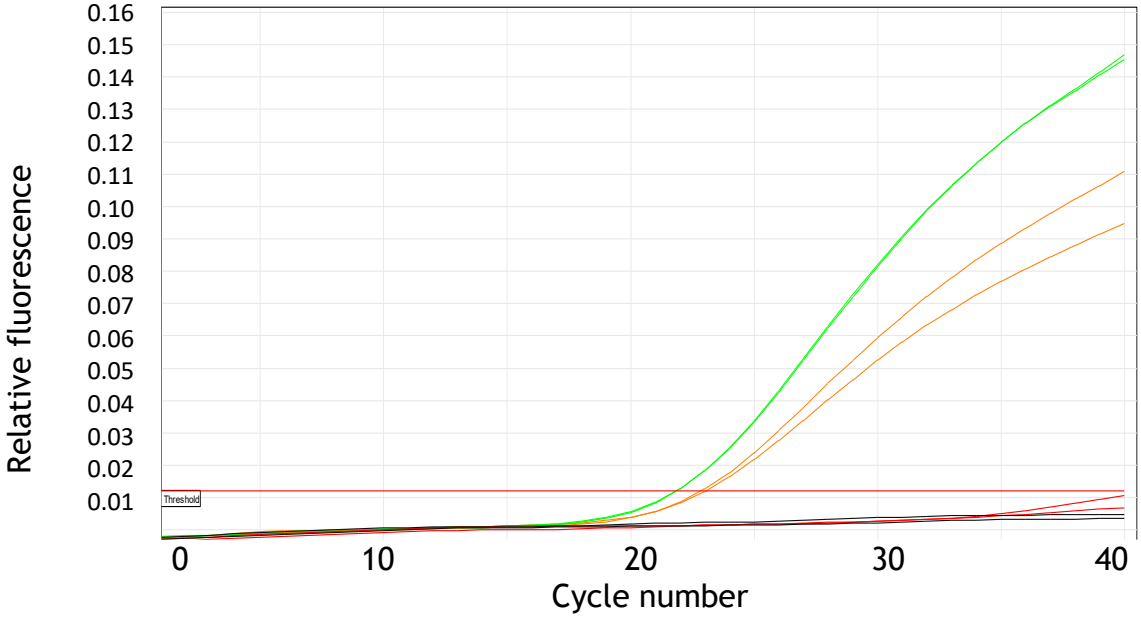

B) Green channel (*E. rhusiopathiae*)

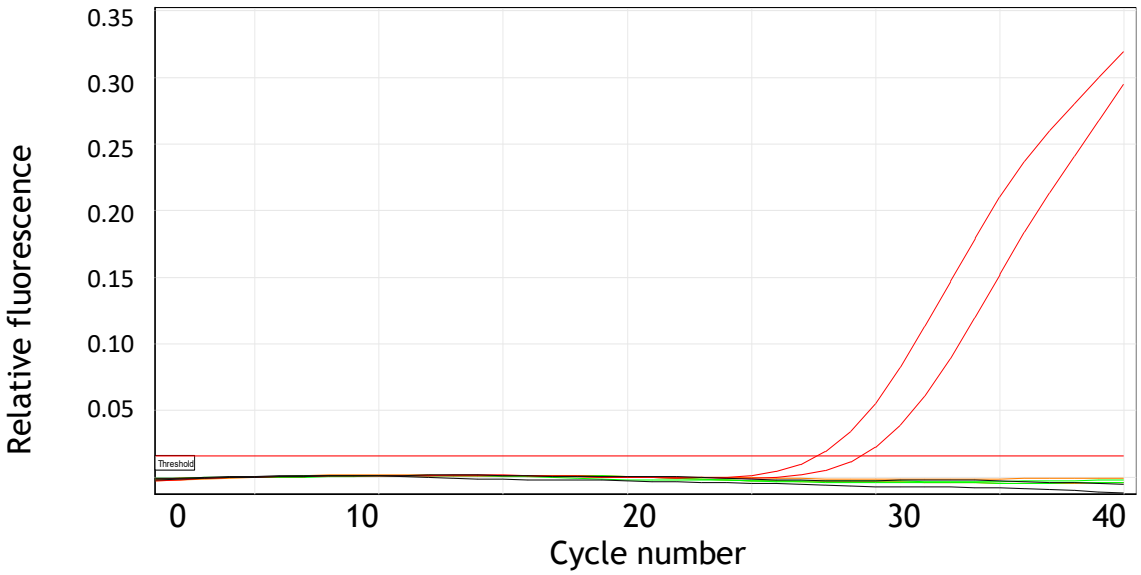

C) Red channel (*E. tonsillarum*)

Figure 3-4 Amplification curves of all three channels of the triplex qPCR. Panel A shows the yellow channel, Panel B the green channel, and Panel C the red channel. All three channels were subjected to 10% outlier removal. All *Erysipelothrix rhusiopathiae* Arctic clone samples were colour coded with orange, *E. rhusiopathiae* non-Arctic clone samples were coloured green and *E. tonsillarum* were coloured red.

The Qubit HS dsDNA kit was used to determine the concentration of the DNA extracts. The concentration of the extracts was calculated by dividing the original Qubit concentration by 100 to account for the 100-fold dilution. The generated C_t values were compared against the respective DNA concentrations of the samples used in the qPCR Table 3-10. The more notable difference in concentration between the samples 7 and 8 (6.7×10^{-3} vs. 5.82×10^{-2} ng/μl) was not sufficient to be reflected in the difference of C_t in the triplex qPCR in the green channel (21.86 vs. 21.84).

Table 3-10 Comparison of DNA concentrations with threshold cycle (C_t) values from the triplex qPCR. The DNA concentration was determined using a Qubit High Sensitivity kit, measured on the original DNA extract and adjusted based on the dilution factor. Ac stands for *Erysipelothrix rhusiopathiae* Arctic clone, Nac stands for non-Arctic clone. The numbers in the 'Target' column represents the sample numbers as shown in Table 3-1. N/A = no amplification.

Target	DNA concentration (ng/μL)	C_t Yellow channel	C_t Green channel	C_t Red channel
E. rhusiopathiae **(Ac) (1&2)**	7.84×10^{-2}/ 7.39×10^{-2}	18.61/18.57	22.84/23.01	N/A
E. rhusiopathiae **(Nac) (7&8)**	6.7×10^{-3}/ 5.82×10^{-2}	N/A	21.86/21.84	N/A
E. tonsillarum **(13&14)**	2.36×10^{-2}/ 6.3×10^{-3}	N/A	N/A	29.46/27.70

3.3.4 Further assay optimisation

3.3.4.1 Specificity testing

To test the specificity of the triplex qPCR, a selection of 16 isolates (Table 3-4) were tested, alongside three positive controls, one representing each of the three targets of the triplex qPCR. All three positive controls amplified, while none of the negative qPCR controls amplified. None of the 16 test isolates showed up on any of the three channels.

3.3.4.2 Efficiency comparison

A comparison to identify any potential loss of qPCR efficiency was conducted using the C_t values of six isolate extracts representing the three targets. The results summarised in Table 3-11 showed no observable loss of qPCR efficiency in

the yellow and green channel, while the red channel suffered a small loss of qPCR efficiency.

The C_t differences observed were between 0.13 to 0.25 cycles for the two Ac samples on the yellow channel across runs; and between 0.02 to 0.14 on the green channel. C_t values differed between 0.1 and 0.48 between the two Nac samples, with the biggest difference observed was between the duplex (10.61) and the triplex (11.09) assays. On the red channel, the two *E. tonsillarum* samples had a difference of 0.94 to 1.5 C_t, which was the biggest deviation observed.

Table 3-11 Threshold cycle comparison between *Erysipelothrix* spp. extracts on single-plex, duplex and triplex qPCR. The three strains include *E. rhusiopathiae* Arctic clone (Ac), *E. rhusiopathiae* non-Arctic clone (Nac) and *E. tonsillarum* (Tons). The DNA concentration was obtained using the Qubit High Sensitivity DNA quantification kit. The single-plex, duplex and triplex qPCRs were run in the same run, using the same DNA extracts, with different prepared master mix. The threshold values to determine the threshold cycle (C_t) were 0.02 for the yellow channel, 0.012 for the green channel and 0.016 for the red channel. N/A: not applicable; samples not included on respective single-plex run.

	DNA concentration (ng/µL)	Single-plex C_t	Duplex C_t	Triplex C_t
Yellow channel				
358-DMX014.2-He (Ac)	7.84	7.16	7.14	7.03
358-DMX07.1-Lu (Ac)	7.39	9.85	9.89	9.64
Green channel				
358-DMX014.2-He (Ac)	7.84	N/A	7.03	7.17
358-DMX07.1-Lu (Ac)	7.39	N/A	10.54	10.52
620-A1627895 (Nac)	16.2	10.38	10.30	10.28
622-2019384 (Nac)	10.3	11.01	10.61	11.09
Red channel				
ERY0041 (Tons)	2.36	20.08	20.84	21.02
ERY0037 (Tons)	0.63	21.01	21.84	22.51

3.3.4.3 Limit of detection

Three samples, one representative for each of the target strains – sample 1 (Ac), sample 7 (Nac) and sample 13 (Tons) for the triplex qPCR – were serially diluted and subjected to the qPCR to identify the limit of detection of the protocol (Figure 3-5). The triplex qPCRs could each detect as little as 10^{-4} of the original DNA stock concentration (Figure 3-5). The Ac qPCR (yellow channel) detection limit was 7.84×10^{-6} ng/µL of DNA, the *E. rhusiopathiae* qPCR (green channel) detection limit was 6.7×10^{-8} ng/µL of DNA, and the *E. tonsillarum* qPCR (red

channel) detection limit was 2.36×10^{-5} ng/µL of DNA. The R^2 value shown in the standard curve shows how well each dilution fits within the standard curve, with 1 being a perfect fit. The efficiency of each qPCR channel was also calculated, with 1 being 100% efficient.

When comparing the C_t difference between the two channels (yellow and green) on which the Ac is detected, the relationship stayed consistent, with yellow amplifying around 5.3 cycles sooner than for the same dilution factor on the green channel (Table 3-12).

Table 3-12 Threshold cycle (C_t) difference of *Erysipelothrix rhusiopathiae* Arctic clone (Ac) serial dilution on different channels. The number in the 'Target' column shows the dilution factor of the original DNA extract: 10^2-fold means it was 100-fold diluted. The 'C_t difference' column was calculated by subtracting the yellow channel C_t from the green channel C_t.

Target	Yellow channel C_t	Green channel C_t	C_t difference
Ac 10^2-fold	18.17	23.46	5.29
Ac 10^3-fold	21.45	26.74	5.29
Ac 10^4-fold	24.89	30.07	5.18
Ac 10^5-fold	28.26	33.66	5.40
Ac 10^6-fold	31.24	36.74	5.50

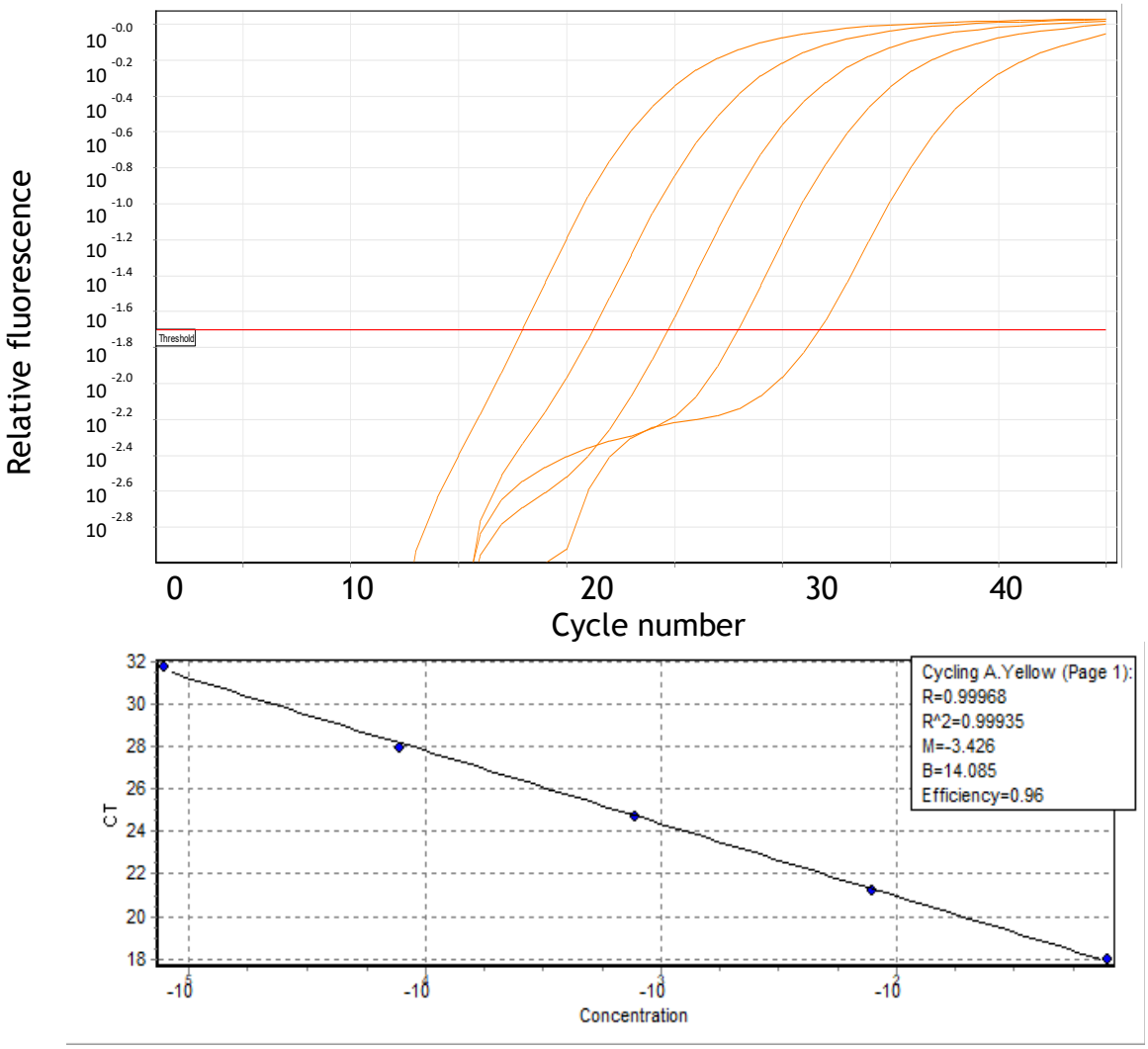

A) Yellow channel

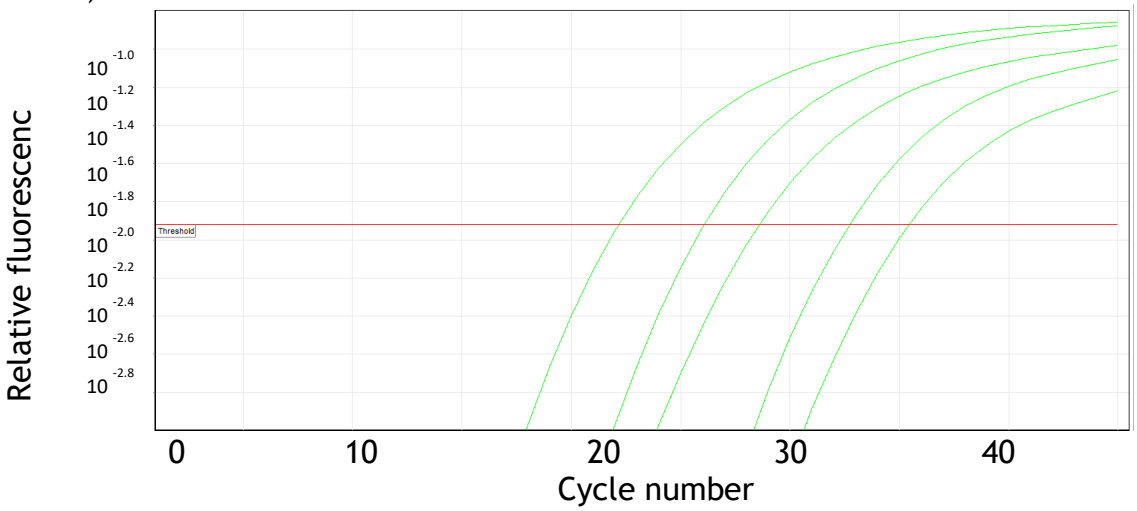

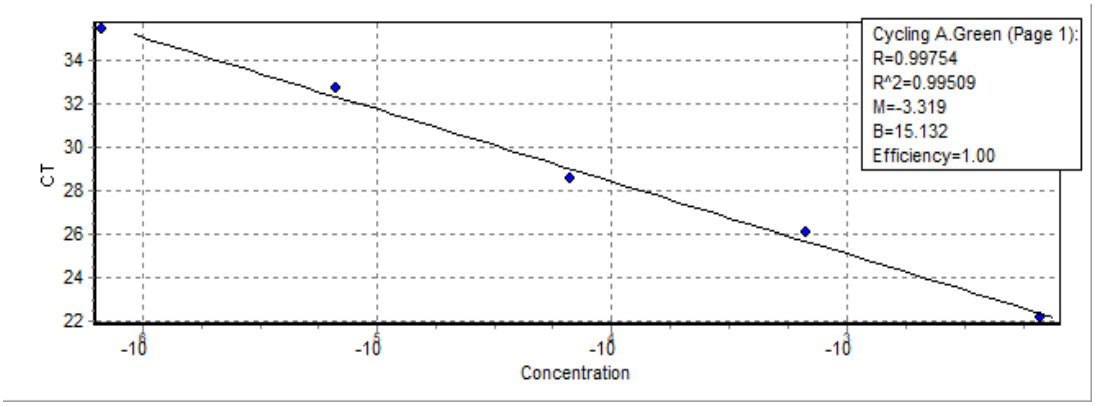

B) Green channel

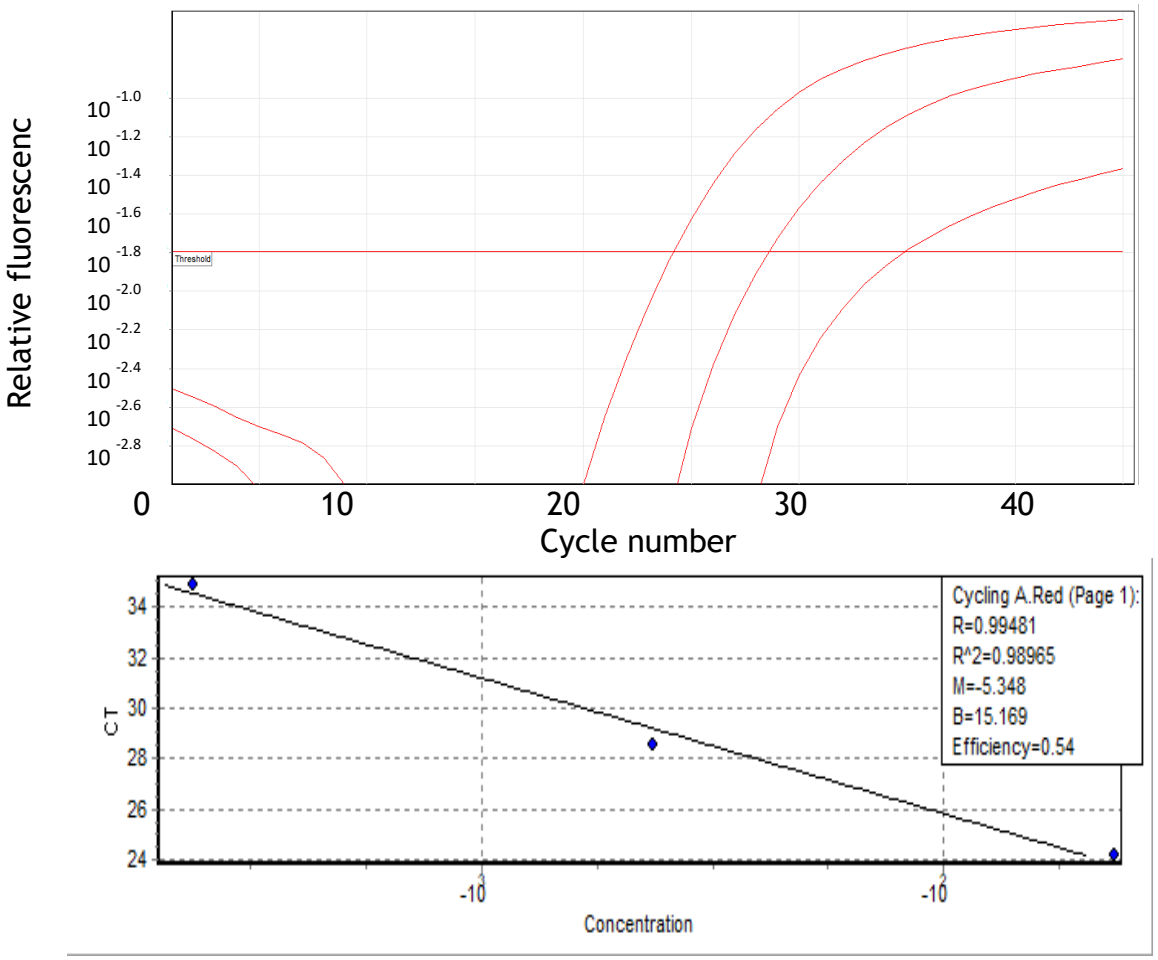

C) Red channel

Figure 3-5 Serial dilution of on-target DNA for all three triplex qPCR channels. Amplification curves (in log-scale) are shown in Panel A for the yellow channel, Panel B for the green channel and Panel C for the red channel. All *Erysipelothrix rhusiopathiae* Arctic clone (Ac) samples were colour coded with orange, *E. rhusiopathiae* non-Arctic clone (Nac) samples were coloured green and *E. tonsillarum* were coloured red. For each series of amplification curves, the curve with the lowest C_t has the highest concentration, going from a dilution factor of 10^{-2} on the left to 10^{-4} for *E. tonsillarum* and 10^{-6} for Ac and Nac. The standard curves shown below each amplification curve were generated by the Rotorgene qPCR software using the DNA concentrations obtained through Qubit.

3.3.4.4 Channel fluorescence interactions

To test if there were signal leaks from the strongest fluorophore, FAM (208), two serial dilutions of Nac were subjected to the triplex qPCR, one with the FAM (Ery) probe and one without (Figure 3-6). In the yellow channel (Panel A), only the Ac controls amplified (green and orange), and in the red channel (Panel C), there were no amplifications. In the green channel, the serial dilution of Nac with the FAM probe was detected, along with the Ac positive control with the FAM probe. The same samples were not detected in the other channels, which meant that there were no signal leaks in the triplex qPCR.

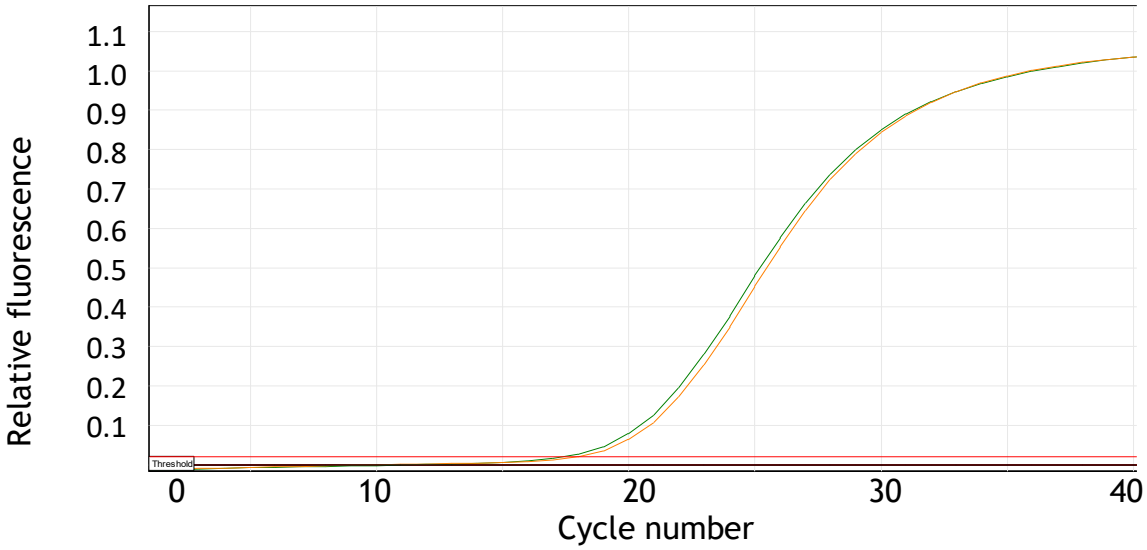

A) Yellow channel

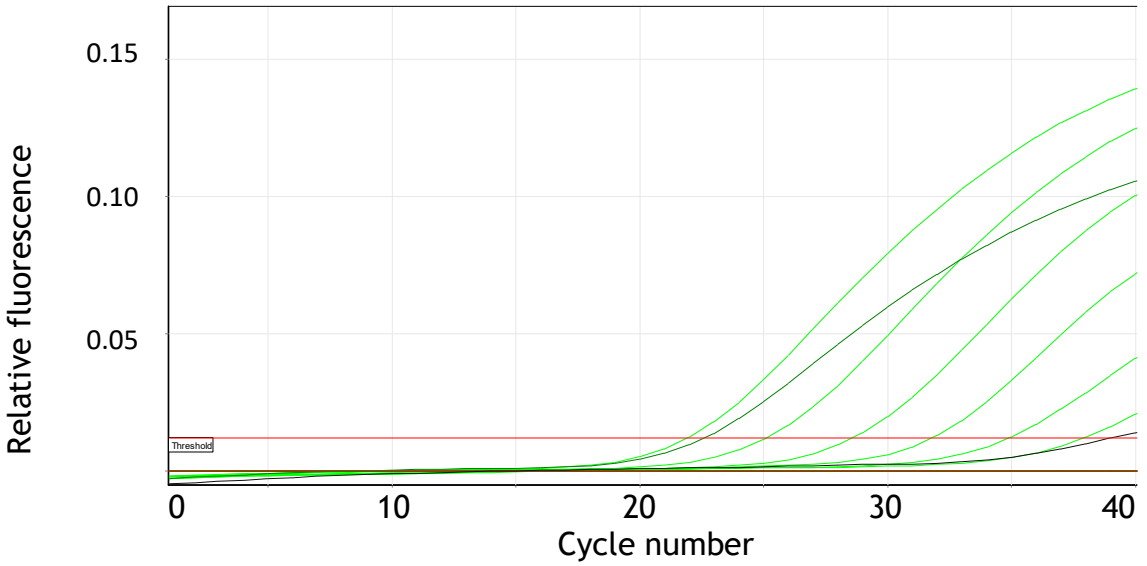

B) Green channel

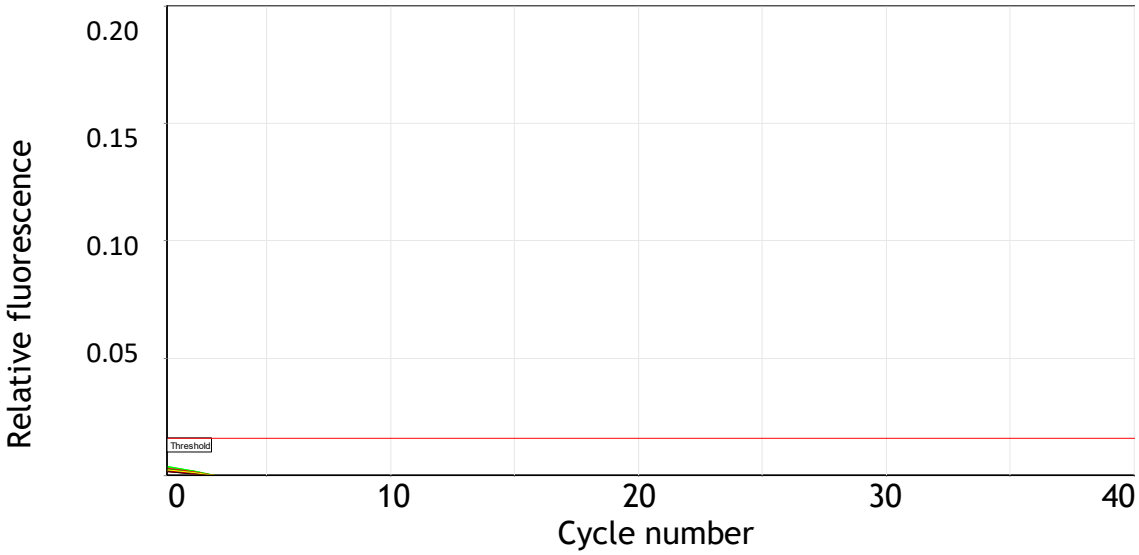

C) Red channel

Figure 3-6 Two sets of serial dilutions of *Erysipelothrix rhusiopathiae* non-Arctic clone (Nac), one containing the FAM probe in the Mastermix, one without. The serial dilution of Nac was coloured light green, the Ac positive controls were coloured orange (without FAM) and dark green (with FAM) and the negative controls were coloured black. Except for the contamination of one of the negative controls (as shown by late amplification in Panel B), the Nac serial dilution with the FAM probe was detected as expected on the green channel, along with the *E. rhusiopathiae* Arctic clone (Ac) positive control with the FAM probe. No amplification of Nac samples was detected in the yellow channel (Panel A) or in the red channel (Panel C).

3.3.4.5 Evaluation of the triplex qPCR on mock 'co-infection' samples

To test the ability of the triplex qPCR to detect two different targets simultaneously (e.g. in DNA extracted from a mixed sample), a series of two tests were conducted. For the first test, a consistent and relatively higher concentration (100-fold dilution of the original extraction) of Nac was spiked into the Ac serial dilution. The higher concentration of Nac has masked the expected C_t shift of the Ac serial dilution within the same reaction well. The ability to differentiate the strains relies explicitly on the results of the yellow channel (Figure 3-7, Panel A).

In the second experiment (serial dilution of *E. tonsillarum* into which 100-fold diluted Nac was spiked; Figure 3-7, panels C and D), the red amplification curve was seen on the green channel due to the 100-fold Nac being spiked in the sample. This showed that in the same qPCR reaction, two different targets can be amplified, even if present at different concentrations.

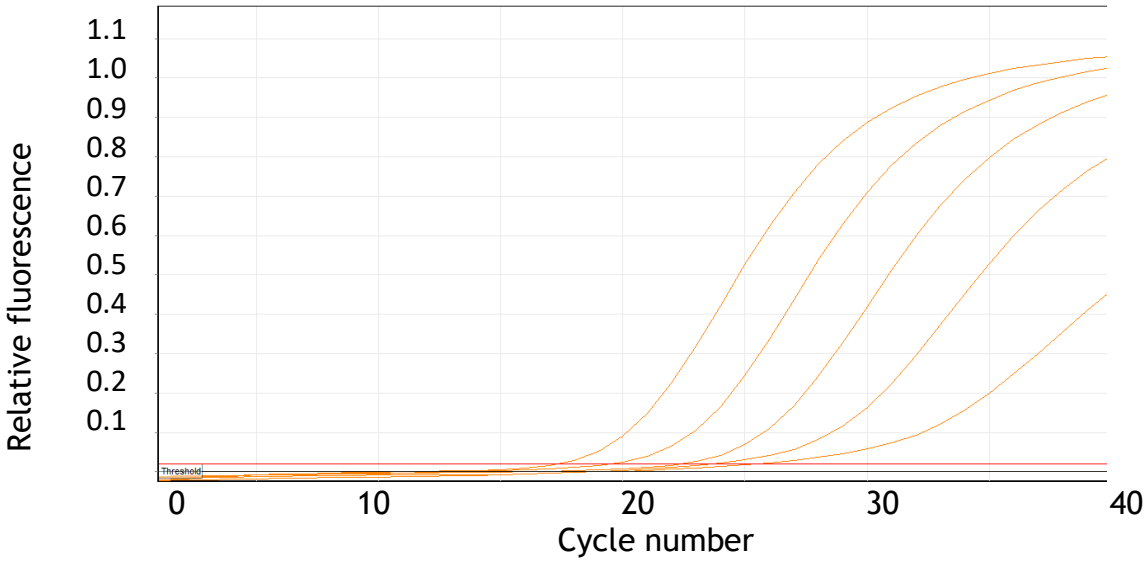

A) Yellow channel (*E. rhusiopathiae* Arctic clone)

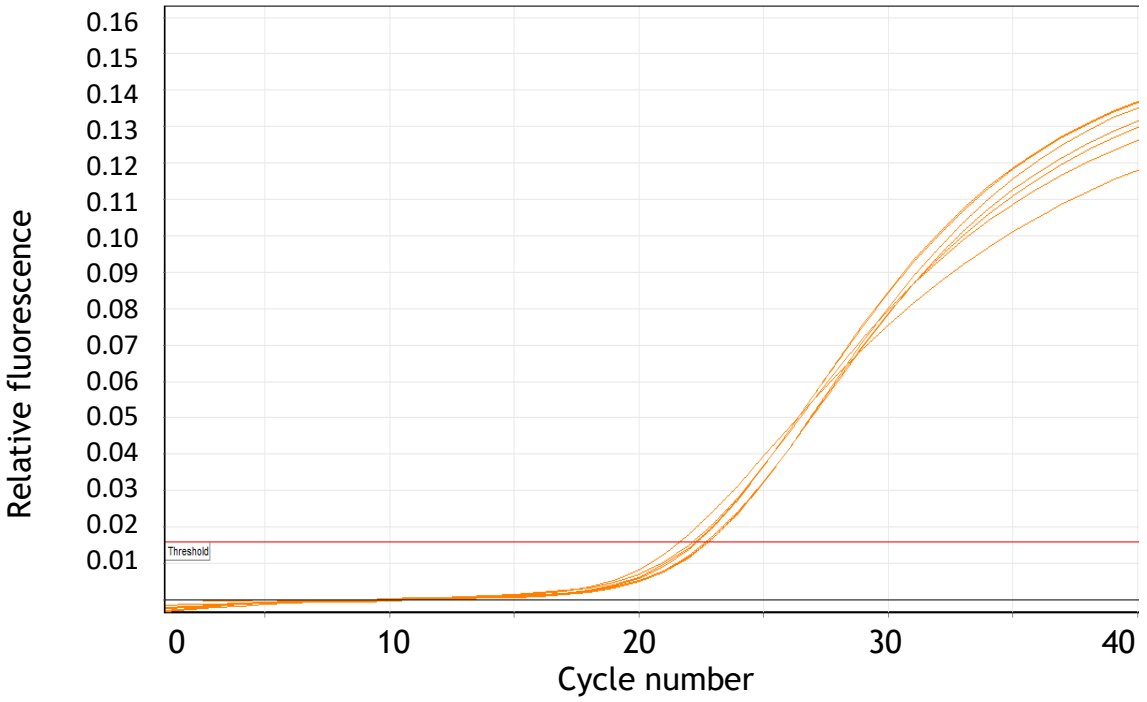

B) Green channel (*E. rhusiopathiae*)

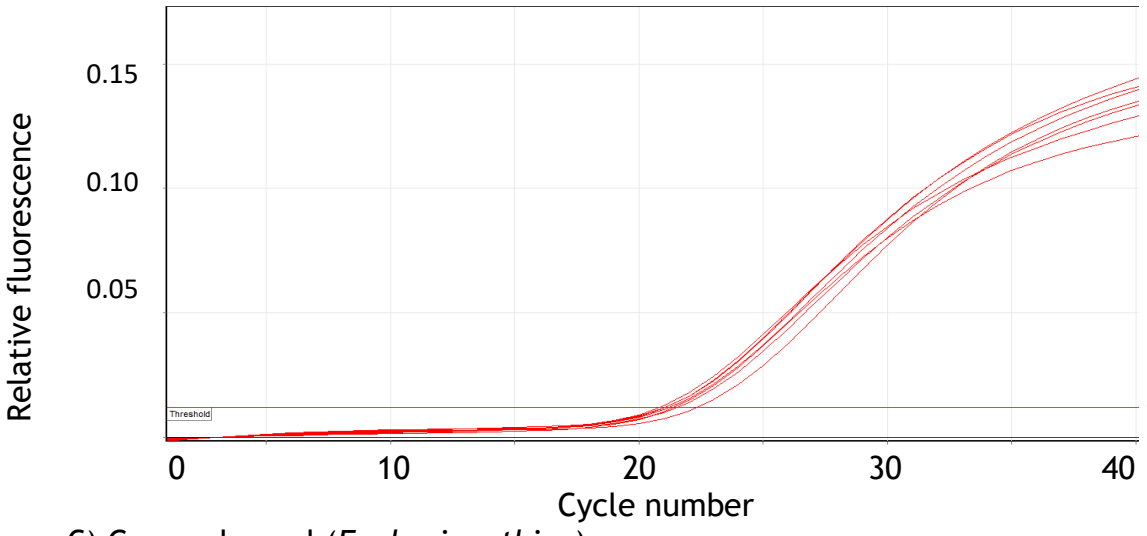

C) Green channel (*E. rhusiopathiae*)

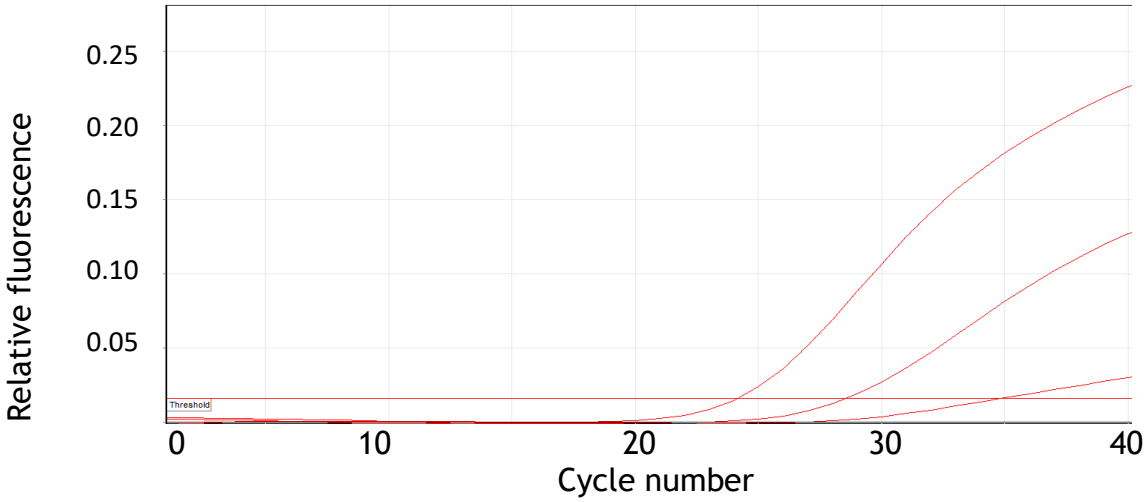

D) Red channel (*E. tonsillarum*)

Figure 3-7 Serial dilutions of *Erysipelothrix rhusiopathiae* Arctic clone (Ac) and *E. tonsillarum* 'spiked' with a 100-fold dilution of *E. rhusiopathiae* non-Arctic clone (Nac). Ac serial dilution spiked with Nac, as seen on yellow channel (Panel A) and green channel (Panel B). *E. tonsillarum* spiked with 100-fold Nac, on green channel (Panel C) and red channel (Panel D).

3.3.4.6 Investigations into Ac imposter sequences

A number of DNA extracts sent from collaborators in Calgary (Table 3-6) were flagged as 'interesting', as their Ac single-plex qPCR results deviated from identification through sequencing data analysis. These extracts were submitted run with the triplex qPCR and there was a clear difference in C_t when compared to other known Ac positive isolates. On the yellow channel, it was clear that there was a big gap between the four Ac 'imposters': these all had C_t ranging from 18 to 20, whereas suspect Ac isolate extracts amplified around cycle 10 on the yellow channel. In the green channel, the Arctic clone positives and three of the 'imposters' had C_t around 13 to 17, while one 'imposter' (sample 683-PB-skin) had C_t at 36.78. On the red channel, there was one amplification, with C_t at 18.17, this was the same sample that had a high C_t on the green channel (Table 3-13). A p-value of 8.69×10^{-14} was obtained when comparing the C_t values obtained from the Ac isolates versus the imposters, meaning these two groups are statistically different from each other. Based on these results, all four Ac suspects were classified to be *E. rhusiopathiae* Arctic clone. Further analyses were conducted on the four 'imposters'.

Table 3-13 Threshold cycle of suspected *Erysipelothrix rhusiopathiae* Arctic clone (Ac) and four 'Imposters'. Ac amplifies on yellow channel, whereas *E. rhusiopathiae* amplifies on green, and *E. tonsillarum* on red.

Samples	Yellow channel C_t	Green channel C_t	Red channel C_t
Suspect Ac 1	10.26	16.10	No amplification
Suspect Ac 2	10.53	16.71	No amplification
Suspect Ac 3	8.21	13.80	No amplification
Suspect Ac 4	9.38	15.35	No amplification
659-MX-WilRiv-BM	18.42	17.58	No amplification
637-BIS-22-779-Spleen	20.78	15.43	No amplification
616-Bathurst-BM – Rib	19.16	13.22	No amplification
683-PB-Skin	20.84	36.78	18.17

3.3.4.6.1 Outlier identification

Using the data compiled from a qPCR of 20 confirmed AC isolates (Table 3-14), two standard curves were generated by plotting the C_t values obtained on the Ac-specific yellow channel against C_t values on the *E. rhusiopathiae* green channel, and against DNA concentrations obtained from the respective isolates. The goal was to determine whether these relationships could be used to identify potential outliers, indicating DNA contamination with more than one clone or species. As described above in Table 3-12, there is normally a clearly conserved relationship between the C_t values obtained on both yellow and green channels for DNA extracted from known Ac isolates. Figure 3-8-A plots this relationship, with the four imposters showing a clear deviation from this trend. This suggests that if there is a larger-than-expected difference between the two C_t values, this is unlikely to be a pure Ac isolate. Furthermore, when plotting the DNA concentration against the C_t values obtained on the yellow channel (Figure 3-8-B), there was again a clear relationship between these values for known Ac isolates that was violated by the imposters. Together, these suggest an issue of contamination.

Table 3-14 Comparison of DNA concentration vs. cycle threshold (C_t) values for *Erysipelothrix rhusiopathiae* Arctic clone isolates and imposters in yellow and green channel (n = 20). These data were used for the construction of the standard curve shown in Figure 3-8. The sample ID was used for identification of the isolate. DNA concentration was determined using Qubit High Sensitivity Quantification kit, the C_t of the yellow and green channels was determined using the triplex qPCR, with the thresholds set at 0.02 and 0.012, respectively.

Sample ID	DNA concentration (ng/µL)	Yellow channel threshold cycle (C_t)	Green channel threshold cycle (C_t)
358-DMX014.2-He	7.8	17.40	12.33
358-DMX07.1-Lu	7.4	17.05	12.20
459-Mould1-BM	7.7	17.46	12.34
459-Mould2-Lu	11.0	16.64	11.74
358-DMX07.2-He	20.3	16.21	10.94
358-DMX07.3-Blood	46.5	15.01	9.77
364-Seal-Lu	13.3	16.70	11.58
364-Seal-He	13.5	16.82	11.67
364-Seal-Blood	37.4	15.24	10.24
459-Mould1-Soil	19.6	16.91	11.38
459-Mould2-He	10.5	17.26	11.95
459-Mould2-SI	15.6	16.65	11.41
459-Mould2-BM	53.0	16.72	10.72
459-Mould2-Soil	33.2	15.36	10.42
459-Mould3-BM	34.5	14.93	9.91
459-Mould3-Soil	52.0	13.86	9.00
459-Mould6-PC-BM	80.0	13.17	8.36
459-Mould12-BM	60.0	13.63	9.00
459-Mould13-Bone(fox)	54.0	13.82	9.20
459-Mould14-BM	49.0	13.91	8.93
659-MX-WILRIV-BM	5.1	27.05	19.03
637-BIS-22-779-Spleen	16.5	32.97	19.69
661-22-1431-BM	12.5	31.81	15.58
616-Bathurst-BM-rib	45.3	29.89	18.18

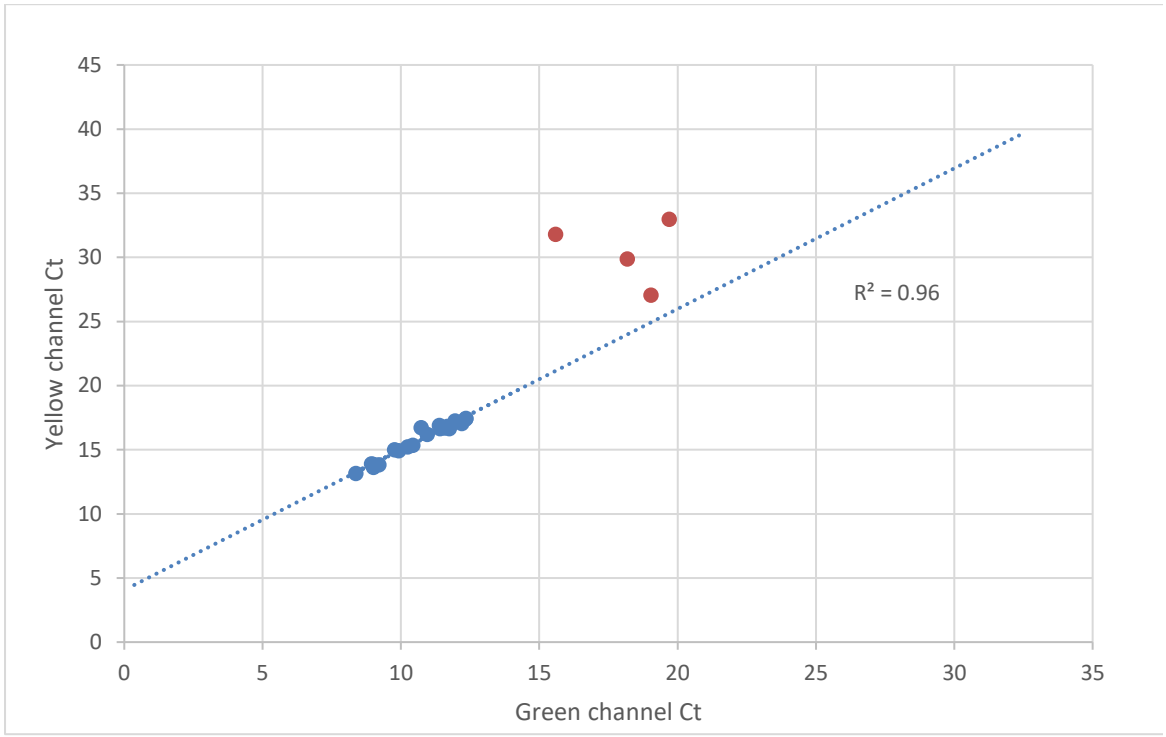

A

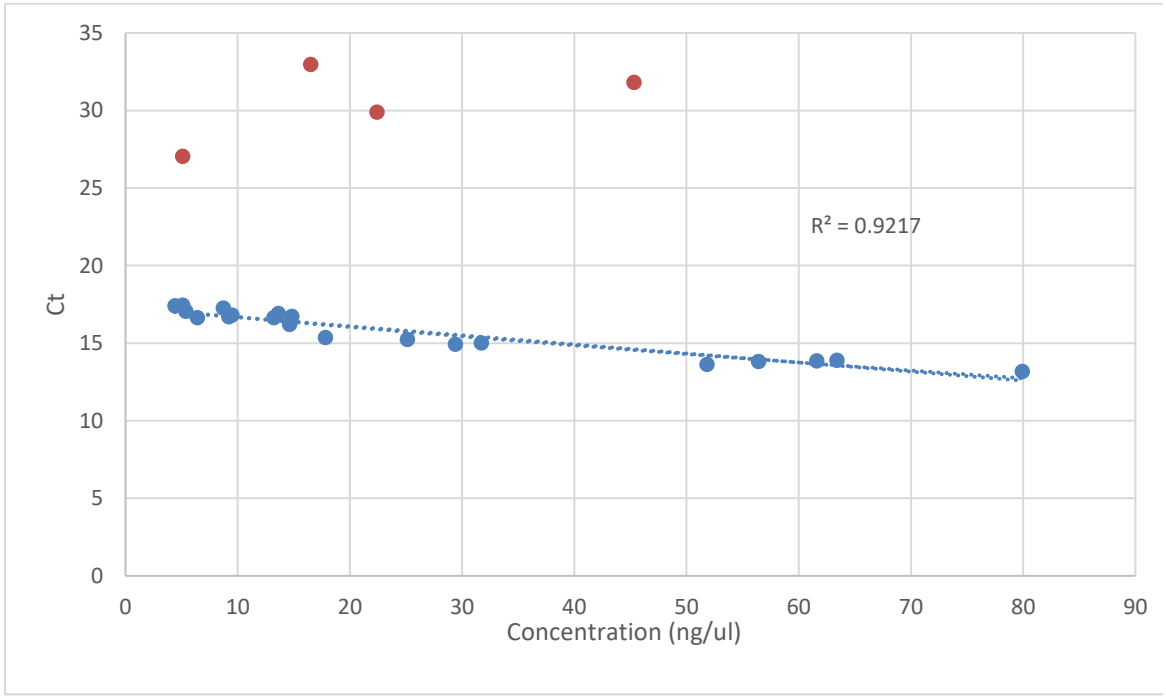

B

Figure 3-8 Relationship between threshold cycle (C_t) on the yellow channel (y-axis) and A) C_t on the green channel; B) DNA concentration (ng/ul), as measured on Qubit for *Erysipelothrix rhusiopathiae* Arctic clone (Ac) isolates. Scatterplots were constructed in Microsoft Excel. The blue plots points are known Ac isolates; the orange plots points are the imposter isolates.

3.3.4.6.2 Whole genome sequence data analyses

The fasta assemblies previously generated for the four imposter isolates were obtained. Initially, the Ac primer and probes sequences were used as templates for the BLAST search using Geneious Prime on the genome sequences of the imposters, the Fujisawa reference genome (NCBI: txid650150 (209)) and a

confirmed Ac assembly. The Ac primer and probes sequences were found in the Ac assembly but were not found in the imposters or the reference genome. Moreover, the BLAST search of the Ac amplicon sequence found no results within the non-Ac assemblies, even when using low similarity thresholds. In summary, we could not find any genomic basis for the imposters to show late amplification in the Ac specific yellow channel, e.g. due to the presence of a similar sequence that might result in weaker non-specific binding.

3.3.4.6.3 Digital PCR

An opportunity to utilise digital PCR (DPCR) to confirm the suspicion of post-extraction contamination was brought up from a neighbouring lab at the vet school at University of Glasgow. Using the absolute quantification option from the QIAcuity software suite (version 3.1.0.0), the copy number (cp) per µL could be identified for each of the samples using the Arctic clone target and the *E. rhusiopathiae* target. Three repeats of the same extract were used for the DPCR, and the mean of the three repeats was reported. The same DNA extracts were also quantified using a Qubit High sensitivity quantification kit and a triplex qPCR. The corresponding results are summarised in Table 3-15. With the data compiled, a correlation could be observed between the qPCR Ct values and the copy number established by the DPCR. Both Arctic clone isolates were very similar in terms of DNA concentration: within 0.5 ng/µL of each other (7.84 and 7.39) and threshold cycles within 0.2 of each other (19.84 and 19.94 for yellow, 20.24 and 20.09 for green) (Table 3-15). The two Nac isolates had a greater difference in concentration, as shown by both Qubit results and DPCR amplicon concentration in the green channel (6 ng/µL for DNA and ~600 cp/µL for amplicon). All isolates had amplification in the green channel, with threshold cycles within 2 of each other, and the range of amplicon concentration going from 457.4 to 1325.4. All Nac and imposter isolates had less than 1 cp/µL of the Arctic clone amplicon.

Table 3-15 Comparison among DNA concentration, qPCR and DPCR results. Data are compiled for six *Erysipelothrix rhusiopathiae* extracts. The DNA concentration was obtained from a Qubit high sensitivity quantification kit, the mean threshold cycle (C_t) was obtained from a triplex qPCR and the mean amplicon concentration (copies (cp)/µL) was obtained from a duplex DPCR, both the latter based on three technical replicates. The six isolates included two *E. rhusiopathiae* Arctic clones (Ac), two *E. rhusiopathiae* non-Arctic clones (Nac) and two Arctic clone 'imposters'. Ac amplifies on the yellow channel; both variants of *E. rhusiopathiae* amplify on green.

	Qubit	**Yellow channel**		**Green channel**	
		qPCR	DPCR	qPCR	DPCR
Isolate ID	DNA concentration (ng/µL)	Mean C_t	Mean Ac amplicon concentration (cp/µL)	Mean C_t	Mean *E. rhusiopathiae* amplicon concentration (cp/µL)
358-DMX014.2-He (Ac)	7.84	19.84	533.7	20.24	498.7
358-DMX07.1-Lu (Ac)	7.39	19.94	658.6	20.09	631.4
620-A1627895 (Nac)	16.2	N/A	0.3	18.94	1325.4
622-2019384 (Nac)	10.3	N/A	0.4	19.69	780.1
637-BIS-Spleen-22-779 (imposter)	16.5	28.38	0.2	19.51	1125.7
659-MX-WILRIV-BM (imposter)	5.08	27.93	0.6	20.67	457.4

3.3.4.7 Diagnostic application

Samples collected in the summer of 2024 from Ellesmere Island in the Canadian Arctic were selectively cultured for *E. rhusiopathiae*. From the 606 samples collected, only nine were culture positive for *E. rhusiopathiae*. All samples were then subjected to direct DNA extraction and tested on the triplex qPCR. Positive control samples of the three *Erysipelothrix* spp. targets were included. Overall, 78 extracts tested positive for *E. rhusiopathiae*, of which 65 extracts were also Ac positive. The amplification (C_t values) from the triplex qPCRs conducted in Calgary were generally higher than those observed in Glasgow, as seen in Figure 3-9. On the yellow channel, the Ac positive controls had C_t at 19.5 and 19.0 while the rest of the samples which were positive amplified after C_t 27.1. On the green channel, the two Ac positives had C_t at 19.3 and 18.7 respectively. The

Nac positive control had a C_t of 16.1, with the samples amplifying at C_t of 25.4 and above.

We also applied the triplex qPCR assay to a collection of 367 further DNA extracts from samples and isolates that had previously tested qPCR positive for *E. rhusiopathiae*. Most samples (n =344) that previously tested positive again showed amplification of the *E. rhusiopathiae* target on the green channel, with 329 (90%) extracts also testing positive on the yellow (Ac) channel. Four isolates tested positive on the yellow channel but showed no amplification on the green channel, the other 19 tested negative on all channels for all three targets. The 23 extracts that tested negative on the green channel were re-run using Calgary's original duplex protocol (*E. rhusiopathiae* + *E. tonsillarum*): the four samples that tested positive on yellow but negative on green using my triplex assay showed late amplification (C_t above 35) on the green channel of the duplex qPCR and were thus classified as Ac. Five extracts tested negative for all three channels in the triplex but amplified in the green channel for both runs of the duplex and were thus classified as Nac. The remaining 14 extracts were classified as negative.

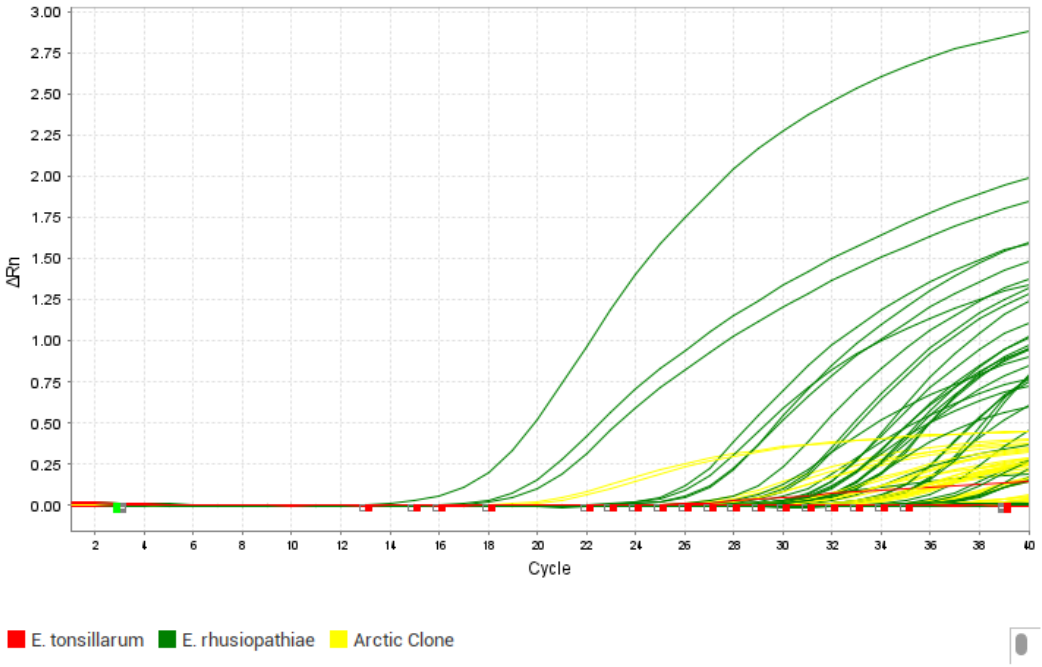

Figure 3-9 Triplex qPCR of samples collected from the Canadian Arctic. The qPCR was conducted on a QuantStudio™ 5 system in Calgary, with samples ranging from soil to bone marrow.

3.4 Discussion

The aim of this chapter was to implement previously designed qPCR assays into a new triplex qPCR assay for simultaneously distinguishing among *E. tonsillarum* and *E. rhusiopathiae*, and determining whether the latter was Ac. The results of the developed triplex qPCR demonstrate that DNA isolated from Ac, Nac and *E. tonsillarum* can be clearly identified and distinguished using this assay. Investigations into the limit of detection, channel fluorescence interactions and false positive test results were conducted to ensure that the qPCR is robust and has high specificity. The initial suspicion of Ac false positive amplification of previously identified Nac strains was partially rectified by redesigning a new respective forward primer and further explored through additional analyses of the WGS results. In order to identify future potential contamination issues in DNA extracts of presumptive Ac-positive samples, standard curves were created comparing Ac amplicon C_t values with those of the *E. rhusiopathiae* amplicon and with DNA concentration. The developed triplex qPCR was applied for *E. rhusiopathiae,* and specifically Ac detection, in a broad range of DNA extracted from field samples. While there was not enough time during my placement in Calgary to optimise the triplex qPCR assay for the detection of direct DNA extracts, initial testing shows great promise for the triplex qPCR to be utilised in the monitoring of outbreaks in the Canadian Arctic.

3.4.1 Triplex Assembly

One of the potential issues from the assembly of the three single-plex assays into a triplex was the decrease of qPCR efficiency (i.e., analytical sensitivity). The compiled results of a summary run of the triplex qPCR were presented in Table 3-11. It showed that the efficiency of the triplex PCR was not noticeably different than the duplex and single-plex qPCRs of the same DNA samples. There were very small C_t differences observed (Table 3-11), however these deviations should be interpreted with caution as there were no repeats conducted for further investigation. As the investigation on the compatibility of the three single-plex assays progressed, an issue of false positive amplification appeared. During the duplex reaction qPCR tests, the Nac and *E. tonsillarum* extracts showed amplification in the yellow channel, which was specific to Ac amplification (Figure 3-3). This raised a suspicion of either DNA cross-

contamination during sample loading, or a wider issue of contamination of reagents. A decision was made to create new aliquots of the working reagents, including the forward and reverse primers, the probes and the nuclease-free water. This process resulted in the elimination of any false positives in the triplex test (Figure 3-4) and reinforced the importance of clean working practices.

3.4.2 Fluorescent signal interference

Since the FAM and HEX emission wavelengths are in close proximity, with the FAM probe emitting light at 520 nm and HEX probe emitting light at 555 nm (201), it was important to rule out any signals being incorrectly picked up by the machine (i.e. cross-channel leakage). Specifically, we aimed to test if the FAM probe, which would in theory emit the strongest fluorescence out of the three probes in the triplex (201,208), would be picked up on in the two other channels not meant to detect this probe. Hence, if the Rotor-Gene has a broader bandwidth for the channel for reading of the emitted fluorescence signal, it could also absorb fluorescence from the neighbouring excited fluorophore. A lower wavelength leads to higher frequency of peaks per second, where the higher frequency of peaks directly correlates to higher energy output (210). Based on guidance documents on multiplex developments and online resources, (200,208,211), the assumption was made that the FAM should have the highest fluorescence, which explained why our tests were focused on green channel leakage into the yellow and red. However, despite this assumption, I found that the yellow channel was reaching 1.05 on the fluorescence scale while the green channel was at 0.15 and the red was at 0.30 (Figure 3-4). The brightness of a fluorophore is only one of the factors which affects the detection in the Rotor-Gene qPCR machine. Primers and probe concentration and PCR efficiency may also affect the maximum fluorescence signal reached. Since the inflection point on the amplification curves, i.e. when amplification is detected, is the important part of the amplification curve, the signal strength did not affect the detection of different strains on the triplex. The lower limit of detection of the red channel could be an indication of lower efficiency, as observed in Figure 3-5. This part of the assay could have been further optimised, but as it was determined to be less important when compared to the strain differentiation of the *E. rhusiopathiae* extracts, it was not deemed a priority.

During the placement in Calgary when the triplex qPCR was tested on DNA extracted from field samples, the fluorophore of the Ac probe was changed to TAMRA due to the limitations of the PCR machine in that laboratory. The new fluorophore had an emission wavelength of 578 nm. From the DNA included in the qPCR shown in Figure 3-9, selecting only the positive controls of the qPCR (which were isolate extractions as opposed to direct sample extracts), the fluorescence strength of each probe is seen in Figure 3-10. The y-axis is represented by ΔRN, which is relative fluorescence (212). The FAM probe, showing the *E. rhusiopathiae* positive control, had the highest fluorescence difference at around 1.8, followed by TAMRA (Ac) at around 0.45 and Cy5 (*E. tonsillarum*) at around 0.2. This result followed the expected trend in fluorophore emission, highlighting differences in fluorescence signal measurement across different qPCR platforms. Many factors could affect the detection of fluorescent signals. This can include the monitoring chemistry, the type of DNA input (purity, GC content and amplicon length determining the melting temperature, as well as secondary DNA structure), target sequence and PCR efficiency (213). The target sequence was the same between the two labs; however, the chemistry, DNA concentration and the efficiency of the PCR could be different. The Rotor-Gene machine's efficiency was explicitly tested, as shown in Figure 3-5, but the detection limit of the qPCR in the QuantStudio 5 at Calgary was not. Different qPCR instruments' PCR efficiencies (214), coupled with the use of a new fluorophore, could explain the differences we observed across platforms. Another factor that would affect the efficiency of detection is the state of the reagents and the reagents themselves. The isolates used in Glasgow were extracted two or more years ago; the length of storage combined with the frequent freeze-thaws of these extracts and the primers and probes during the development of the triplex qPCR could cause some DNA degradation and lower the DNA concentration (215). An investigation to fully explore the reasons behind the difference in fluorescent strength could be conducted but since it did not alter the triplex qPCR's ability to differentiate between the three strains, no further actions were taken.

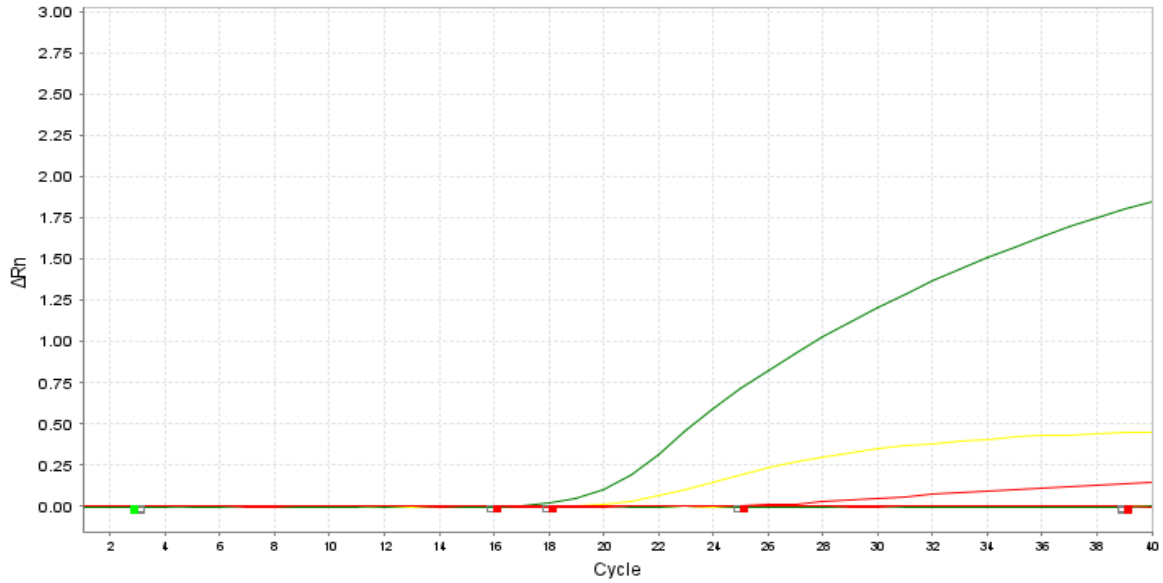

Figure 3-10 Triplex qPCR amplification curve of the positive control DNA used in Calgary. The figure was developed to compare the fluorescence strength of each fluorophore used in the triplex. The green channel is used for detection of *Erysipelothrix rhusiopathiae* (FAM probe), yellow is used for *E. rhusiopathiae* Arctic clone (TAMRA probe) and red is for *E. tonsillarum* (Cy5 probe).

3.4.3 Detection of mixed infections

It was important to make sure that the triplex qPCR could distinguish among more than one *Erysipelothrix* variant in the same sample, since we know that co-infection is possible, and i) errors can arise in culturing where a single isolate is not selected during sub-culture onto the purity plate (25), and ii) DNA may be extracted directly from samples (as opposed to isolates). The fact that the three fluorescent probes are target specific meant that certain co-infections could be detected by identifying different combinations of fluorescence in the three respective channels. Table 3-12 showed that using the triplex qPCR, there was a consistent difference of 5 C_t between the yellow and green channels despite the copy numbers of their respective amplicons being similar (Table 3-15). The interpretation of strain type using copy number differences between Ac and Nac is clearer when using DPCR as opposed to qPCR, especially as the same DPCR results reveals the performance difference between the channels given that the copy numbers should be identical. Panel B of Figure 3-8 shows that despite the C_t difference, all 20 Ac isolates follow a consistent trend. The only deviation observed were the imposters, which were not 'true' Ac. Due to the direct relationship between the two channels for Ac isolates, any deviations from this trend could either be classified as contamination or potential mixed infections using this panel.

3.4.4 Imposter elimination

The imposter isolates showed slightly different results from typical Ac isolates, wherein the C_t values were higher than other DNA extracts, despite having a similar DNA concentration. A hypothesis was formed on the basis of the two distinct clusters of C_t values: we hypothesized that the 'true' Arctic clones (i.e. pure isolates) have a C_t value around 10-15 that is comparable to that observed for Ery (green channel) (given that both the Ac and Ery targets are believed to exist in single copies within the genome), whereas higher amplification in the yellow channel of C_t value around 25 and greater (i.e. fewer copies of the *hhaIM-1* gene) likely indicates an issue of contamination with a second strain.

Numerous actions were taken to root out the false positive amplification exhibited by the 'imposter' isolates described in Table 3-6, i.e., those that showed late amplification of the Ac target, but had been classified as Nac based on WGS. Firstly, the cycling protocol was modified to suit the manufacturers' recommendation for the master-mix: namely, the annealing temperature was increased by 3°C to 60°C and the annealing time was decreased from 30 s to 20 s. This change did not have a noticeable effect on the false amplification of the imposters, but the new annealing temperature was used onwards to keep the protocol within the manufacturer's recommendations for the master mix and the primers and probes, specifically within 6-7°C higher than the Tm (general consensus of around 53°C) of the primers, which would allow the binding process of the primers to be much easier.

To further investigate the issue, a hypothesis was formed in relation to whether there was a related genetic sequence within these genomes, either to the *hhaIM-1* gene, or at least the primer/probe sequences being targeted, that was binding/allowing amplification in these 'imposters', albeit with lower specificity and amplification success rate. The lack of BLAST hits against both Nac reference assemblies and the 'imposter assemblies' using either the Ac primer/probe or the Ac amplicon as a reference query (vs. positive hits for the Ac assembly) showed that the amplification of the 'imposters' on the yellow channel was unlikely to be occurring for this reason; i.e., the false positives were more likely an issue of contamination post-extraction, rather than a lack of specificity of the Ac qPCR target.

By plotting the C_t in the yellow channel and vs. the DNA concentration and the C_t of the same isolates on in the green channel (Figure 3-8), all the imposters were identified as outliers to the general trend. The qPCR targets for both strains exist as a single target site per genome, as shown in Figure 3-1 and further demonstrated using DPCR (which showed similar copy numbers of both targets in Nac isolates), which meant that the relationship between C_t of the Ac on green and yellow channels stays consistent.

To test for statistical significance of the outliers, ANOVA testing analysis was conducted on the C_t values which compared the mean of the Ac C_t vs the imposters' C_t, and it showed that the imposters were significantly different ($p=8.69 \times 10^{-14}$). This was further reinforced when a more accurate measure of amplicon copy number with DPCR was provided. The analysis showed the substantially lower copy numbers of the amplicon in the Nac and imposter samples when compared to Ac (Table 3-15). Both Ac isolates had more than 500 copies per µL, while the others remained at less than 0.6 copies per µL. The copy numbers of the Ac isolates also reinforces the trend that normal pure Ac should have a consistent C_t on in yellow and green channels since the copy numbers of the amplicons were similar, with Ac 1 having 533.7 cp/µL in the yellow channel and 498.7 cp/µL in the green channel and Ac 2 having 658.6 cp/µL in the yellow channel and 631.4 cp/µL in the green channel. Both the Nac and imposters had similar copy numbers on DPCR and also showed amplification in the yellow channel. When subjected to the 10% outlier removal step, which was standard practise for the testing, the Nac did not show amplification in the yellow channel, although before this step a slight amplification trend could be observed. These discrepancies suggest that late amplification – associated with the presence of the very low copy numbers – could be indicative of low background contamination, but that such results are challenging to interpret.

With the abundance of evidence collected, including the negative BLAST search results of the imposter assemblies, the deviation from normal Ac trends, low copy numbers from the DPCR and the exhibition of trends similar to contaminated samples, it was decided that the occurrence of the false amplification of the imposter isolates was very likely due to contamination of the extracted DNA and was not due to the lack of specificity of the triplex qPCR.

3.4.5 Diagnostic interpretation

Since the qPCR was optimised for the detection of DNA extracted from pure isolates, the use of the current triplex qPCR protocol was not necessarily optimised for the detection of the three targets from DNA extracted directly from field and clinical samples. One of the observations made while conducting tests on the triplex qPCR in Calgary was that the C_t of the samples in Calgary were generally higher than those from Glasgow, with the range going from 25 and above (Figure 3-9). This is expected, given the much lower levels of *Erysipelothrix* DNA in sample extracts than in cultured isolates. The samples collected included tissues, soil, water and plant material. The variations of these sample types, combined with the difference of associated extraction techniques, could have influenced the DNA yield from the sample or be associated with different levels of qPCR inhibition (216). I did not have the opportunity to test if or how this might influence the limit of detection in such samples.

As part of the outbreak investigation for the emergence of *E. rhusiopathiae i*n the Canadian Arctic, the collaborators at the University of Calgary collected samples from Ellesmere Island over four consecutive years. Each year, carcass sites were visited and samples brought back to the lab to be cultured for *E. rhusiopathiae* (47). Samples that were not culture positive were further subjected to direct DNA extraction to recover any potential *E. rhusiopathiae* DNA from non-viable bacteria. The standard protocol used in Calgary was to classify any amplification in the channels as positive, provided that there was no amplification of the negative controls. The triplex protocol that I introduced was able to detect different strains from non-culturable samples which contained very limited pathogen DNA concentration. As culture attempts of these samples were unsuccessful, qPCR remains the only effective method to detect the traces of *E. rhusiopathiae* in the environment and to determine the strain type. While the detection of *E. rhusiopathiae* Ac in older muskox or other animal carcasses does not necessarily mean that it was the cause of death, monitoring for the Ac in comparison to other strains is valuable for understanding the spatio-temporal spread of this clone. For example, mortalities from which *E. rhusiopathiae* is isolated in novel geographic locations could quickly be tested to understand whether it is the Ac, rather than waiting for sequencing results. Although there

were issues with a low number of older DNA extracts (5%) when re-testing the previous duplex qPCR-positives on the newer triplex assay, this issue could be linked to the low concentration of pathogen DNA, since C_t values of these samples were ~35. Increasing the number of qPCR replicates could be conducted to enhance the chances of positive amplification where low pathogen copy numbers are anticipated for future diagnostic purposes.

3.4.6 Threshold cut-off for false amplification

Of the six isolates included in the DPCR analyses, only the two Arctic clone extracts should have amplified on the yellow channel. However, the imposters had later amplification in the yellow channel in the triplex qPCR that was run in tandem. The DPCR showed that even at very small copy numbers per sample (0.4 cp/µL), the amplification curve crossed the threshold value of 0.02 on the yellow channel around cycle 28, which is above the limit of detection of cycle 32 as shown in Figure 3-5. It was established that any isolate extraction that amplified after the limit of detection in the yellow channel, after cycle 28, should be treated as a likely false positive or contamination due to the disproportionate quantity of isolate DNA compared to the concentration of Ac amplicons. Using the data from Table 3-15 and the trend established in Figure 3-8, in the future, false positives could potentially be identified for DNA extracted from pure isolates using the trendline, since we showed that the imposters were outliers on the Ac trend. This method could only be applied for the detection of false positives from *E. rhusiopathiae* isolates, since mixed infections could not be ruled out in sample extracts. Due to the different conditions the qPCR was conducted in, including the difference in qPCR efficiency between the machines used, it would be important to adjust the scale as to what would be classified as each Ac or Nac strain according to the amplification detected in the qPCR. The established standard curve from the samples in Glasgow would only be used in Glasgow, for instance, provided that the protocol was not significantly altered. A new standard curve should be established in Calgary, using the methodology described in 3.2.3.6.2, with Qubit results and the C_t of confirmed positives.

It was interesting to note that the qPCR conducted in tandem with the DPCR investigation was conducted five months after the previous qPCR investigation.

During this time, a brand-new stock of the Ery probe was ordered and reconstituted, whereas the previous stock was from before 2020. The new stock of probe may have contributed to the reduced Ct gap between amplification seen with the FAM probe and the HEX probe as previously observed. Instead of the average of 5 cycle difference, this newer qPCR had threshold cycles within 0.4 of each other (19.84 and 19.94 for yellow, 20.24 and 20.09 for green). This suggests that the relationship between yellow and green-channel amplification can change between run conditions, and several control samples should be included in the same run as unknown samples where such a relationship is being investigated.

3.4.7 Benefits and drawbacks

The aim of the development of a triplex qPCR that could detect three major *Erysipelothrix* strains of interest in one single reaction was to increase the throughput of analysis in the outbreak investigation among muskoxen in the Canadian Arctic and wider surveillance efforts. Before the development of this triplex qPCR, all samples collected were selectively cultured for *Erysipelothrix* spp., with any culture positives then being extracted for a single-plex qPCR to confirm that the species was *E. rhusiopathiae*, before being sent off to be sequenced to determine whether an isolate belonged to the Ac. The entire process is labour intensive due to the sheer number of samples the lab technicians have to go through. This process currently takes roughly six weeks for each sample because of the lengthy selective culture method and the long sequencing turnaround as the sequencing is outsourced to another company. This is before any bioinformatics analyses. The combination of extensive labour and high costs (sequencing of one isolate is roughly £65) was a major hurdle for a thorough outbreak investigation. The creation and optimisation of the triplex qPCR meant that the cost of the sample processing and downstream analysis was reduced significantly since sequencing was no longer required for identifying strain differences. Direct sample extraction was used, instead of selective culture then followed by DNA extraction. This further reduced the time required to obtain results from six weeks to two days. The sample processing and analysis cost was also reduced to approximately £6, excluding labour time and cost. The decreased sample cost and reduced time required for results would be beneficial

for future monitoring programs, allowing prompt feedback to communities and wildlife authorities.

The testing of previous duplex qPCR positives showed that there is still optimisation needed to adapt the triplex qPCR protocol for the use of detection of environmental extracts. Nine of these DNA samples still tested positive on their duplex run but failed to amplify on the green channel of our triplex assay. The failure of the other 14 previously positive extracts to amplify on either assay could be partly due to DNA degradation during storage and repeated freeze/thaw cycles, especially with samples that had low *Erysipelothrix*-specific DNA loads, or it could be due to chance, where the current template volume of 2 µL may not pick up a single copy of the target if the copy number per µL is lower than 1. This could be partly mitigated by increasing the number of replicates in the qPCR for samples suspected of having lower DNA concentrations (e.g., soil or water samples).

3.4.7.1 Contamination

Due to the high sensitivity of qPCR and the small volumes of solution and small size of the vessels that contain the reagents, a few contamination issues arose over the duration of the investigation. It is believed that part of the issues encountered were due to poor laboratory practise. During one of the investigations into the 'Imposter' false positives, the BLAST search of the expected amplicon in the assembly of the Ac imposters (Table 3-2) yielded no results, meaning that it was imperative to investigate what was actually being amplified in the qPCR which allowed for the binding of the Ac primer and probes. A 'nested' qPCR has been described to be more sensitive than a qPCR; it uses the PCR product from the first round of amplification as a template for the second (217,218). In a side investigation not described in this thesis, we ran a nested PCR to amplify the Ac target for the imposters and a handful of known Ac strains, with the goal of yielding a high number of amplicons to submit for Sanger sequencing. Between the two PCRs, the tubes were opened to aliquot the product into a fresh master mix. This step was conducted right after the initial PCR run had finished and it was not conducted in a PCR cabinet or fume hood. The result of this oversight meant that highly concentrated amplicons of Ac were likely released into the laboratory environment. Despite exercising extra caution

and using DNA-erase (219) to sterilise the lab environment, amplifications of the negative controls of the qPCR continued for the next few weeks. This halted the qPCR optimisation and ultimately lead to the redesign of the forward primer to combat the contamination issue. The new forward primer for Ac was designed to be 22 bases ahead of the original, which increased the amplicon size from 111 bases to 133 bases. This was done with the goal of any background contamination with Ac amplicons would no longer be amplified in the qPCR.

Several steps were taken to reduce the possibility of contamination: the OHRBID lab has dedicated areas and workflow for culture, DNA extraction, PCR mix preparation, amplification and post-amplification processing, the work surface was thoroughly cleaned with lab specific protocols, extra care was taken when handling the small volumes while preparing the master-mix for the qPCR, such as slow and gentle movements when pipetting the master mix and the template into the PCR tube to avoid aerosol creation. The lids of the PCR tubes were shut as soon as the sample was loaded into the master mix. The template tubes were only open for the pipette to collect the DNA, before being immediately shut again. Extra negative controls for the qPCR were placed in between samples instead of being placed at the end of the samples. This was used to easily identify any contamination which was the result of the splash over of the template onto the nearby qPCR tubes.

The current layout of the Glasgow lab has a biological side and a molecular side. The two sides are inter-connected by two walkways and there is no physical separation in between. This is likely the main reason why the contamination from the nested PCR caused such a long-lasting contamination issue. Since this is a limitation of the layout of the building, there was no way of changing this. A PCR cabinet (220) could be introduced to the lab for the preparation of PCRs as well, since the current preparation (addition of template DNA) occurs on the bench top. This cabinet would come with a UV filter for the airflow which could minimise any airborne contaminants. Any spilling of reagents could also be easily contained within the cabinet to prevent a widespread contamination.

3.4.8 Future research

There has already been precedent wherein WGS data was used to develop qPCR assays with specific targets. One study conducted by Subhash et al., 2022 has designed patient specific assays for the quantitation of tumour cells (221). Another study has used WGS to identify a single-nucleotide polymorphism (SNP) within a target gene and designed the qPCR assay to target that SNP for diagnostic purposes (222). Another use for WGS in diagnostic purposes is to help validate the qPCR results (223,224). The next steps of adapting the research of this qPCR protocol into a standard diagnostic test would be to further optimise this assay to increase the PCR efficiency, especially for the red channel, more in-house validation, adding internal amplification control to eliminate any false negatives and inter-laboratory validation. All of these steps would aid the protocol's adherence to international standards such as the ISO standards (188,225). Future work to aid in the rapid detection of *E. rhusiopathiae* could also involve the development of a faster assay which could be conducted at the site of harvest, which would reduce travel time and risk factors for the transportation of contaminated samples to the lab. This could, for example, be in the form of a loop-mediated isothermal amplification (LAMP) assay, which can be incorporated into a lateral-flow device for onsite detection (226); however, this can also have its own drawbacks due to higher risk of contamination and the lower specificity of the LAMP assay.

3.4.9 Conclusion

The result of the optimisation steps led to confidence in the specificity of the triplex qPCR. The establishment of the standard curves for DNA extracted from presumptively pure isolates to identify potential contamination of suspected Ac isolates based on scatterplots (Figure 3-8) made the visual detection of any potential contamination and mixed infection easier. There was sufficient evidence to demonstrate that the triplex qPCR is able to detect and clearly distinguish among both *E. rhusiopathiae* Arctic clone and non-Arctic clone and *E. tonsillarum*. This protocol can be adapted to other qPCR instruments and reagents, although modifications could be required depending on the difference in platforms used. The triplex qPCR provides a quicker and cheaper diagnostic

alternative than existing methods and that can be implemented in future outbreak investigations.

4 General Discussion

In the Arctic, local Inuit communities rely heavily on the wildlife for cultural and economic wellbeing (22). The aim of this project was to aid in the investigations into outbreaks of Ac in muskoxen the Canadian Arctic as part of the CINUK-funded ArcticEID project (26). One component of the epidemiological triad (67), specifically the pathogenicity of the Ac, was studied in Chapter 2 of this thesis by testing the use of the *in vivo* model of *Galleria mellonella* for the bacterium *E. rhusiopathiae*. The other main goal of this thesis was to develop a molecular assay for the key strains of *Erysipelothrix* spp. in the Canadian Arctic, which was summarised in Chapter 3. The results from both of these chapters have provided novel information that will be of value for future research on this bacterial species to build on.

The use of murine models have revolutionised biomedical sciences due to their availability as a model for a wide range of human diseases (227). Transgenic mice have been used for cancer research (228) while rat models play a vital role in the research of cardiovascular diseases (229). Other examples of *in vivo* models being used in disease research include rabbits (230), guinea pigs (231) and zebra fish (232). Due to logistical constraints and ethical considerations, current research practise has set a preference for the replacement of the tradition animal models (110,233). *Ex vivo* models such as tissue culture have also been used to study bacterial virulence (234). *Ex vivo* models use tissues or organs extracted from animals or humans that are cultured using *in vitro* methods. The benefit of such systems is that they preserve the surface topography of the tissue, which makes the study of bacteria attachment and biofilm formation easier to study (235). I was unable to find any literature wherein such techniques were used to study the virulence of *E. rhusiopathiae*. One promising *in vivo* model uses Wax Moth larvae (*Galleria mellonella*) as a host for the bacterial infection that has been described in many publications as a good alternative to animal models (154,162,164,236). To our knowledge, this model had not been previously tested on *E. rhusiopathiae* or its Arctic clone. My investigation included the establishment of the growth kinetics of *E. rhusiopathiae*, numerous troubleshooting steps for the use of the *G. mellonella* model and statistical analysis of the results. The data obtained from this chapter demonstrated that this model is unsuitable for the investigation of differential

virulence among *E. rhusiopathiae* strains. The absence of significant mortalities 24-h post inoculation differs from most models which reported success in the use of the model on other bacterial species (102,121,122,237,238). The comparison of the Kaplan-Meier curves (Figure 2-5,Figure 2-6,Figure 2-7,Figure 2-8), supported by a Cox proportional hazards model (Table 2-7) showed that the majority of the test groups were not statistically significant from the controls. The only test group that tested statistically different from the controls was the undiluted Nac group. Future studies could alter the methodology to increase the concentration of the inoculum used for the injections.

The methodology and the results provided in Chapter 2 aid future investigations of virulence of *E. rhusiopathiae* and its Ac by establishing that the *Galleria* model is not suitable for the investigation of virulence in this species and suggesting that alternative approaches would be more appropriate. The high prevalence of the Ac in the muskox outbreak on Ellesmere and Axel Heiberg islands, confirmed using the rapid diagnostic tool developed in chapter 3, necessitates continued research into the drivers for its pathogenicity. Future investigations could build upon this research by using the rapid qPCR method to screen a large number of samples quickly. Future virulence screening could potentially make use of different *in vivo* models, such as the *Drosophila melanogaster* model (fruit fly) (239) or *Caenorhabditis elegans* (transparent nematode) (112). These models could provide better results as there are more standardised protocols (240,241). The existence of such protocols could provide a fair comparison between different bacterial species or strains (128). Another advantage of using other models is that the immune proteins have not all been identified yet (242), as the whole genome of *G. mellonella* was only recently assembled (243). This limits the knowledge regarding the larval immune system. Whether *E. rhusiopathiae*-induced virulence is more apparent in these models would require initial testing, as I have done here for *G. mellonella*.

Molecular assays have been used for the detection of various bacteria and their specific strain types (189,192,217). The emergence of Ac in the Canadian Arctic has been monitored using a combination of selective culturing and WGS (22,61,66), a process which is time consuming, labour intensive and expensive, often requiring up to 6 weeks from start to finish and up to £65 to provide results on the strain type. The aim of Chapter 3 was to develop a multiplex assay

by combining assays previously designed by other researchers (103,104). The combined assay would detect strain differences between *E. rhusiopathiae* Ac and Nac and also *E. tonsillarum*, all of which are species/strain-types of importance in the current outbreak investigation (39,66). The development of the triplex qPCR included sensitivity and specificity testing, the determination of the limit of detection and the exclusion of cross-channel fluorescence contamination. The emergence of the 'imposter' isolates and the subsequent series of contamination issues highlighted the requirement for the establishment of a standard curve and a trendline for the Ac specific-yellow channel. Through converging investigations, the 'imposters' were determined to be contaminated extractions since they did not follow the general trend set by the other Ac isolates (i.e. showed a different relationship between the C_t obtained on the yellow and green channels) and based on the low copy numbers obtained from the DPCR, despite having similar DNA concentrations. The triplex qPCR was also used as a preliminary diagnostic tool during a 3-month placement that was undertaken in Calgary. Extracts from different tissue types and sample variations were tested on the qPCR and showed promising results. The qPCR protocol required minimal optimisation when adapting it to the conditions in Calgary, namely the different systems (244) and reagents used. The current qPCR protocol was optimised for the detection of isolate extracts; the occurrence of 19 likely false negatives among DNA extracts that previously texted positive for *E. rhusiopathiae* shows that further steps could be taken to optimise the protocol for the detection of extracts with significantly lower bacterial DNA yields. These 19 false negatives only made up 5% of all previous positives and there were numerous factors which could affect this, including the age of the samples, the number of freeze/thaw cycles and different cycling conditions. Due to limited time and resources, it was not possible to investigate it further in Calgary. Future work could involve the establishment of a standard curve/trend and more optimisation for the triplex qPCR to be more sensitive and specific when used to detect direct extracts (187).

The assembled triplex was able to differentiate the three different species/strains of interest and was able to reduce the cost tenfold, from £65 to £6 and reduce the time required for strain/species identification from six weeks to one day. The development of this qPCR has provided a cheaper and quicker

alternative to the established methodology and has already proven to be successful in detecting Ac-positive samples from the outbreak investigation. In summary, both chapters have provided data which has advanced the current research on *E. rhusiopathiae* and its Ac.

List of References

1. Louca S, Mazel F, Doebeli M, Parfrey LW. A census-based estimate of Earth's bacterial and archaeal diversity. PLOS Biol. 2019 Feb 1;17(2):e3000106.
2. Taylor LH, Latham SM, Woolhouse MEJ. Risk factors for human disease emergence. Philos Trans R Soc B Biol Sci. 2001 July 29;356(1411):983–9.
3. Tang KWK, Millar BC, Moore JE. Antimicrobial Resistance (AMR). Br J Biomed Sci. 2023;80:11387.
4. Hasso-Agopsowicz M, Hwang A, Hollm-Delgado MG, Umbelino-Walker I, Karron RA, Rao R, et al. Identifying WHO global priority endemic pathogens for vaccine research and development (R&D) using multi-criteria decision analysis (MCDA): an objective of the Immunization Agenda 2030. eBioMedicine. 2024 Nov 4;110:105424.
5. WHO bacterial priority pathogens list, 2024: Bacterial pathogens of public health importance to guide research, development and strategies to prevent and control antimicrobial resistance [Internet]. [cited 2025 Aug 28]. Available from: https://www.who.int/publications/i/item/9789240093461
6. Spinelley A. Issue 5 1 General Commentaries Citation: Spinelley A. Endemic Diseases: Understanding Their Persistent Nature, Impact on Communities, and Strategies for Effective Management and Prevention in Affected Regions. J Infect Med Microbiol. 2024;8(5):225.
7. Pruvot M, Kutz S, van der Meer F, Musiani M, Barkema HW, Orsel K. Pathogens at the livestock-wildlife interface in Western Alberta: does transmission route matter? Vet Res. 2014 Feb 12;45(1):18.
8. Cleaveland S, Laurenson MK, Taylor LH. Diseases of humans and their domestic mammals: pathogen characteristics, host range and the risk of emergence. Woolhouse MEJ, Dye C, editors. Philos Trans R Soc Lond B Biol Sci. 2001 July 29;356(1411):991–9.
9. Daszak P, Cunningham AA, Hyatt AD. Emerging Infectious Diseases of Wildlife-- Threats to Biodiversity and Human Health. Science. 2000 Jan 21;287(5452):443–9.
10. Byrne AW, Morgan ER. Emerging and Endemic Infections in Wildlife: Epidemiology, Ecology and Management in a Changing World. Pathogens. 2024 June;13(6):513.
11. Bengis RG, Leighton FA, Fischer JR, Artois M, Mörner T, Tate CM. The role of wildlife in emerging and re-emerging zoonoses. Rev Sci Tech Int Off Epizoot. 2004 Aug;23(2):497–511.
12. Kamath PL, Foster JT, Drees KP, Luikart G, Quance C, Anderson NJ, et al. Genomics reveals historic and contemporary transmission dynamics of a bacterial disease among wildlife and livestock. Nat Commun. 2016 May 11;7(1):11448.
13. Ní Bhuachalla D, Corner LA, More SJ, Gormley E. The role of badgers in the epidemiology of Mycobacterium bovis infection (tuberculosis) in cattle in the United Kingdom and the Republic of Ireland: current perspectives on control strategies. Vet Med Res Rep. 2014 Dec 19;6:27–38.
14. Tomaselli M, Elkin B, Kutz S, Harms NJ, Nymo HI, Davison T, et al. A Transdisciplinary Approach to Brucella in Muskoxen of the Western Canadian Arctic 1989–2016. EcoHealth. 2019 Sept 1;16(3):488–501.
15. Aguilar XF, Mavrot F, Surujballi O, Leclerc LM, Tomaselli M, Kutz S. Brucellosis emergence in the Canadian Arctic. One Health. 2024 June 1;18:100712.
16. Tomaselli et al. Muskox health, status and trends - crossing the boundaries. 2023 May.

17. Fereidouni S, Freimanis GL, Orynbayev M, Ribeca P, Flannery J, King DP, et al. Mass Die-Off of Saiga Antelopes, Kazakhstan, 2015. Emerg Infect Dis. 2019 June 1;25(6):1169.
18. Di Francesco J, Hanke A, Milton T, Leclerc LM, Association KA, Gerlach C, et al. Documenting Indigenous Knowledge to Identify and Understand the Stressors of Muskoxen (Ovibos moschatus) in Nunavut, Canada. Arctic. 2021;74(4):418–36.
19. Kutz S, Bollinger T, Branigan M, Checkley S, Davison T, Dumond M, et al. Erysipelothrix rhusiopathiae associated with recent widespread muskox mortalities in the Canadian Arctic. Can Vet J. 2015 June 1;56(6):560.
20. Mavrot F, Orsel K, Hutchins W, Adams LG, Beckmen K, Blake JE, et al. Novel insights into serodiagnosis and epidemiology of Erysipelothrix rhusiopathiae, a newly recognized pathogen in muskoxen (Ovibos moschatus). PloS One. 2020;15(4):e0231724.
21. Tomaselli M, Kutz S, Gerlach C, Checkley S. Local knowledge to enhance wildlife population health surveillance: Conserving muskoxen and caribou in the Canadian Arctic. Biol Conserv. 2018 Jan;217:337–48.
22. Mavrot F, Aleuy OA, Forde T, Kutz SJ. Erysipelas in Arctic and Northern Regions. In: Tryland M, editor. Arctic One Health: Challenges for Northern Animals and People [Internet]. Cham: Springer International Publishing; 2022 [cited 2025 Sept 16]. p. 363–75. Available from: https://doi.org/10.1007/978-3-030-87853-5_16
23. Davison T, Baryluk S. Aerial Survey of Muskoxen and Peary Caribou on Banks Island, July and August 2019. Environment and Natural Resources Government of the Northwest Territories; 2021 Aug.
24. Davison T, Williams J. Aerial Survey of Muskoxen (Ovibos moschatus) and Peary Caribou (Rangifer tarandus pearyi) on Northwest Victoria Island, May 2019. 2022 Dec.
25. Forde TL, Orsel K, Zadoks RN, Biek R, Adams LG, Checkley SL, et al. Bacterial genomics reveal the complex epidemiology of an emerging pathogen in arctic and boreal ungulates. Front Microbiol. 2016 Nov 7;7(NOV).
26. ArcticEID - community-based wildlife surveillance - CINUK [Internet]. [cited 2023 Nov 13]. Available from: https://www.cinuk.org/projects/arcticeid/
27. Contact | Kutz Research Group | Faculty of Veterinary Medicine (UCVM) | University of Calgary [Internet]. [cited 2025 Sept 24]. Available from: https://vet.ucalgary.ca/groups/arctic-wildlife-health/contact
28. OHRBID [Internet]. [cited 2025 Sept 24]. Home. Available from: https://www.ohrbidglasgow.com
29. Wang Q, Chang BJ, Riley TV. Erysipelothrix rhusiopathiae. Vet Microbiol. 2010 Jan 27;140(3–4):405–17.
30. MSD Veterinary Manual [Internet]. [cited 2025 Aug 18]. Overview of Erysipelothrix rhusiopathiae Infection in Animals - Infectious Diseases. Available from: https://www.msdvetmanual.com/infectious-diseases/erysipelothrix-rhusiopathiae-infection/overview-of-erysipelothrix-rhusiopathiae-infection-in-animals
31. Mavrot F, Aleuy A, Forde T, Kutz SJ. Erysipelas in Arctic and Northern Regions. In: Arctic One Health: Challenges for Northern Animals and People. Springer International Publishing; 2022. p. 363–75.
32. Jsseldijk LLI, Begeman L, Duim B, Gröne A, Kik MJL, Klijnstra MD, et al. Harbor Porpoise Deaths Associated with Erysipelothrix rhusiopathiae, the Netherlands, 2021. Emerg Infect Dis. 2023 Apr 1;29(4):835.
33. Chang RK, Miller MA, Tekedar HC, Rose D, García JC, LaFrentz BR, et al. Pathology, microbiology, and genetic diversity associated with Erysipelothrix

rhusiopathiae and novel Erysipelothrix spp. infections in southern sea otters (Enhydra lutris nereis). Front Microbiol [Internet]. 2024 Feb 1 [cited 2025 Sept 16];14. Available from: https://www.frontiersin.org/journals/microbiology/articles/10.3389/fmicb.2023.1303235/full
34. Rouse N, Huntington KB, Goertz C, Hunter N, Radhakrishnan S, Forde T. Erysipelothrix in Cook Inlet, Alaska, USA: an emerging bacterial pathogen of the endangered Cook Inlet beluga whale. Dis Aquat Organ. 2025 July 3;163:1–16.
35. Spraker TR, White PA. Shaggy Lame Fox Syndrome in Pribilof Island Arctic Foxes (Alopex lagopus pribilofensis), Alaska. Vet Pathol. 2017 Mar 1;54(2):258–68.
36. Prod'hom G, Bille J. Chapter 167 - Aerobic Gram-positive bacilli. In: Cohen J, Opal SM, Powderly WG, editors. Infectious Diseases (Third Edition) [Internet]. London: Mosby; 2010 [cited 2025 Sept 16]. p. 1660–75. Available from: https://www.sciencedirect.com/science/article/pii/B9780323045797001672
37. Brooke CJ, Riley TV. Erysipelothrix rhusiopathiae: Bacteriology, epidemiology and clinical manifestations of an occupational pathogen. J Med Microbiol. 1999;48(9):789–99.
38. Ogawa Y, Ooka T, Shi F, Ogura Y, Nakayama K, Hayashi T, et al. The genome of Erysipelothrix rhusiopathiae, the causative agent of swine erysipelas, reveals new insights into the evolution of Firmicutes and the organism's intracellular adaptations. J Bacteriol. 2011 June;193(12):2959–71.
39. Takahashi T, Fujisawa T, Benno Y, Tamura Y, Sawada T, Suzuki S, et al. Erysipelothrix tonsillarum sp. nov. Isolated from Tonsils of Apparently Healthy Pigs. Int J Syst Evol Microbiol. 1987;37(2):166–8.
40. Verbarg S, Rheims H, Emus S, Frühling A, Kroppenstedt RM, Stackebrandt E, et al. Erysipelothrix inopinata sp. nov., isolated in the course of sterile filtration of vegetable peptone broth, and description of Erysipelotrichaceae fam. nov. Int J Syst Evol Microbiol. 2004;54(1):221–5.
41. Bang BH, Rhee MS, Chang DH, Park DS, Kim BC. Erysipelothrix larvae sp. nov., isolated from the larval gut of the rhinoceros beetle, Trypoxylus dichotomus (Coleoptera: Scarabaeidae). Antonie Van Leeuwenhoek. 2015 Feb 1;107(2):443–51.
42. Pomaranski EK, Griffin MJ, Camus AC, Armwood AR, Shelley J, Waldbieser GC, et al. Description of Erysipelothrix piscisicarius sp. nov., an emergent fish pathogen, and assessment of virulence using a tiger barb (Puntigrus tetrazona) infection model. Int J Syst Evol Microbiol. 2020;70(2):857–67.
43. Zhong J, Medvecky M, Tornos J, Clessin A, Le Net R, Gantelet H, et al. Erysipelothrix amsterdamensis sp. nov., associated with mortalities among endangered seabirds. Int J Syst Evol Microbiol. 2024;74(2):006264.
44. Erysipelothrix anatis sp. nov., Erysipelothrix aquatica sp. nov. and Erysipelothrix urinaevulpis sp. nov., three novel species of the genus, and emended description of Erysipelothrix. 2022 July 1;005454.
45. Opriessnig T, Forde T, Shimoji Y. Erysipelothrix Spp.: Past, Present, and Future Directions in Vaccine Research. Front Vet Sci. 2020 Apr 15;7:532026.
46. Wood RL. Survival of Erysipelothrix rhusiopathiae in soil under various environmental conditions. Cornell Vet. 1973 July;63(3):390–410.
47. Mccaide Wooten. Insights from a three-year observational study of High Arctic muskoxen (Ovibos moschatus) following an acute infectious disease epidemic [Internet]. International Conference of the Wildlife Disease Association; Unpublished; 2025 [cited 2025 Sept 1]; Victoria, British Columbia, Canada. Available from: https://rgdoi.net/10.13140/RG.2.2.21956.95360

48. Reboli AC, Farrar WE. Erysipelothrix rhusiopathiae: An occupational pathogen. Clin Microbiol Rev. 1989;2(4):354–9.
49. Barnett JH, Estes SA, Wirman JA, Morris RE, Staneck JL. Erysipeloid. 1982.
50. Stephenson EH, Berman DT. Isolation of Erysipelothrix rhusiopathiae from tonsils of apparently normal swine by two methods. Am J Vet Res. 1978 Jan;39(1):187–8.
51. Opriessnig T, Coutinho TA. Erysipelas. In: Diseases of Swine [Internet]. John Wiley & Sons, Ltd; 2019 [cited 2025 Aug 13]. p. 835–43. Available from: https://onlinelibrary.wiley.com/doi/abs/10.1002/9781119350927.ch53
52. Erysipeloid - Infectious Diseases - MSD Manual Professional Edition [Internet]. [cited 2024 Jan 4]. Available from: https://www.msdmanuals.com/professional/infectious-diseases/gram-positive-bacilli/erysipeloid
53. Frasch CE. [12] Serogroup and serotype classification of bacterial pathogens. In: Methods in Enzymology [Internet]. Academic Press; 1994 [cited 2025 Sept 18]. p. 159–74. (Bacterial Pathogenesis Part A: Identification and Regulation of Virulence Factors; vol. 235). Available from: https://www.sciencedirect.com/science/article/pii/0076687994351384
54. KUCSERA G. Proposal for Standardization of the Designations Used for Serotypes of Erysipelothrix rhusiopathiae (Migula) Buchanan. Int J Syst Evol Microbiol. 1973;23(2):184–8.
55. Ding Y, Zhu D, Zhang J, Yang L, Wang X, Chen H, et al. Virulence determinants, antimicrobial susceptibility, and molecular profiles of Erysipelothrix rhusiopathiae strains isolated from China. Emerg Microbes Infect. 2015 Nov 11;4(11):69.
56. Nakato H, Shinomiya K, Mikawa H. Possible Role of Neuraminidase in the Pathogenesis of Arteritis and Thrombocytopenia Induced in Rats by Erysipelothrix Rhusiopathiae. Pathol - Res Pract. 1986 June 1;181(3):311–9.
57. Nakato H, Shinomiya K, Mikawa H. Adhesion of Erysipelothrix rhusiopathiae to Cultured Rat Aortic Endothelial Cells: Role of Bacterial Neuraminidase in the Induction of Arteritis. Pathol - Res Pract. 1987 Apr 1;182(2):255–60.
58. Shimoji Y. Pathogenicity of Erysipelothrix rhusiopathiae: Virulence factors and protective immunity. Microbes Infect. 2000;2(8):965–72.
59. Nørrung V. Studies on Erysipelothrix Insidiosa S. Rhusiopathiae. Acta Vet Scand. 1970 Dec 1;11(4):577–85.
60. Lachmann PG, Deicher H. Solubilization and characterization of surface antigenic components of Erysipelothrix rhusiopathiae T28. Infect Immun. 1986;52(3):818–22.
61. Seru LV, Forde TL, Roberto-Charron A, Mavrot F, Niu YD, Kutz SJ. Genomic characterization and virulence gene profiling of Erysipelothrix rhusiopathiae isolated from widespread muskox mortalities in the Canadian Arctic Archipelago. BMC Genomics. 2024 Dec 1;25(1):691.
62. Bender JS, Kinyon JM, Kariyawasam S, Halbur PG, Opriessnig T. Comparison of conventional direct and enrichment culture methods for Erysipelothrix spp. from experimentally and naturally infected swine. J Vet Diagn Invest. 2009;21(6):863–8.
63. Grieco MH, Sheldon C. Erysipelothrix Rhusiopathiae. Ann N Y Acad Sci. 1970;174(2):523–32.
64. Forde T, Biek R, Zadoks R, Workentine ML, De Buck J, Kutz S, et al. Genomic analysis of the multi-host pathogen Erysipelothrix rhusiopathiae reveals extensive recombination as well as the existence of three generalist clades with wide geographic distribution. BMC Genomics. 2016 June 14;17(1).

65. Forde TL, Kollanandi Ratheesh N, Harvey WT, Thomson JR, Williamson S, Biek R, et al. Genomic and Immunogenic Protein Diversity of Erysipelothrix rhusiopathiae Isolated From Pigs in Great Britain: Implications for Vaccine Protection. Front Microbiol. 2020 Mar 13;11.
66. Wooten MT, Forde TL, Roberto-Charron A, Fredlund M, Mullin T, Christensen OA, et al. Erysipelothrix rhusiopathiae clone associated with recurrent mass mortality events in High Arctic muskoxen (Ovibos moschatus) [Internet]. Research Square; 2025 [cited 2025 Sept 11]. Available from: https://www.researchsquare.com/article/rs-7384235/v1
67. Snieszko SF. The effects of environmental stress on outbreaks of infectious diseases of fishes. J Fish Biol. 1974;6(2):197–208.
68. van Seventer JM, Hochberg NS. Principles of Infectious Diseases: Transmission, Diagnosis, Prevention, and Control. Int Encycl Public Health. 2017;22–39.
69. Prewer E, Kutz S, Leclerc LM, Kyle CJ. Already at the bottom? Demographic declines are unlikely further to undermine genetic diversity of a large Arctic ungulate: muskox, Ovibos moschatus (Artiodactyla: Bovidae). Biol J Linn Soc. 2020 Jan 30;129(2):459–69.
70. Pečnerová P, Lord E, Garcia-Erill G, Hanghøj K, Rasmussen MS, Meisner J, et al. Population genomics of the muskox' resilience in the near absence of genetic variation. Mol Ecol. 2024;33(2):e17205.
71. Hellberg RS, Chu E. Effects of climate change on the persistence and dispersal of foodborne bacterial pathogens in the outdoor environment: A review. Crit Rev Microbiol. 2016 July 3;42(4):548–72.
72. Kock RA, Orynbayev M, Robinson S, Zuther S, Singh NJ, Beauvais W, et al. Saigas on the brink: Multidisciplinary analysis of the factors influencing mass mortality events. Sci Adv. 2018 Jan 17;4(1):eaao2314.
73. Bacterial Virulence - an overview | ScienceDirect Topics [Internet]. [cited 2025 Sept 7]. Available from: https://www.sciencedirect.com/topics/immunology-and-microbiology/bacterial-virulence
74. Biology LibreTexts [Internet]. 2025 [cited 2025 Sept 7]. 17: Pathogenicity and Virulence Factors. Available from: https://bio.libretexts.org/Courses/City_College_of_San_Francisco/Introduction_to_Microbiology_(Liu_et_al.)/17%3A_Pathogenicity_and_Virulence_Factors
75. Zhu W, Cai C, Li J, Zhang Q, Huang J, Jin M. Characterization of protective antigen CbpB as an adhesin and a plasminogen-binding protein of Erysipelothrix rhusiopathiae. Res Vet Sci. 2019 June 1;124:352–6.
76. Shimoji Y, Ogawa Y, Tsukio M, Shiraiwa K, Nishikawa S, Eguchi M. Genome-Wide Identification of Virulence Genes in Erysipelothrix rhusiopathiae: Use of a Mutant Deficient in a tagF Homolog as a Safe Oral Vaccine against Swine Erysipelas. Infect Immun. 2019 Dec 1;87(12):e00673-19.
77. Lipke PN, Ragonis-Bachar P. Sticking to the Subject: Multifunctionality in Microbial Adhesins. J Fungi. 2023 Apr 1;9(4):419.
78. Patel S, Mathivanan N, Goyal A. Bacterial adhesins, the pathogenic weapons to trick host defense arsenal. Biomed Pharmacother. 2017 Sept 1;93:763–71.
79. Hallstrom KN, McCormick BA. Pathogenicity Islands: Origins, Structure, and Roles in Bacterial Pathogenesis. Mol Med Microbiol. 2015 Jan 1;303–14.
80. Klemm P, Schembri MA. Bacterial adhesins: Function and structure. Int J Med Microbiol. 2000;290(1):27–35.
81. Maresso AW. Bacterial Invasion of the Host Cell. Bact Virulence. 2019;89–102.

82. Shimoji Y, Ogawa Y, Osaki M, Kabeya H, Maruyama S, Mikami T, et al. Adhesive surface proteins of Erysipelothrix rhusiopathiae bind to polystyrene, fibronectin, and type I and IV collagens. J Bacteriol. 2003 May;185(9):2739–48.
83. Zhao A, Sun J, Liu Y. Understanding bacterial biofilms: From definition to treatment strategies. Front Cell Infect Microbiol. 2023;13:1137947.
84. Maresso AW. Biofilms. Bact Virulence. 2019;145–53.
85. Rajagopal M, Walker S. Envelope Structures of Gram-Positive Bacteria. Curr Top Microbiol Immunol. 2017 Jan 1;404:1.
86. Ma L, Conover M, Lu H, Parsek MR, Bayles K, Wozniak DJ. Assembly and development of the Pseudomonas aeruginosa biofilm matrix. PLoS Pathog [Internet]. 2009 Mar [cited 2025 June 18];5(3). Available from: https://pubmed.ncbi.nlm.nih.gov/19325879/
87. CDP-glycerol glycerophosphotransferase (IPR007554) - InterPro entry - InterPro [Internet]. [cited 2025 Sept 28]. Available from: https://www.ebi.ac.uk/interpro/entry/InterPro/IPR007554/
88. CDP-glycerol:poly(glycerophosphate) glycerophosphotransferase, which is involved in the synthesis of the major wall teichoic acid in Bacillus subtilis 168, is encoded by tagF (rodC) [Internet]. [cited 2025 Sept 28]. Available from: https://journals.asm.org/doi/epdf/10.1128/jb.174.2.646-649.1992
89. Fitzgerald SN, Foster TJ. Molecular Analysis of the tagF Gene, Encoding CDP-Glycerol:Poly(glycerophosphate) Glycerophosphotransferase of Staphylococcus epidermidis ATCC 14990. J Bacteriol. 2000 Feb 15;182(4):1046–52.
90. Maresso AW. The Acquisition and Consumption of Host Nutrients. Bact Virulence. 2019;131–44.
91. Palmer LD, Skaar EP. Transition Metals and Virulence in Bacteria. Annu Rev Genet. 2016 Nov 23;50(Volume 50, 2016):67–91.
92. Kwok AH, Li Y, Jiang J, Jiang P, Leung FC. Complete genome assembly and characterization of an outbreak strain of the causative agent of swine erysipelas – Erysipelothrix rhusiopathiae SY1027. BMC Microbiol. 2014 July 2;14(1):176.
93. Peraro MD, Van Der Goot FG. Pore-forming toxins: Ancient, but never really out of fashion. Nat Rev Microbiol. 2016 Feb 1;14(2):77–92.
94. Sharifi-Mood B, Metanat M, Sharifi-Mood B, Metanat M, Sharifi-Mood B, Metanat M. Diagnosis, Clinical Management, Prevention, and Control of Cholera; A Review Study. Int J Infect 2014 11 [Internet]. 2014 Mar 31 [cited 2025 Aug 1];1(1). Available from: https://brieflands.com/articles/iji-14679
95. Maresso AW. Bacterial Protein Toxins and Effectors. Bact Virulence. 2019;115–29.
96. Liddington RC. Assembly and Function of the Anthrax Toxin Protein Translocation Complex. Subcell Biochem. 2021;96:563–77.
97. Di Bella S, Ascenzi P, Siarakas S, Petrosillo N, di Masi A. Clostridium difficile Toxins A and B: Insights into Pathogenic Properties and Extraintestinal Effects. Toxins. 2016 May 1;8(5):134.
98. Lyras D, O'Connor JR, Howarth PM, Sambol SP, Carter GP, Phumoonna T, et al. Toxin B is essential for virulence of Clostridium difficile. Nature. 2009 Apr 30;458(7242):1176–9.
99. Wagley S, Borne R, Harrison J, Baker-Austin C, Ottaviani D, Leoni F, et al. Galleria mellonella as an infection model to investigate virulence of Vibrio parahaemolyticus. Virulence. 2018 Dec 31;9(1):197–207.
100. Pereira TC, Barros PP de, de Oliveira Fugisaki LR, Rossoni RD, Ribeiro F de C, Menezes RT de, et al. Recent Advances in the Use of Galleria mellonella

Model to Study Immune Responses against Human Pathogens. J Fungi [Internet]. 2018 [cited 2024 Jan 6];4(4). Available from: /pmc/articles/PMC6308929/
101. Ménard G, Rouillon A, Cattoir V, Donnio PY. Galleria mellonella as a Suitable Model of Bacterial Infection: Past, Present and Future. Front Cell Infect Microbiol. 2021 Dec 22;11.
102. Elizalde-Bielsa A, Aragón-Aranda B, Loperena-Barber M, Salvador-Bescós M, Moriyón I, Zúñiga-Ripa A, et al. Development and evaluation of the Galleria mellonella (greater wax moth) infection model to study Brucella host-pathogen interaction. Microb Pathog. 2023 Jan 1;174:105930.
103. Pal N, Bender JS, Opriessnig T. Rapid detection and differentiation of Erysipelothrix spp. by a novel multiplex real-time PCR assay. J Appl Microbiol. 2010;108(3):1083–93.
104. Fang T. Designing PCR assays for distinguishing among the three broad clades of multi-host pathogen Erysipelothrix rhusiopathiae and for identifying the 'Arctic Clone' strain [Final Masters project report]. University of Glasgow; 2023.
105. Shi F, Ogawa Y, Sano A, Harada T, Hirota J, Eguchi M, et al. Characterization and identification of a novel candidate vaccine protein through systematic analysis of extracellular proteins of Erysipelothrix rhusiopathiae. Infect Immun. 2013 Dec;81(12):4333–40.
106. Zhu W, Wu C, Kang C, Cai C, Wang Y, Li J, et al. Evaluation of the protective efficacy of four newly identified surface proteins of Erysipelothrix rhusiopathiae. Vaccine. 2018 Dec 18;36(52):8079–83.
107. Kiani AK, Pheby D, Henehan G, Brown R, Sieving P, Sykora P, et al. Ethical considerations regarding animal experimentation. J Prev Med Hyg. 2022 June 1;63(2 Suppl 3):E255.
108. Baertschi B, Gyger M. Ethical Considerations in Mouse Experiments. Curr Protoc Mouse Biol. 2011 Mar;1(1):155–67.
109. PETA Staff. Giant 'Mouse' and More Than 30 PETA Supporters Protest NIH-Funded Experiments in D.C. (Photos). PETA website [Internet]. 2018 Jan 25 [cited 2025 June 19]; Available from: https://www.peta.org/news/photos-peta-giant-mouse-protest-nih-funded-sepsis-experiments/
110. Tannenbaum J, Bennett BT. Russell and Burch's 3Rs Then and Now: The Need for Clarity in Definition and Purpose. J Am Assoc Lab Anim Sci JAALAS. 2015 Mar 1;54(2):120.
111. The Principles of Humane Experimental Technique. Med J Aust. 1960 Mar;1(13):500–500.
112. Lavigne JP, Blanc-Potard AB, Bourg G, O'Callaghan D, Sotto A. Caenorhabditis elegans : modèle d'étude in vivo de la virulence bactérienne. Pathol Biol. 2006 Oct 1;54(8–9):439–46.
113. Kwadha CA, Ong'Amo GO, Ndegwa PN, Raina SK, Fombong AT. The biology and control of the greater wax moth, Galleria mellonella. Insects. 2017 June 9;8(2).
114. Kavanagh K, Sheehan G. The Use of Galleria mellonella Larvae to Identify Novel Antimicrobial Agents against Fungal Species of Medical Interest. J Fungi Basel Switz [Internet]. 2018 [cited 2025 Nov 6];4(3). Available from: http://dx.doi.org/10.3390/jof4030113
115. Pereira MF, Rossi CC, da Silva GC, Rosa JN, Bazzolli DMS. Galleria mellonella as an infection model: an in-depth look at why it works and practical considerations for successful application. Pathog Dis. 2020 Nov 23;78(8):ftaa056.
116. Söderhäll K, Cerenius L. Role of the prophenoloxidase-activating system in invertebrate immunity. Curr Opin Immunol. 1998 Feb 1;10(1):23–8.

117. Loh JMS, Adenwalla N, Wiles S, Proft T. Galleria mellonella larvae as an infection model for group A streptococcus. Virulence. 2013;4(5):419–28.
118. Evans BA, Rozen DE. A Streptococcus pneumoniae infection model in larvae of the wax moth Galleria mellonella. Eur J Clin Microbiol Infect Dis. 2012 Oct;31(10):2653–60.
119. Lam LN, Brunson DN, Kajfasz JK, Lemos JA. Methods for Using the Galleria mellonella Invertebrate Model to Probe Enterococcus faecalis Pathogenicity. Methods Mol Biol Clifton NJ. 2022;2427:177–83.
120. Mylonakis E, Moreno R, El Khoury JB, Idnurm A, Heitman J, Calderwood SB, et al. Galleria mellonella as a model system to study Cryptococcus neoformans pathogenesis. Infect Immun. 2005 July;73(7):3842–50.
121. Prakoso D, Zhu X, Rajeev S. Galleria mellonella infection model to evaluate pathogenic and nonpathogenic Leptospira strains. Vet Microbiol. 2022 Jan 1;264:109295.
122. Banfi D, Bianchi T, Mastore M, Brivio MF. Optimization of Experimental Infection of the Animal Model Galleria mellonella Linnaeus 1758 (Lepidoptera: Pyralidae) with the Gram-Positive Bacterium Micrococcus luteus. Insects. 2024 Aug 1;15(8):618.
123. Livefood UK Ltd. [Internet]. [cited 2025 Jan 2]. Available from: https://www.livefoods.co.uk/index.php
124. Radhakrishnan S. High-resolution genomic analyses offer unique insights into the emergence of a bacterial pathogen of ungulates in the Canadian Arctic. In Berlin: Annual Conference of The 650 Society for Veterinary Epidemiology and Preventive Medicine (The Society for Veterinary Epidemiology 651 and Preventive Medicine, Berlin, Germany, 2025); 2025.
125. Kumar A, Murthy LN, Jeyakumari A. 5. PLATING TECHNIQUES IN ISOLATION OF MICRO-ORGANISMS.
126. Miles AA, Misra SS, Irwin JO. The estimation of the bactericidal power of the blood. Epidemiol Infect. 1938;38(6):732–49.
127. GitHub - therneau/survival: Survival package for R [Internet]. [cited 2025 July 7]. Available from: https://github.com/therneau/survival
128. Pereira MF, Rossi CC, Da Silva GC, Rosa JN, Bazzolli DMS. Galleria mellonella as an infection model: An in-depth look at why it works and practical considerations for successful application. Pathog Dis. 2020 Nov 1;78(8).
129. Ménard G, Rouillon A, Ghukasyan G, Emily M, Felden B, Donnio PY. Galleria mellonella Larvae as an Infection Model to Investigate sRNA-Mediated Pathogenesis in Staphylococcus aureus. Front Cell Infect Microbiol [Internet]. 2021 Apr 19 [cited 2025 Nov 6];11. Available from: https://www.frontiersin.org/journals/cellular-and-infection-microbiology/articles/10.3389/fcimb.2021.631710/full
130. Malmquist JA, Rogan MR, McGillivray SM. Galleria mellonella as an Infection Model for Bacillus anthracis Sterne. Front Cell Infect Microbiol [Internet]. 2019 Oct 18 [cited 2025 Nov 6];9. Available from: https://www.frontiersin.org/journals/cellular-and-infection-microbiology/articles/10.3389/fcimb.2019.00360/full
131. Dalton JP, Uy B, Swift S, Wiles S. A Novel Restraint Device for Injection of Galleria mellonella Larvae that Minimizes the Risk of Accidental Operator Needle Stick Injury. Front Cell Infect Microbiol [Internet]. 2017 Mar 28 [cited 2025 Nov 6];7. Available from: https://www.frontiersin.org/journals/cellular-and-infection-microbiology/articles/10.3389/fcimb.2017.00099/full
132. Ignasiak K, Maxwell A. Galleria mellonella (greater wax moth) larvae as a model for antibiotic susceptibility testing and acute toxicity trials. BMC Res Notes. 2017 Aug 29;10(1):428.

133. Chen RY, Keddie BA. Galleria mellonella (Lepidoptera: Pyralidae) Hemocytes Release Extracellular Traps That Confer Protection Against Bacterial Infection in the Hemocoel. J Insect Sci. 2021 Nov 1;21(6):17.
134. Serrano I, Verdial C, Tavares L, Oliveira M, Serrano I, Verdial C, et al. The Virtuous Galleria mellonella Model for Scientific Experimentation. Antibiotics [Internet]. 2023 Mar 2 [cited 2025 Nov 6];12(3). Available from: https://www.mdpi.com/2079-6382/12/3/505
135. Curtis A, Kavanagh K, Murphy F. Galleria Mellonella as a Potential Bridging Model for Nanotoxicology. In: Alfaro-Moreno E, Murphy F, editors. Nanosafety: A Comprehensive Approach to Assess Nanomaterial Exposure on the Environment and Health [Internet]. Cham: Springer Nature Switzerland; 2025 [cited 2025 Nov 6]. p. 313–36. Available from: https://doi.org/10.1007/978-3-031-93871-9_12
136. Wuensch A, Trusch F, Iberahim NA, van West P. Galleria melonella as an experimental in vivo host model for the fish-pathogenic oomycete Saprolegnia parasitica. Fungal Biol. 2018 Feb 1;122(2):182–9.
137. Lethal Dose 50 (LD50) - everything you need to know [Internet]. [cited 2025 Nov 5]. Available from: https://bpca.org.uk/news-and-blog/Feature/ld50-everything-you-need-to-know/278076
138. Ogawa Y, Minagawa Y, Shi F, Eguchi M, Muneta Y, Shimoji Y. Immunostimulatory Effects of Recombinant Erysipelothrix rhusiopathiae Expressing Porcine Interleukin-18 in Mice and Pigs. Clin Vaccine Immunol CVI. 2012 Sept;19(9):1393–8.
139. Zhao D, Hu Y, Wu H, Feng Z, Hu C, Hu H, et al. Phenotypic and Genotypic Characterization of a Highly Virulent Erysipelothrix rhusiopathiae Strain. Transbound Emerg Dis. 2024;2024:5401707.
140. Dunn MJ, Woodruff AL, Anderson MZ. The Galleria mellonella Waxworm Infection Model for Disseminated Candidiasis. J Vis Exp JoVE. 2018 Nov 17;(141).
141. Wojda I. Immunity of the greater wax moth Galleria mellonella. Insect Sci. 2017;24(3):342–57.
142. Wu G, Liu Y, Ding Y, Yi Y. Ultrastructural and functional characterization of circulating hemocytes from *Galleria mellonella* larva: Cell types and their role in the innate immunity. Tissue Cell. 2016 Aug 1;48(4):297–304.
143. Gizzi AB da R, Oliveira ST, Leutenegger CM, Estrada M, Kozemjakin DA, Stedile R, et al. Presence of infectious agents and co-infections in diarrheic dogs determined with a real-time polymerase chain reaction-based panel. BMC Vet Res. 2014 Jan 16;10(1):23.
144. Howell AK, McCann CM, Wickstead F, Williams DJL. Co-infection of cattle with Fasciola hepatica or F. gigantica and Mycobacterium bovis: A systematic review. PloS One. 2019;14(12):e0226300.
145. Nishi K, Gondaira S, Hirano Y, Ohashi M, Sato A, Matsuda K, et al. Biofilm characterisation of Mycoplasma bovis co-cultured with Trueperella pyogenes. Vet Res. 2025 Jan 30;56(1):22.
146. Tomaselli M, Ytrehus B, Opriessnig T, Duignan P, Dalton C, van der Meer F, et al. Contagious Ecthyma Dermatitis as a Portal of Entry for Erysipelothrix rhusiopathiae in Muskoxen (Ovibos moschatus) of the Canadian Arctic. J Wildl Dis. 2022 Jan 1;58(1):228–31.
147. Jensen HE, Gyllensten J, Hofman C, Leifsson PS, Agerholm JS, Boye M, et al. Histologic and Bacteriologic Findings in Valvular Endocarditis of Slaughter-Age Pigs. J Vet Diagn Invest. 2010 Nov 1;22(6):921–7.
148. Parkinson AJ, Evengard B, Semenza JC, Ogden N, Børresen ML, Berner J, et al. Climate change and infectious diseases in the Arctic: establishment of a circumpolar working group. Int J Circumpolar Health. 2014 Sept 30;73:10.3402/ijch.v73.25163.

149. Takahashi T, Takagi M, Yamaoka R, Ohishi K, Norimatsu M, Tamura Y, et al. Comparison of the pathogenicity for chickens of Erysipelothrix rhusiopathiae and Erysipelothrix tonsillarum. Avian Pathol J WVPA. 1994 June;23(2):237–45.
150. Silva LN, Campos-Silva R, Ramos LS, Trentin DS, Macedo AJ, Branquinha MH, et al. Virulence of Candida haemulonii complex in Galleria mellonella and efficacy of classical antifungal drugs: a comparative study with other clinically relevant non-albicans Candida species. FEMS Yeast Res. 2018 Nov 1;18(7):82.
151. Fallon JP, Troy N, Kavanagh K. Pre-exposure of Galleria mellonella larvae to different doses of Aspergillus fumigatus conidia causes differential activation of cellular and humoral immune responses. Virulence. 2011;2(5):413–21.
152. Lin Z, Wang JL, Cheng Y, Wang JX, Zou Z. Pattern recognition receptors from lepidopteran insects and their biological functions. Dev Comp Immunol. 2020 July;108:103688.
153. Tsai CJY, Loh JMS, Proft T. Galleria mellonella infection models for the study of bacterial diseases and for antimicrobial drug testing. Virulence. 2016 Apr 2;7(3):214–29.
154. Wojda I, Staniec B, Sułek M, Kordaczuk J. The greater wax moth Galleria mellonella: biology and use in immune studies. Pathog Dis. 2020 Dec 18;78(9):57.
155. Beck SD. Neural and Hormonal Control of Pupation in Galleria mellonella (Lepidoptera: Galleriidae). Ann Entomol Soc Am. 1970 Jan 15;63(1):144–9.
156. Śmietanko A, Wiśniewski JR, Cymborowski B. Effect of low rearing temperature on development of Galleria mellonella larvae and their sensitivity to juvenilizing treatment. Comp Biochem Physiol A Physiol. 1989 Jan 1;92(2):163–9.
157. Copplestone D, Coates CJ, Lim J. Low dose γ-radiation induced effects on wax moth (Galleria mellonella) larvae. Sci Total Environ. 2023 June 10;876:162742.
158. Nojima Y, Bono H, Yokoyama T, Iwabuchi K, Sato R, Arai K, et al. Superoxide dismutase down-regulation and the oxidative stress is required to initiate pupation in Bombyx mori. Sci Rep. 2019 Dec 1;9(1).
159. Banville N, Browne N, Kavanagh K. Effect of nutrient deprivation on the susceptibility of Galleria mellonella larvae to infection. Virulence. 2012;3(6):497–503.
160. Fredericks LR, Lee MD, Roslund CR, Crabtree AM, Allen PB, Rowley PA. The design and implementation of restraint devices for the injection of pathogenic microorganisms into Galleria mellonella. PLoS ONE. 2020 July 30;15(7):e0230767.
161. Büyükgüzel E, Kalender Y. Penicillin-induced oxidative stress: effects on antioxidative response of midgut tissues in instars of Galleria mellonella. J Econ Entomol. 2007 Oct;100(5):1533–41.
162. Champion OL, Wagley S, Titball RW. Galleria mellonella as a model host for microbiological and toxin research. Virulence. 2016 Oct 2;7(7):840–5.
163. Wojda I. Immunity of the greater wax moth Galleria mellonella. Insect Sci. 2017 June 1;24(3):342–57.
164. Brown SE, Howard A, Kasprzak AB, Gordon KH, East PD. A peptidomics study reveals the impressive antimicrobial peptide arsenal of the wax moth Galleria mellonella. Insect Biochem Mol Biol. 2009 Nov;39(11):792–800.
165. Jorjão AL, Oliveira LD, Scorzoni L, Figueiredo-Godoi LMA, Prata MCA, Jorge AOC, et al. From moths to caterpillars: Ideal conditions for galleria mellonella rearing for in vivo microbiological studies. Virulence. 2018 Jan 1;9(1):383–9.

166. Serrano I, Verdial C, Tavares L, Oliveira M. The Virtuous Galleria mellonella Model for Scientific Experimentation. Antibiot 2023 Vol 12 Page 505. 2023 Mar 3;12(3):505.
167. Sadeghi R, Heidari F, Ebadollahi A, Chen G. Effects of High-Pressure Carbon Dioxide on the Sensory and Chemical Properties of Dried Dates and Its Toxicity against Galleria mellonella (L.) and Plodia interpunctella (Hübner). J Food Prot. 2022 Sept 1;85(9):1329–34.
168. Gulati R, Kaushik HD. Enemies of honeybees and their management – A review. Agric Rev. 2004;25(3):189–200.
169. Brain Heart Infusion Broth for microbiology BHI Broth [Internet]. [cited 2025 Sept 23]. Available from: https://www.sigmaaldrich.com/GB/en/product/sial/53286
170. Columbia Agar Base with 5% Defibrinated Sheep Blood [Internet]. E & O Laboratories Ltd. [cited 2025 Sept 23]. Available from: https://eolabs.com/product/pp1747-columbia-agar-with-5-sheep-blood/
171. Why Must Pipette Tips Be Changed Between Dilutions? - News [Internet]. [cited 2025 Sept 24]. Available from: https://www.marvnier.com/news/why-must-pipette-tips-be-changed-between-dilut-75502896.html
172. Harada T, Ogawa Y, Eguchi M, Shi F, Sato M, Uchida K, et al. Erysipelothrix rhusiopathiae exploits cytokeratin 18-positive epithelial cells of porcine tonsillar crypts as an invasion gateway. Vet Immunol Immunopathol. 2013 June 15;153(3):260–6.
173. Di Francesco J, Navarro-Gonzalez N, Wynne-Edwards K, Peacock S, Leclerc LM, Tomaselli M, et al. Qiviut cortisol in muskoxen as a potential tool for informing conservation strategies. Conserv Physiol. 2017 Jan 1;5(1):cox052.
174. What's killing muskox in the Arctic Islands? [Internet]. [cited 2025 Nov 6]. Available from: https://canadiangeographic.ca/articles/whats-killing-muskox-in-the-arctic-islands/
175. Kleppe K, Ohtsuka E, Kleppe R, Molineux I, Khorana HG. Studies on polynucleotides: XCVI. Repair replication of short synthetic DNA's as catalyzed by DNA polymerases. J Mol Biol. 1971 Mar 14;56(2):341–61.
176. Mullis KB, Faloona FA. [21] Specific synthesis of DNA *in vitro* via a polymerase-catalyzed chain reaction. In: Methods in Enzymology [Internet]. Academic Press; 1987 [cited 2025 Aug 13]. p. 335–50. (Recombinant DNA Part F; vol. 155). Available from: https://www.sciencedirect.com/science/article/pii/0076687987550236
177. Borst P. Ethidium DNA agarose gel electrophoresis: How it started. IUBMB Life. 2005;57(11):745–7.
178. Galindo-Murillo R, Cheatham TE. Ethidium bromide interactions with DNA: an exploration of a classic DNA–ligand complex with unbiased molecular dynamics simulations. Nucleic Acids Res. 2021 Mar 25;49(7):3735–47.
179. Introduction & Historical Timelines [Internet]. [cited 2025 Aug 14]. Available from: https://www.sigmaaldrich.com/GB/en/technical-documents/technical-article/genomics/pcr/pcr-introduction-and-historical-timelines
180. Higuchi R, Fockler C, Dollinger G, Watson R. Kinetic PCR analysis: real-time monitoring of DNA amplification reactions. Biotechnol Nat Publ Co. 1993 Sept;11(9):1026–30.
181. Kralik P, Ricchi M. A Basic Guide to Real Time PCR in Microbial Diagnostics: Definitions, Parameters, and Everything. Front Microbiol. 2017 Feb 2;8:108.

182. SYBR™ Green Universal Master Mix 1 x 5 mL | Buy Online | Applied Biosystems™ [Internet]. [cited 2025 Aug 18]. Available from: https://www.thermofisher.com/order/catalog/product/4309155
183. TaqMan® Real-Time PCR Products | Thermo Fisher Scientific - UK [Internet]. [cited 2025 Aug 18]. Available from: https://www.thermofisher.com/uk/en/home/brands/taqman/taqman-pcr-products.html
184. Holland PM, Abramson RD, Watson R, Gelfand DH. Detection of specific polymerase chain reaction product by utilizing the 5'----3' exonuclease activity of Thermus aquaticus DNA polymerase. Proc Natl Acad Sci. 1991 Aug 15;88(16):7276–80.
185. QIAcuity Digital PCR System | QIAGEN [Internet]. [cited 2025 Aug 12]. Available from: https://www.qiagen.com/us/products/instruments-and-automation/pcr-instruments/qiacuity-digital-pcr-system
186. Kubista M, Andrade JM, Bengtsson M, Forootan A, Jonák J, Lind K, et al. The real-time polymerase chain reaction. Mol Aspects Med. 2006;27(2–3):95–125.
187. Hays A, Wissel M, Colletti K, Soon R, Azadeh M, Smith J, et al. Recommendations for Method Development and Validation of qPCR and dPCR Assays in Support of Cell and Gene Therapy Drug Development. AAPS J. 2024 Feb 5;26(1):24.
188. Bustin SA, Benes V, Garson JA, Hellemans J, Huggett J, Kubista M, et al. The MIQE Guidelines: Minimum Information for Publication of Quantitative Real-Time PCR Experiments. Clin Chem. 2009 Apr 1;55(4):611–22.
189. Hernández I, Sant C, Martínez R, Fernández C. Design of Bacterial Strain-Specific qPCR Assays Using NGS Data and Publicly Available Resources and Its Application to Track Biocontrol Strains. Front Microbiol [Internet]. 2020 Mar 10 [cited 2025 Aug 18];11. Available from: https://www.frontiersin.org/journals/microbiology/articles/10.3389/fmicb.2020.00208/full
190. Li F, Liu J, Maldonado-Gómez MX, Frese SA, Gänzle MG, Walter J. Highly accurate and sensitive absolute quantification of bacterial strains in human fecal samples. Microbiome. 2024 Sept 7;12(1):168.
191. Johansen P, Vindeløv J, Arneborg N, Brockmann E. Development of quantitative PCR and metagenomics-based approaches for strain quantification of a defined mixed-strain starter culture. Syst Appl Microbiol. 2014 May 1;37(3):186–93.
192. Barbau-Piednoir E, Denayer S, Botteldoorn N, Dierick K, De Keersmaecker SCJ, Roosens NH. Detection and discrimination of five E. coli pathotypes using a combinatory SYBR® Green qPCR screening system. Appl Microbiol Biotechnol. 2018;102(7):3267–85.
193. Grazziotin AL, Vidal NM, Hoepers PG, Reis TFM, Mesa D, Caron LF, et al. Comparative genomics of a novel clade shed light on the evolution of the genus Erysipelothrix and characterise an emerging species. Sci Rep. 2021 Feb 9;11(1):3383.
194. Grazziotin AL, Vidal NM, Hoepers PG, Reis TFM, Mesa D, Caron LF, et al. Author Correction: Comparative genomics of a novel clade shed light on the evolution of the genus Erysipelothrix and characterise an emerging species. Sci Rep. 2021 May 4;11(1):9861.
195. LLC GB. SnapGene Viewer | Free software for plasmid mapping, primer design, and restriction site analysis [Internet]. [cited 2025 Sept 10]. Available from: https://www.snapgene.com/snapgene-viewer
196. Primer designing tool [Internet]. [cited 2025 July 30]. Available from: https://www.ncbi.nlm.nih.gov/tools/primer-blast/

197. Primer3 [Internet]. [cited 2025 Sept 10]. Available from: https://primer3.org/
198. Qiagen. Second Edition Sample & Assay Technologies Rotor-Gene ® Multiplex Handbook Rotor-Gene Multiplex PCR Kit Rotor-Gene Multiplex RT-PCR Kit For fast multiplex real-time PCR, two-step RT-PCR, and one-step RT-PCR using sequence-specific probes on Rotor-Gene cyclers QIAGEN Sample and Assay Technologies [Internet]. 2011. Available from: www.qiagen.com.
199. Jia Y. Chapter 3 - Real-Time PCR. In: Conn PM, editor. Methods in Cell Biology [Internet]. Academic Press; 2012 [cited 2025 Aug 30]. p. 55–68. (Laboratory Methods in Cell Biology; vol. 112). Available from: https://www.sciencedirect.com/science/article/pii/B9780124059146000032
200. How to develop an optimal fluorescence assay [Internet]. [cited 2025 Sept 16]. Available from: https://www.tecan.com/blog/how-to-develop-an-optimal-fluorescence-assay
201. Pazdernik A, PhD, Writer S, Prediger IE, PhD, Writer FSS, et al. Integrated DNA Technologies. [cited 2025 Aug 7]. qPCR Probes: Selecting reporter dyes and quenchers | IDT. Available from: https://eu.idtdna.com/pages/education/decoded/article/qpcr-probes-selecting-the-best-reporter-dye-and-quencher
202. Faster qRT-PCR & Quantitative PCR, Brilliant III Probe MM | Agilent [Internet]. [cited 2025 July 30]. Available from: https://www.agilent.com/en/product/real-time-pcr-(qpcr)/real-time-pcr-(qpcr)-master-mixes/brilliant-iii/brilliant-iii-probe-mm-232721#support
203. Geneious Prime | Molecular Biology and Sequence Analysis Tools - Geneious [Internet]. [cited 2025 July 30]. Available from: https://www.geneious.com/features/prime
204. SnapGene | Software for everyday molecular biology [Internet]. [cited 2025 July 30]. Available from: https://www.snapgene.com/
205. Ostertagová E, Ostertag O. Methodology and Application of Oneway ANOVA. Am J Mech Eng. 2013 Jan 23;1(7):256–61.
206. Wood RL. A selective liquid medium utilizing antibiotics for isolation of Erysipelothrix insidiosa. Am J Vet Res. 1965 Nov;26(115):1303–8.
207. Fidalgo SG, Wang Q, Riley TV. Comparison of Methods for Detection of Erysipelothrix spp. and Their Distribution in Some Australasian Seafoods. Appl Environ Microbiol. 2000 May;66(5):2066–70.
208. Grohmann L, Barbante A, Eriksson R, Gatto F, Georgieva T, Huber I, et al. Guidance document on multiplex real-time PCR methods: European Network of GMO Laboratories [Internet]. Luxembourg: Publications Office of the European Union; 2021 [cited 2025 Sept 15]. (EUR; vol. 30708). Available from: https://plus.cobiss.net/cobiss/si/sl/bib/94024963
209. Schoch CL, Ciufo S, Domrachev M, Hotton CL, Kannan S, Khovanskaya R, et al. NCBI Taxonomy: a comprehensive update on curation, resources and tools. Database. 2020 Jan 1;2020:baaa062.
210. NASA PACE - Section I: Light Properties [Internet]. [cited 2025 Sept 14]. Available from: https://pace.oceansciences.org/prop_of_light.cgi
211. Stephen. PCR and friends: Fluorophores world : part 1 [Internet]. PCR and friends. 2013 [cited 2025 Sept 16]. Available from: https://q-pcr.blogspot.com/2013/01/fluorophores-world-part-1.html
212. What is the delta Rn value? [Internet]. [cited 2025 Sept 14]. Available from: https://www.qiagen.com/us/resources/faq/2681
213. Ruijter JM, Lorenz P, Tuomi JM, Hecker M, van den Hoff MJB. Fluorescent-increase kinetics of different fluorescent reporters used for qPCR depend on

monitoring chemistry, targeted sequence, type of DNA input and PCR efficiency. Mikrochim Acta. 2014;181(13):1689–96.
214. Svec D, Tichopad A, Novosadova V, Pfaffl MW, Kubista M. How good is a PCR efficiency estimate: Recommendations for precise and robust qPCR efficiency assessments. Biomol Detect Quantif. 2015 Mar 11;3:9–16.
215. Lopez MLD, Crichton EM, Allison MJ, Dema AH, Bonderud MT, Helbing CC. Effects of storage conditions on the stability of qPCR reagents: implications for environmental DNA detection. BMC Res Notes. 2024 July 18;17(1):199.
216. Pearce DL, Edson JE, Jennelle CS, Walter WD. Evaluation of DNA yield from various tissue and sampling sources for use in single nucleotide polymorphism panels. Sci Rep. 2024 May 17;14(1):11340.
217. Massung RF, Slater K, Owens JH, Nicholson WL, Mather TN, Solberg VB, et al. Nested PCR assay for detection of granulocytic ehrlichiae. J Clin Microbiol. 1998 Apr;36(4):1090–5.
218. Sharifdini M, Mirhendi H, Ashrafi K, Hosseini M, Mohebali M, Khodadadi H, et al. Comparison of Nested Polymerase Chain Reaction and Real-Time Polymerase Chain Reaction with Parasitological Methods for Detection of Strongyloides stercoralis in Human Fecal Samples. Am J Trop Med Hyg. 2015 Dec;93(6):1285–91.
219. LookOut DNA Erase Decontamination Spray Sigma-Aldrich [Internet]. [cited 2025 Sept 13]. Available from: https://www.sigmaaldrich.com/GB/en/product/sigma/l8917
220. PCR Cabinets | Starlab UK [Internet]. [cited 2025 Sept 14]. Available from: https://www.starlabgroup.com/GB-en/equipment/pcr-cabinets.html
221. Subhash VV, Huang L, Kamili A, Wong M, Chen D, Venn NC, et al. Whole-genome sequencing facilitates patient-specific quantitative PCR-based minimal residual disease monitoring in acute lymphoblastic leukaemia, neuroblastoma and Ewing sarcoma. Br J Cancer. 2022 Feb;126(3):482–91.
222. Mao D, Zhao L, Zhao B, Xu H, Zhang Q. Development of a Strain-Specific Detection and Quantification Method for Bifidobacterium animalis subsp. lactis HN019 Using WGS-SNP Analysis and qPCR. Microorganisms. 2025 July;13(7):1596.
223. Yeung PSW, Wang H, Sibai M, Solis D, Yamamoto F, Iwai N, et al. Evaluation of a Rapid and Accessible Reverse Transcription-Quantitative PCR Approach for SARS-CoV-2 Variant of Concern Identification. J Clin Microbiol. 2022 Apr 25;60(5):e00178-22.
224. Yang Z, Kulka M, Yang Q, Papafragkou E, Yu C, Wales SQ, et al. Whole-Genome Sequencing-Based Confirmatory Methods on RT-qPCR Results for the Detection of Foodborne Viruses in Frozen Berries. Food Environ Virol. 2024;16(2):225–40.
225. ISO 22174:2024(en), Microbiology of the food chain — Polymerase chain reaction (PCR) for the detection and quantification of microorganisms — General requirements and definitions [Internet]. [cited 2025 Sept 25]. Available from: https://www.iso.org/obp/ui/#iso:std:iso:22174:ed-2:v1:en
226. Tang J, Zhu J, Wang J, Qian H, Liu Z, Wang R, et al. Development and clinical application of loop-mediated isothermal amplification combined with lateral flow assay for rapid diagnosis of SARS-CoV-2. BMC Infect Dis. 2024 Jan 15;24(1):81.
227. Khan A, Waqar K, Shafique A, Irfan R, Gul A. Chapter 18 - In Vitro and In Vivo Animal Models: The Engineering Towards Understanding Human Diseases and Therapeutic Interventions. In: Barh D, Azevedo V, editors. Omics Technologies and Bio-Engineering [Internet]. Academic Press; 2018 [cited 2025 Sept 24]. p. 431–48. Available from: https://www.sciencedirect.com/science/article/pii/B978012804659300018X

228. Lampreht Tratar U, Horvat S, Cemazar M. Transgenic Mouse Models in Cancer Research. Front Oncol. 2018 July 20;8:268.
229. Jia T, Wang C, Han Z, Wang X, Ding M, Wang Q. Experimental Rodent Models of Cardiovascular Diseases. Front Cardiovasc Med. 2020 Dec 7;7:588075.
230. Mapara M, Thomas BS, Bhat KM. Rabbit as an animal model for experimental research. Dent Res J. 2012;9(1):111–8.
231. Padilla-Carlin DJ, McMurray DN, Hickey AJ. The Guinea Pig as a Model of Infectious Diseases. Comp Med. 2008 Aug;58(4):324–40.
232. Choi TY, Choi TI, Lee YR, Choe SK, Kim CH. Zebrafish as an animal model for biomedical research. Exp Mol Med. 2021 Mar;53(3):310–7.
233. Calvillo L. Editorial: 3Rs approach (replace, reduce and refine animal models) to improve preclinical research. Front Physiol. 2022 Oct 6;13:1040575.
234. Giugliano LG, Barer M, Mann GF, Drasar BS. Tissue Culture Systems for the Examination of Bacterial Virulence. In: Hill MJ, editor. Models of Anaerobic Infection: Proceedings of the third Anaerobe Discussion Group Symposium held at Churchill College, University of Cambridge, July 30–31, 1983, followed by the abstracts of the first meeting of the Society for Intestinal Microbial Ecology and Disease, Boston, November 1983 [Internet]. Dordrecht: Springer Netherlands; 1984 [cited 2025 Sept 29]. p. 189–200. Available from: https://doi.org/10.1007/978-94-009-6054-1_17
235. Shi D, Mi G, Wang M, Webster TJ. In vitro and ex vivo systems at the forefront of infection modeling and drug discovery. Biomaterials. 2019 Apr;198:228–49.
236. Dijokaite A, Humbert MV, Borkowski E, La Ragione RM, Christodoulides M. Establishing an invertebrate Galleria mellonella greater wax moth larval model of Neisseria gonorrhoeae infection. Virulence. 2021 Dec 31;12(1):1900–20.
237. Guembe M, Hafian R, Díaz-Navarro M, Visedo A, De Maio F, Pimpinelli F, et al. Virulence profile of carbapenem-resistant Klebsiella pneumoniae strains by an in vivo model of Galleria mellonella. Microbiol Spectr. 2025 Feb 4;13(2):e0221524.
238. Tao Y, Duma L, Rossez Y. Galleria mellonella as a Good Model to Study Acinetobacter baumannii Pathogenesis. Pathogens. 2021 Nov 14;10(11):1483.
239. Fruit Fly Model - an overview | ScienceDirect Topics [Internet]. [cited 2025 Sept 29]. Available from: https://www.sciencedirect.com/topics/immunology-and-microbiology/fruit-fly-model
240. Wright CL, Kavanagh O. Galleria mellonella as a Novel In Vivo Model to Screen Natural Product-Derived Modulators of Innate Immunity. Appl Sci. 2022 Jan;12(13):6587.
241. Champion OL, Titball RW, Bates S. Standardization of G. mellonella Larvae to Provide Reliable and Reproducible Results in the Study of Fungal Pathogens. J Fungi. 2018 Sept;4(3):108.
242. Giammarino A, Bellucci N, Angiolella L. Galleria mellonella as a Model for the Study of Fungal Pathogens: Advantages and Disadvantages. Pathogens. 2024 Mar;13(3):233.
243. The genome sequence of the Greater Wax ... | Wellcome Open Research [Internet]. [cited 2025 Sept 29]. Available from: https://wellcomeopenresearch.org/articles/9-101
244. Fisher Scientific T. QuantStudio ™ 5 Real-Time PCR Instrument (for Human Identification) USER GUIDE Installation, maintenance, and administration for use with: HID Real-Time PCR Analysis Software v1.3 and v1.4.